NDE METHOD FOR CHARACTERIZING ANODIZED A1 SURFACES

ROCKWELL INTERNATIONAL SCIENCE CENTER
1049 CAMINO DOS RIOS
THOUSAND OAKS, CALIFORNIA 91360

January 1979

TECHNICAL REPORT AFML-TR-78-146
Final Report for period 1 September 1977 through 31 July 1978

AIR FORCE MATERIALS LABORATORY (LLP)
AIR FORCE SYTSTEMS COMMAND
WRIGHT-PATTERSON AIR FORCE BASE, OHIO 45433

NOTICE

When Government drawings, specifications, or other data are used for any purpose other than in connection with a definitely related Government procurement operation, the United States Government thereby incurs no responsibility nor any obligation whatsoever; and the fact that the Government may have formulated, furnished, or in any way supplied the said drawings, specifications, or other data, is not to be regarded by implication or otherwise as in any manner licensing the holder or any other person or corporation, or conveying any rights or permission to manufacture, use, or sell any patented invention that may in any way be related thereto.

This report has been reviewed by the Information Office (IO) and is releasable to the National Technical Information Service (NTIS). At NTIS, it will be available to the general public, including foreign nations.

This technical report has been reviewed and is approved for publication.

R.L.Crane

ROBERT L. CRANE
Project Engineer

DONALD M. FORNEY, Jr., Chief
Nondestructive Evaluation Branch
Metals and Ceramics Division

FOR THE COMMANDER

LAWRENCE N. HJELM, Asst Chief
Metals and Ceramics Division

"If your address has changed, if you wish to be removed for our mailing list, or if the addressee is no longer employed by your organization please notify AFML/LLP, WPAFB, OH 45433 to help us maintain a current mailing list."

Copies of this report should not be returned unless return is required by security considerations, contractual obligations, or notice on a specific document.

unclassified

SECURITY CLASSIFICATION OF THIS PAGE *(When Data Entered)*

REPORT DOCUMENTATION PAGE		READ INSTRUCTIONS BEFORE COMPLETING FORM
1. REPORT NUMBER AFML-TR-78-146	2. GOVT ACCESSION NO.	3. RECIPIENT'S CATALOG NUMBER
4. TITLE *(and Subtitle)* NDE Method for Characterizing Anodized Al Surfaces		5. TYPE OF REPORT & PERIOD COVERED Final Report 09/01/77 thru 07/31/78
		6. PERFORMING ORG. REPORT NUMBER SC5123.23FTR
7. AUTHOR(s) T. Smith		8. CONTRACT OR GRANT NUMBER(s) F33615-77-C-5215
9. PERFORMING ORGANIZATION NAME AND ADDRESS Rockwell International/Science Center 1049 Camino Dos Rios Thousand Oaks, CA 91360		10. PROGRAM ELEMENT, PROJECT, TASK AREA & WORK UNIT NUMBERS Project No. 2418
11. CONTROLLING OFFICE NAME AND ADDRESS Air Force Materials Laboratory (LLP) Air Force Systems Command Wright-Patterson Air Force Base, Ohio 45433		12. REPORT DATE September, 1978 13. NUMBER OF PAGES 101
14. MONITORING AGENCY NAME & ADDRESS*(if different from Controlling Office)*		15. SECURITY CLASS. *(of this report)* unclassified 15a. DECLASSIFICATION/DOWNGRADING SCHEDULE

16. DISTRIBUTION STATEMENT *(of this Report)*

Approved for public release; distribution unlimited

17. DISTRIBUTION STATEMENT *(of the abstract entered in Block 20, if different from Report)*

18. SUPPLEMENTARY NOTES

19. KEY WORDS *(Continue on reverse side if necessary and identify by block number)*
NONDESTRUCTIVE INSPECTION, ADHESIVE BONDING OF ALUMINUM, ELLIPSOMETRY, SURFACE POTENTIAL DIFFERENCE, PHOTOELECTRON EMISSION, WETTABILITY, COMPUTER MAPPING

20. ABSTRACT *(Continue on reverse side if necessary and identify by block number)*

This report describes a study of the relationship between nondestructive inspection (NDI) for contaminants on phosphoric acid anodized (PAA) Al 7075-T6 and bond strength and degradation that results from the contamination. Contamination is used in the broad sense to include surface preparation process errors (e.g., incorrect anodize time or voltage) and handling damage, as well as organic contamination from humans and smog. It is demonstrated that the ellisometric technique

DD FORM 1 JAN 73 1473 EDITION OF 1 NOV 65 IS OBSOLETE

unclassified

SECURITY CLASSIFICATION OF THIS PAGE *(When Data Entered)*

20.

can adequately reveal contamination at levels below and in the range that significantly degrades bond integrity. The ellisometric technique is not restricted to flat panels, as demonstrated by mapping a panel with 7 cm radius of curvature. However, mapping of curved surfaces would be facilitated by passing the sensor head over the panel rather than the panel under the head. This and mapping on NDI of smaller numbers of various shaped parts requires the development of a small miniaturized hand-held contamination tester. The design of such a tester is presented.

TABLE OF CONTENTS

LIST OF FIGURES

LIST OF FIGURES (Cont'd)

LIST OF FIGURES (Cont'd)

LIST OF TABLES

LIST OF TABLES (Cont'd)

FORWARD

This report covers work conducted as Task III "NDE Method for Characterizing Anodized Al Surfaces" from 9/01/77 to 07/29/78, under the direction of Dr. Tennyson Smith, Manager and Principal Investigator, with Gary W. Lindberg assisting. We acknowledge the assistance of P.A. Smith for computer mapping and bond testing.

This work was conducted under United States Air Force Contract F33615-77-C-5215, Project No. 2418, and was administered under the direction of the Metals Behavior Branch, Metals and Ceramics Division, Air Force Materials Laboratory, Wright Patterson Air Force Base, Ohio. The project monitor was Dr. R.L. Crane.

SUMMARY

In the last report (AFML-TR-77-42), it was demonstrated that the ellipsometric computerized inspection technique could detect organic contamination, handling damage and process errors. In this report, we demonstrate the relationships between contamination levels and adhesive joint integrity. By integrity, we mean lap shear strength and bond durability as tested by the humidity wedge test.

It was discovered that contrary to the FPL etch surface treatment, the PAA treatment leaves the surface very insensitive to degradation by organic contamination. However, PAA is very sensitive to degradation by handling damage, process errors and certain other types of contamination (e.g. silicone grease).

Panels of Al 7075-T6 were prepared by the phosphoric acid anodize treatment and contaminated or damaged to controlled levels. These panels were mapped by the ellipsometric technique, then bonded with FM73 adhesive to uncontaminated panels. The joints were tested by the lap shear test and by the wedge humidity durability test. Good correlation was obtained between contamination levels, contamination maps and bond integrity.

The goal of this effort was to demonstrate that the ellipsometric NDI technique could detect contamination below the level that significantly degrades the Al 7075-T6 FM73 joint. This goal has been met.

SECTION I

INTRODUCTION

Recent emphasis in the USAF on structural integrity and durability has focused attention on the use of adhesive bonding in primary structures as a joining technique. Preliminary estimates of weight and cost savings that would result from utilization of adhesive bonding technology are 15 and 20%, respectively. To assure the reliability of this joining method, nondestructive inspection (NDI) tools must be developed to ensure the adequacy of each step in the bonding process.

The program was divided into two tasks. In Task I, a contractor (Northrup Corp., see Ref. 1) developed an (SEM) inspection technique to determine the surface oxide composition, morphology and thickness of anodized panels. In Task II, a contractor (Rockwell International Science Center, see Ref. 2) developed a nondestructive inspection technique that can be used, just prior to layup, to detect contamination on the aluminum surface.

Contamination is used in a broad sense to include surface damage due to handling with cotton gloves and Kraft paper, processing errors during surface preparation, as well as organic contamination from various sources. Table 1 gives a list of contamination sources and whether ellipsometry, SPD or water contact angle was successful in detecting it, Y for yes and N for no.

The conclusion of the Task II study is that the most useful surface tool for monitoring all types of contamination is ellipsometry, although SPD and $\theta H_2 0$ are also very useful. However, the water break test $\theta H_2 0$ is only useful for detecting nonpolar contaminants.

TABLE 1

REPRESENTATIVE CONTAMINATION DUE TO VARIOUS SOURCES AND SURFACE TOOL UTILITY

Type	Compound or Substance	Tool		
		Ellip.	SPD	θH_2O
Processing Errors	Anodize time	y	N	N
	Anodize voltage	y	y	N
	Contamination from bath	y	N	
	Delay in H_3PO_4 before rinse	y	N	N
Handling Damage	Cotton glove	y	N	N
	Kraft paper	y	N	N
	Kimwipe	y	N	N
Human Contamination	Finger prints	y	y	y
	Cough or sneeze	N	N	N
	Cigarette smoke	N	N	N
	Cigarette ashes	N	y	
	Food remnants	y	y	N
Representative Constitutents of Smog	N Docosane	y	y	y
	16-Bromo-9-hexadecanoic acid	y	y	
	Dotriacontane	y	y	y
	Stearic acid	y	N	y
	Erucic acid	y	y	y
	Brassidic acid	y	y	y
	Decanoic acid	y	N	y
	Benzoic acid	y	y	y
	Amino-Benzoic acid	y	y	y
	1,1,2 diamino dodecane	y	y	y
	1-12-diamino decane	y	y	
	decadiene	N	N	
	decacyclene	y	N	N
	1-Eicosene	y	N	y
	1-Hexadeclamine	y	y	y
	Anthracene	N	N	N
	Adamantanol	y	y	N
	2-Adamantanone	y	y	N
	1-Adamantone carbonitrile	N	y	y
	1-Adamantane carbonylic acid	y	N	y

A. The Problem

Having established the utility of ellipsometry to detect very low concentrations of contaminants on PAA Al 7075-T6, it becomes necessary to discover if the ultimate detection level is below that which can significantly degrade bond strength or durability. Also, since all of the measurements were performed on flat panels, it is necessary to establish the utility of ellipsometry for contamination mapping of curved panels.

B. The Solution

The solution to this problem involves mapping controlled contaminated panels and then bonding these panels to uncontaminated panels and testing for bond strength and durability. If it can be demonstrated that the ellipsometer can detect contamination below the level that degrades the bond strength and durability, the utility of the ellipsometer for NDI of Al 7075-T6 just prior to layup will have been established.

The second aspect of the solution involves mapping of curved panels to see what, if any, effect curvature might have on the sensitivity of the ellipsometric mapping technique.

SECTION II

EXPERIMENTAL

The anodizing process, the surface tools and interpretation of their signals, and the automated computer facility have all been described in detail in the last report (Ref. 2).

A. Controlled Contamination

It is difficult to prepare surfaces with a controlled uniform layer of predetermined thickness. We have tried three techniques, aerosol spray, dip-withdrawal and solution-spin.

1. Aerosol Spray

The aerosol spray technique involves dissolution of the organic contaminant in pentane or hexane, then spraying with an air brush past the surface. The amount of deposition depends upon the concentration of this contaminant and the number of exposures. This technique has proved most useful and was originally designed to simulate smog which is an aerosol of low molecular weight material that contains larger molecules of all sorts. The aerosol particles form a fine mist that deposits on the surface. When the pentane evaporates, it leaves tiny particles of the contaminant dispersed over the surface. The average thickness of the contamination is determined by ellipsometry.

2. Dip-Withdrawal

To form thicker films than obtained by the aerosol technique, samples were placed in a solution of pentane or some other high vapor pressure solvent and slowly withdrawn at controlled speeds. As the sample surface raises above the liquid, evaporation causes the deposition of the contaminant. The thickness and quality of the deposit depends on the concentration and speed of withdrawal.

3. Solution-Spin

If a layer of solution is placed on a sample, evaporation will cause the solvent to form drops due to surface tension. The drops will not deposit the solute molecules until saturation is reached. The contaminant is therefore deposited at discrete points rather than in a uniform layer. To overcome this, the sample is spun so that centrifugal force overcomes the surface tension effect and the fluid remains a thin layer during evaporation. This is fairly successful and is commonly used in the semiconductor industry for placing the films of photoresist on chips. There is a tendency to leave solute in rays spreading from the center of the drop.

B. OFF-NULL Ellipsometry

Standard Null ellipsometry has been used throughout this study to calculate optical properties and film thickness values. To facilitate rapid scanning of surfaces for computer mapping, an automated version was invented[3] and used. However, the automated ellipsometer with no moving parts must monitor an elliptically shaped area about 2 cm long and 1 cm wide. In order to increase sensitivity and decrease the spot size to about 1 mm or less, a new "OFF NULL" technique was developed.

Figure 1 is a plot of light intensity vs polarizer azimuth for reflection of red light (λ = 6328Å) from an aluminum panel. For conventional ellipsometry, the intensity minimum (null) is used to obtain the polarizer azimuth which relates to the surface optical properties. If the optical properties change, the polarizer is rotated to a new null. In "OFF NULL" ellipsometry, the polarizer is set at null and optical changes are noted by the change in light intensity. For example, the null position for the aluminum plate (solid line in Fig. 1) is P = 43.5°. The addition of a contamination film shifts the null position to 33.5° (dashed curve). If the polarizer is left at 43.5°, the light intensity follows the arrow from I = 4 to I = 22.

The advantage of using the "OFF NULL" technique lies in increased sensitivity and optical changes can also be followed without mechanical motion of the ellipsometer parts. These properties are ideal for rapid scanning of a

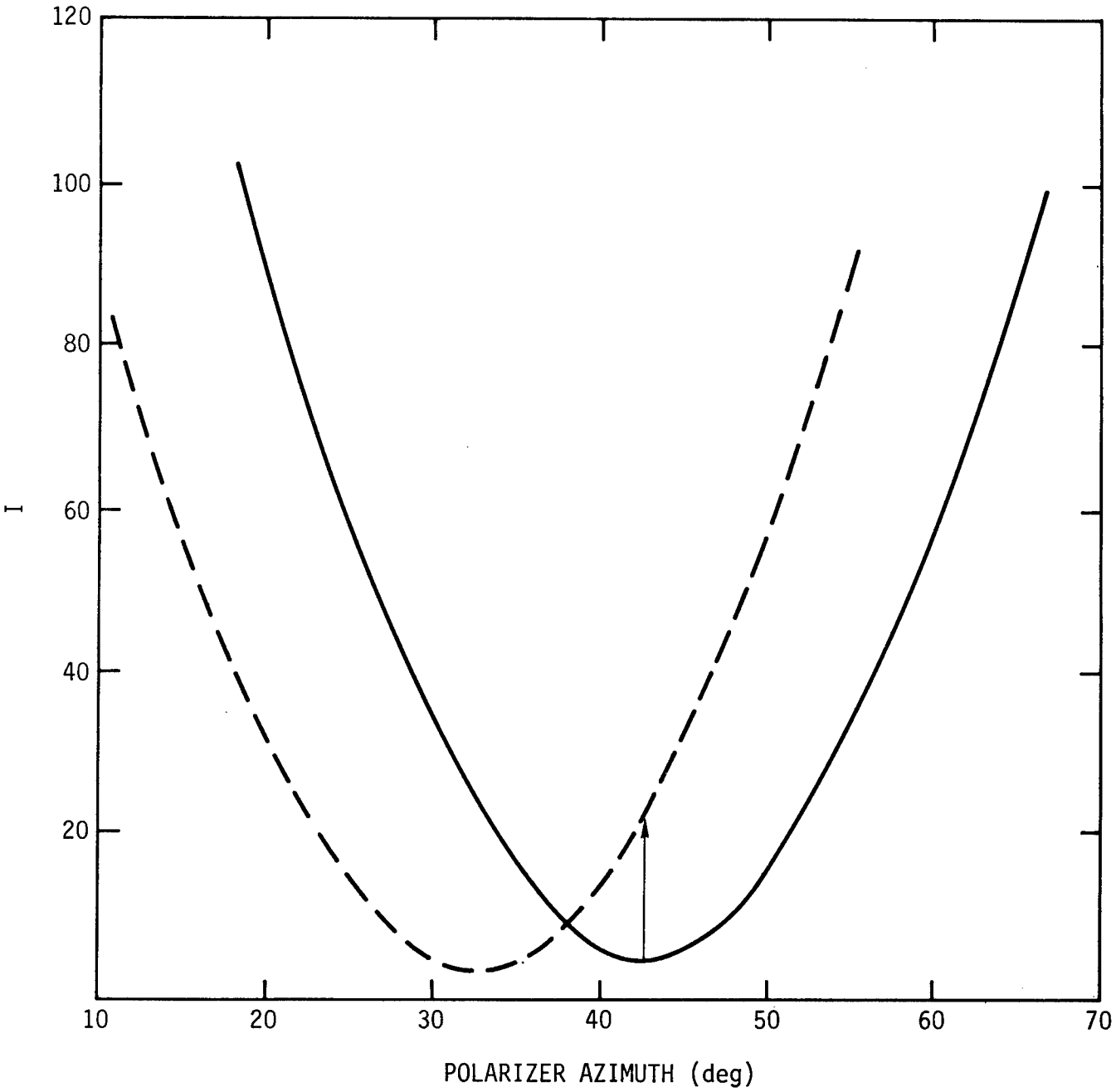

Fig. 1 Light intensity, I, vs polarizer asimuth.

geometrical area or for rapid following of changes with time. To illustrate the sensitivity, Fig. 2 shows plots of I vs position (1 to 4 inches) on the phosphoric acid analyzed panel 3-28-7-76, Fig. 3 (see last year's report Fig. C25a AFML-TR-77-42). The lower dashed curve is the intensity profile for the uncontaminated surface, the dotted curve is for brassidic acid contamination between position 1 and 2, 2 and 3, 3 and 4, the solid line is for contamination with erucic acid. Any area of this panel with $I < 20$ would be considered acceptable, any area with $I > 20$ would be contaminated.

Figure 4 shows the intensity profile across the panel (6-21-4-76C) contaminated with 1-Hexadecylamine (see Fig. 5). The increased contamination is noted from left to right. Figure 4 also indicates the great increase in sensitivity with increase in angle of incidence (AI) from 60^{o} to 70^{o}.

The standard ellipsometric measurements are given in Fig. 6, the deviation of Δ from the control value (163) is $\delta\Delta \sim 23^{o}$, -18^{o} and $+10^{o}$ for positions 6, 7 and 8, respectively. Since the deviation of Δ from a mean value for the control area is about $\delta\Delta_c \sim 3^{o}$, the ratio $[\delta\Delta/\delta\Delta_c] \sim 7$ for the most contaminated region. This can be compared to $[\delta I/\delta I_c] \sim 20$ by the "OFF NULL" technique.

C Curved Surfaces

All of the work reported in the previous report (Ref. 2) was for flat panels. However, factory use of an automated NDI system will certainly involve curved surfaces. In principle, automated ellipsometry can work just as well for curved surfaces as for flat surfaces as long as the angle of incidence remains unchanged. The part must be maneuvered to satisfy this requirement. Automated computer controlled positioning equipment is commonly used for machining and other purposes.

We have constructed an auxiliary unit to fit our planar mapping unit for the purpose of positioning a curved panel during mapping. This facility is shown in Fig. 7. The curved Al 7075-T6 panel (7 cm radius) is moved in one direction on the standard positioner stage. Motion in the other direction is accomplished by rotating the panel with a cord attached to a pulley and stepping motor. The black cube at the left of the photograph contains the

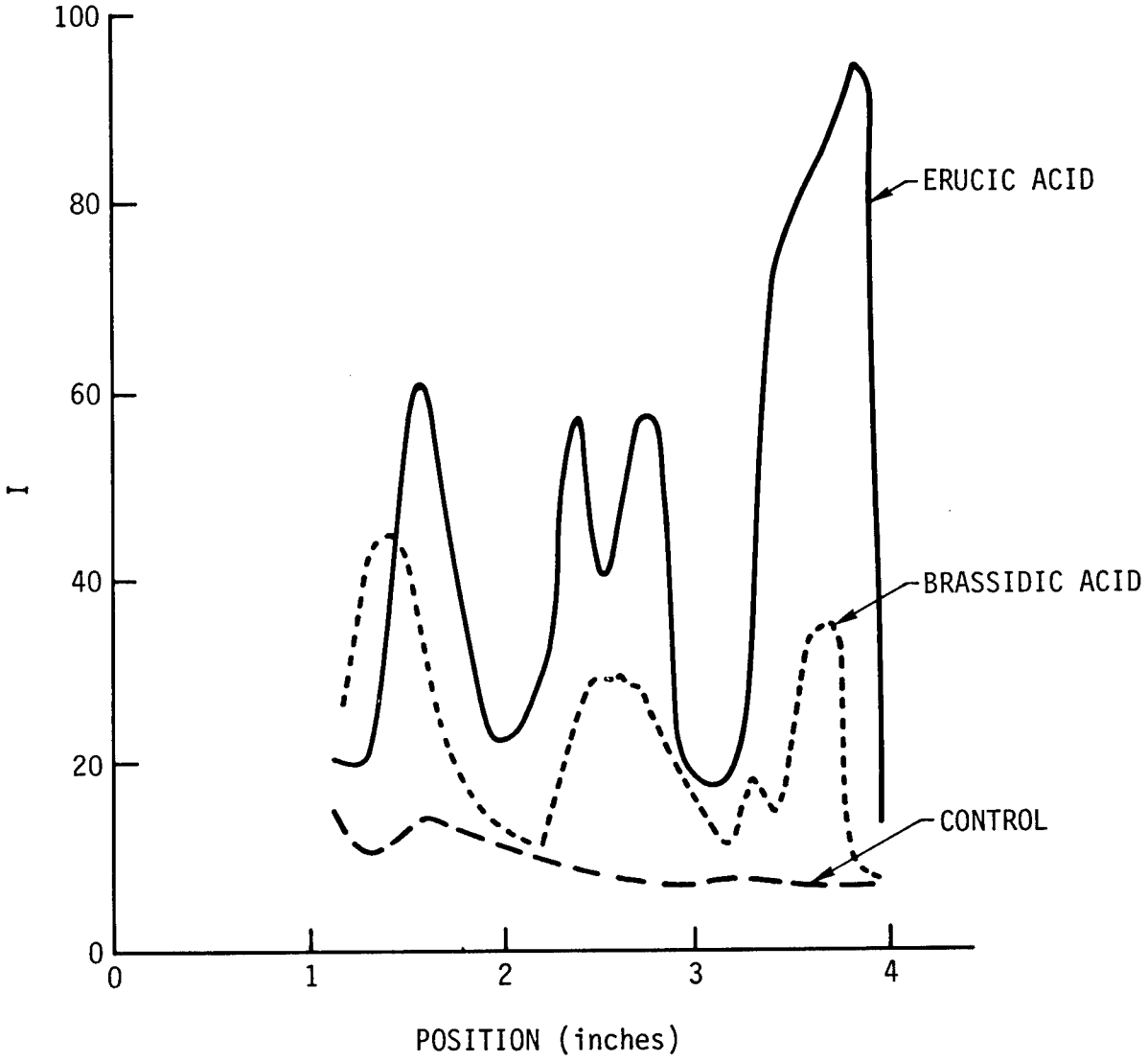

Fig. 2 Intensity vs position for contamination on Al panel 3-27-7-76. (see Fig. 3)

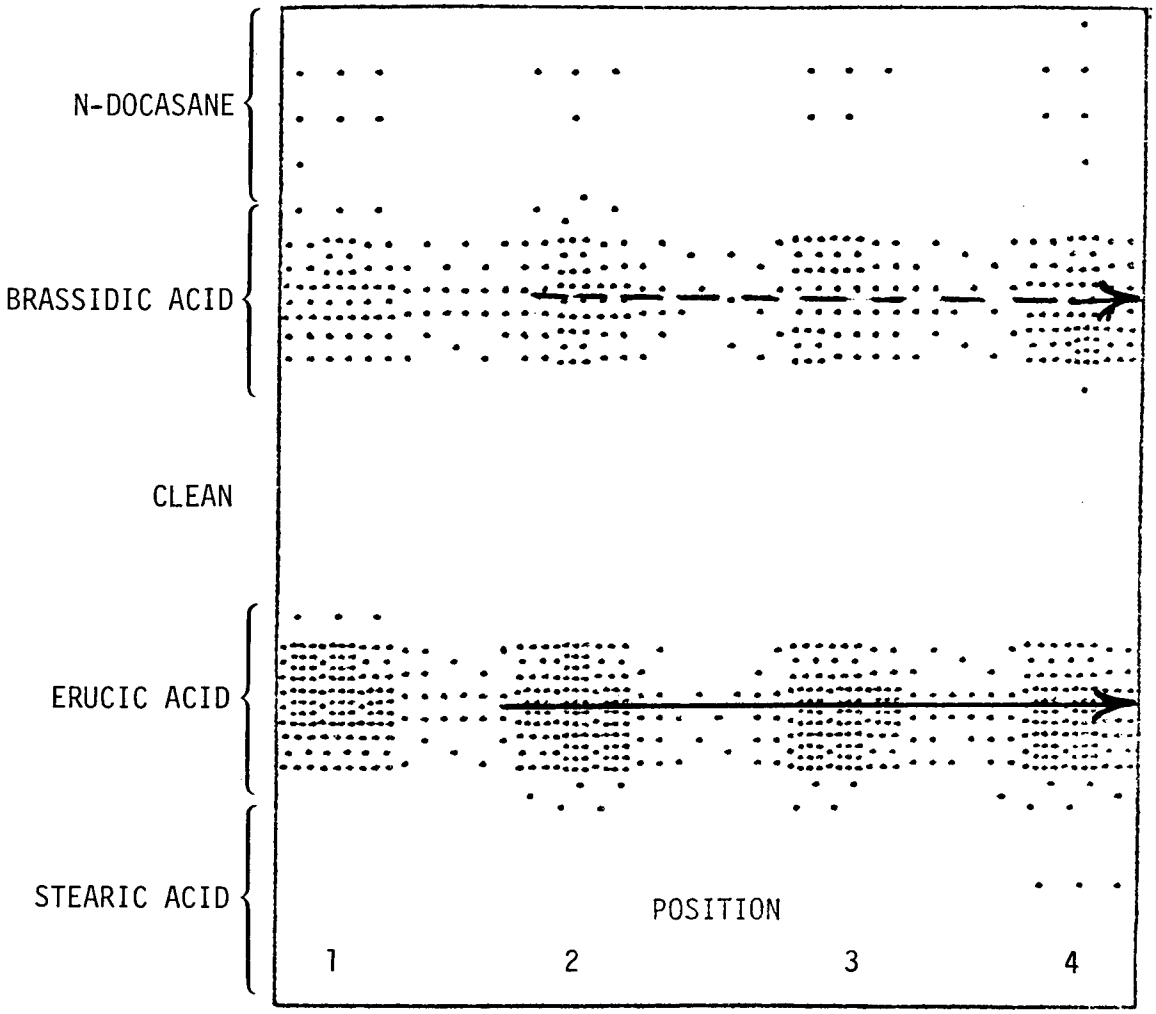

Fig. 3 A Δ plot ($165 < \Delta < 163$) for a panel that was contaminated in four regions but left clean in the center region.

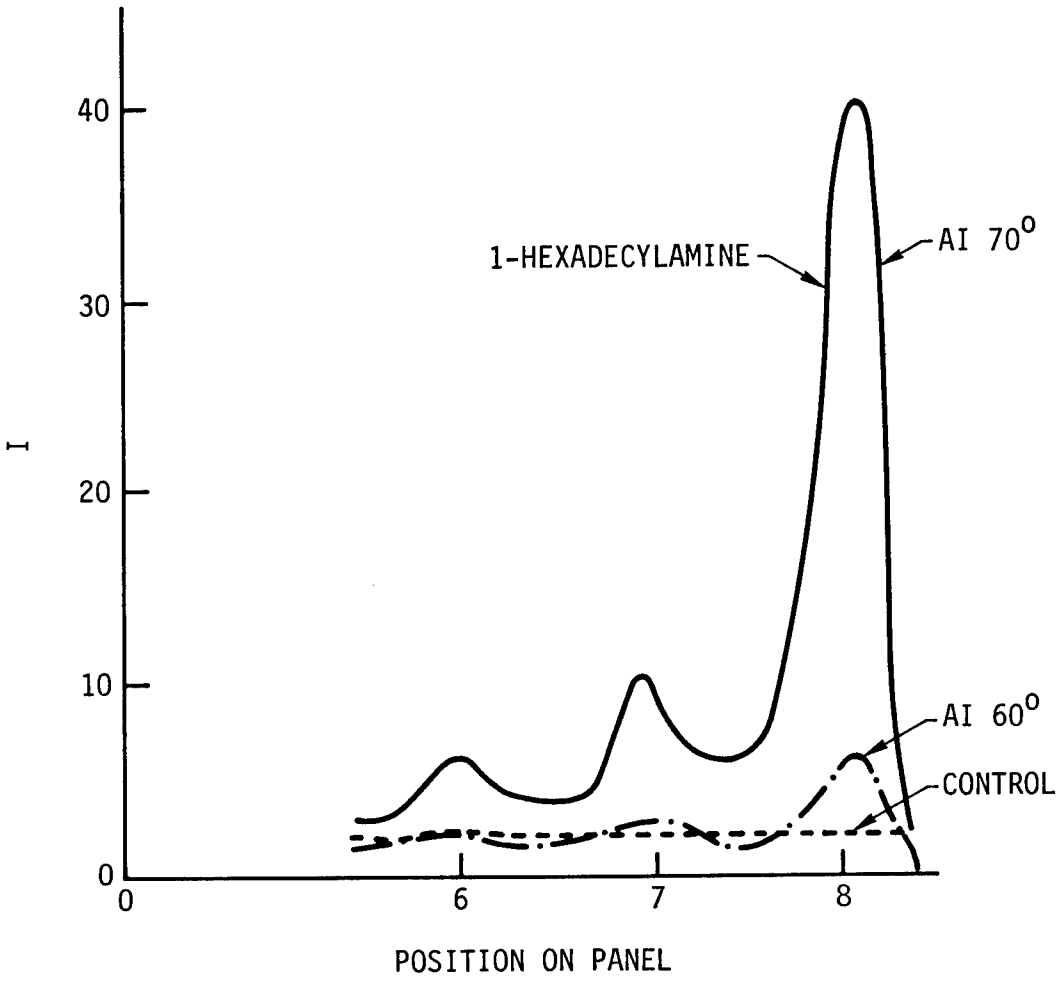

Fig. 4 Plot of I vs position on Al panel contaminated with 1-Hexadecylamine. (see Fig. 5)

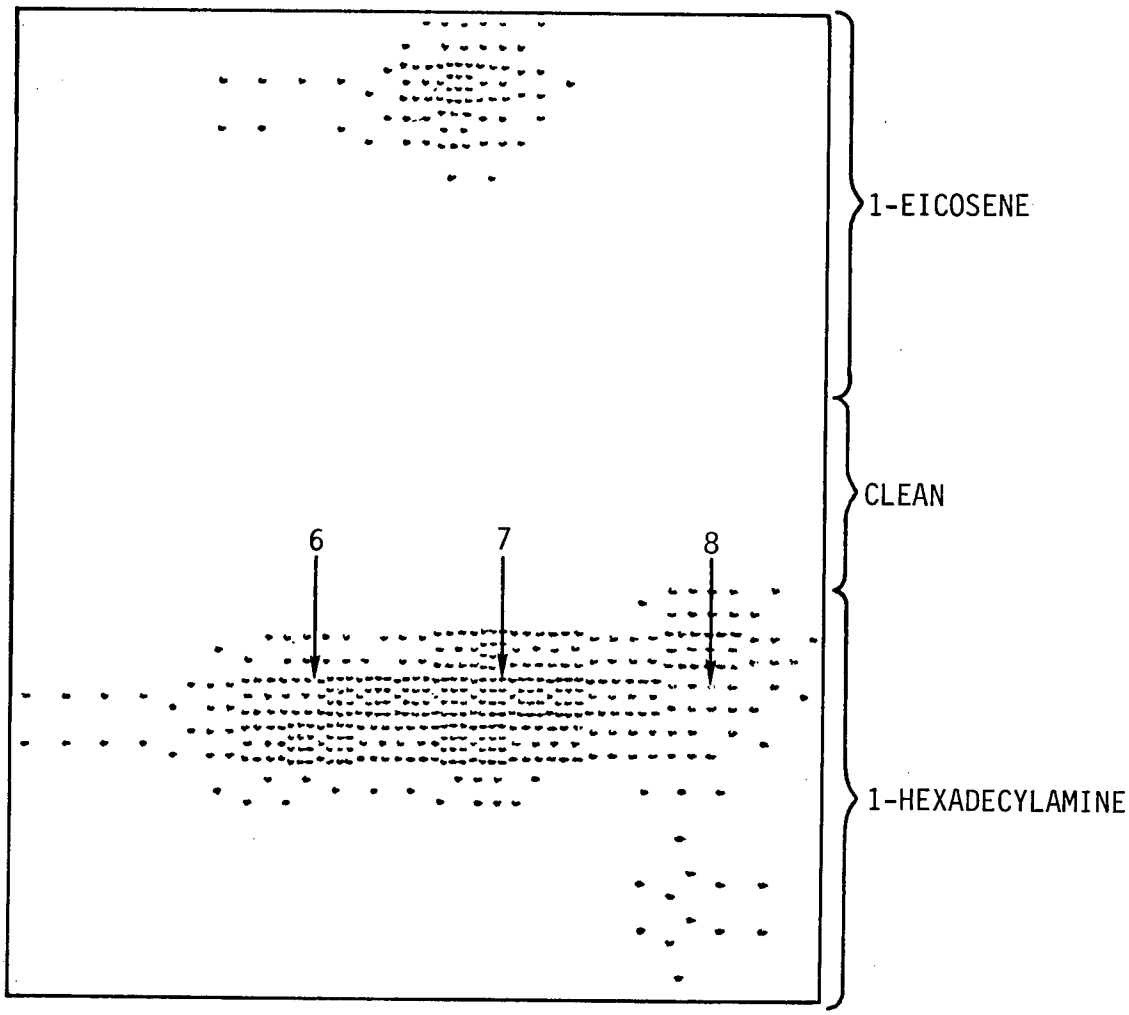

Fig. 5 Computer plot of $162 < \Delta < 160$ for contamination.
Top: 1-Eicosene; Middle: Clean; Bottom 1-Hexadecylamine.

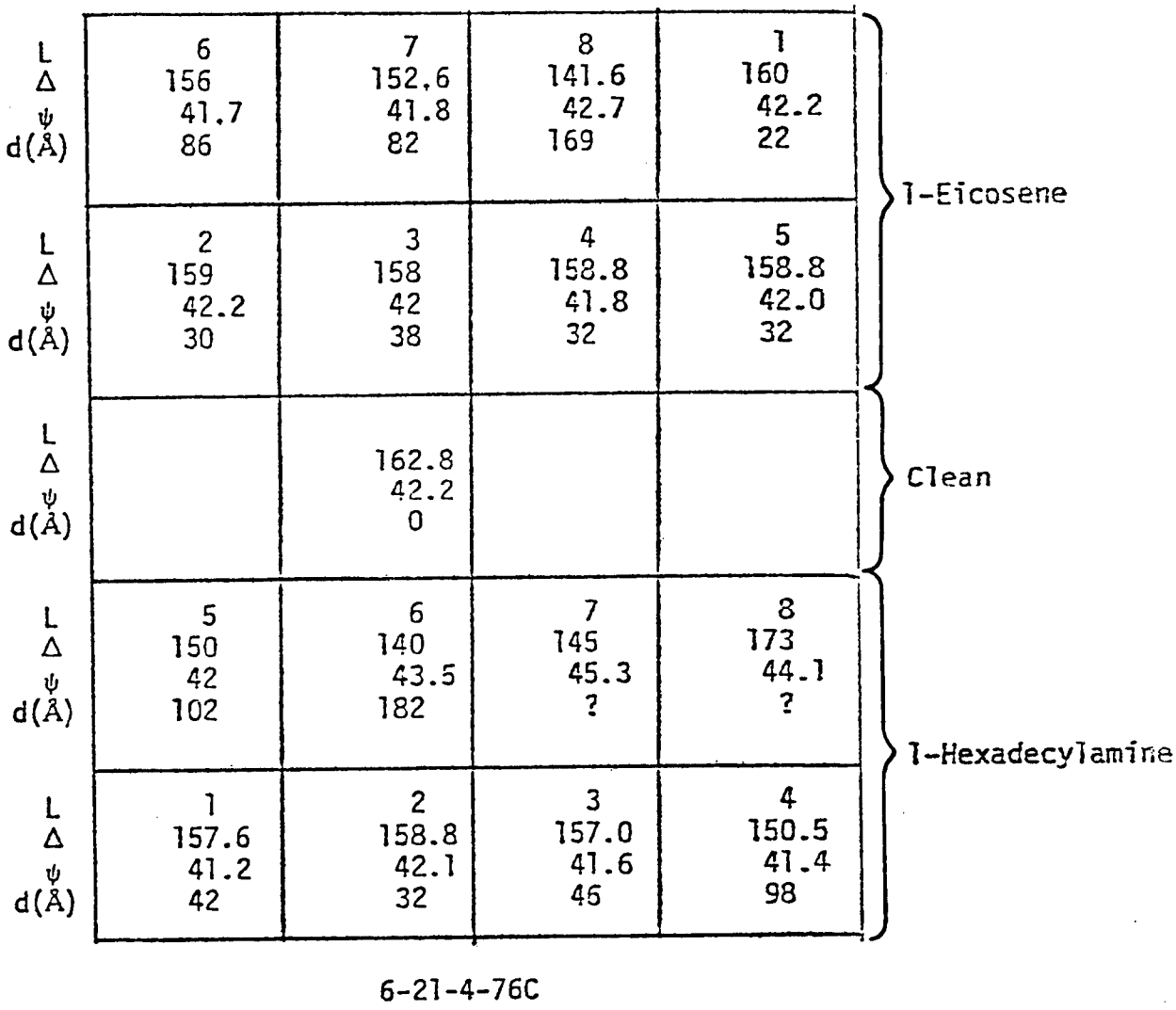

Fig. 6 Regions on a phosphoric acid anodized Al 7075-T6 panel with various contamination levels. Top: 1-Eicosene; Middle: Clean; Bottom: 1-Hexadecylamine.

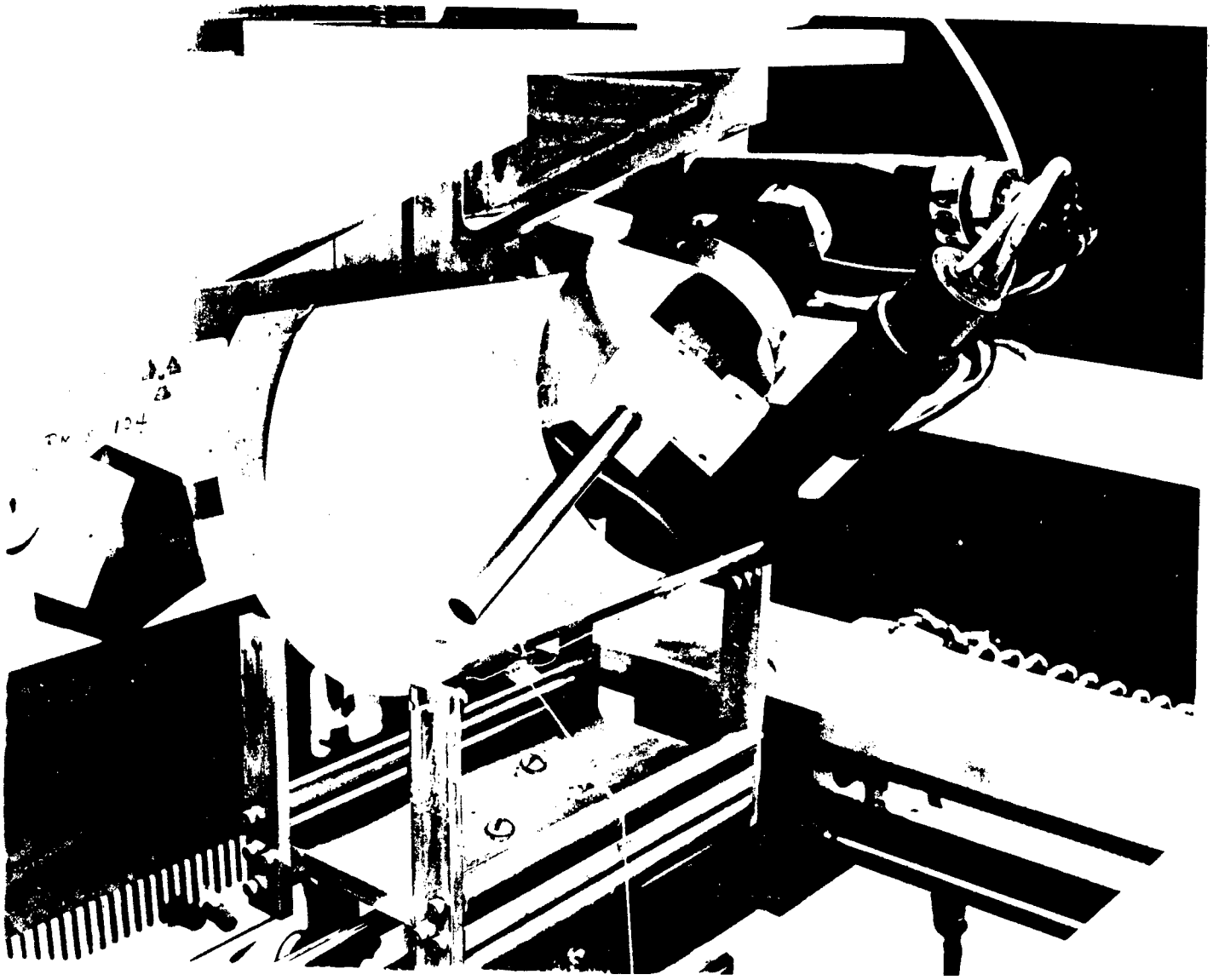

Fig. 7 Photograph of the mechanism for mapping curved panels.

ellipsometer compensator prism. The aluminum (silver colored) block at the right holds the analyzer prism. The photomultiplier tubes were positioned to receive light from the orthogonal beams from the beam splitting analyzer. The laser is on the shelf at the top and the beam is directed through the polarizer and compensator on to the metal surface via mirrors (not seen at the left). The spot on the panel just below the end of the receiver tube has been polished for alignment purposes.

SECTION III

EXPERIMENTAL RESULTS

A Effect of Contamination on Surface Properties and Bond Quality

1. Human Contamination

Twelve lap shear specimens were prepared by the standard PAA surface treatment and analyzed with respect to Δ, ψ, SPD and θH_2O. A consistent set of surface properties are reported in Table 2 as "Initial Preparation". The average values of Δ and ψ are $162 \pm 5^{\circ}$ and $36.4 \pm 0.8^{\circ}$, respectively. These values correspond to about 3400Å of anodic hydroxide. The SPD value of 0.18 ± 0.02 volts corresponds to about 3400Å of aged PAA anodized Al 7075-T6 (see Fig. 11, AFML-TR-77-42). The water contact angles average $6 \pm 1^{\circ}$ for wettable hydroxide.

Sample 1-6-6-78 was not contaminated and was used as a control. Five of the other samples were contaminated with materials that we often found in a factory bonding facility, i.e. exhaled cigarette smoke, cigarette smoke, fingerprints, soda pop (Coca Cola) and coffee. The surface properties, measured by ellipsometry, SPD and water contact angle, are reported for the contaminated specimens at the bottom of Table 2. Although the smoke, and fingerprints are detected by all of the tools, the lap shear strength is essentially the same as for the control (5.0 Ksi) and the estimated percent interfacial failure is 10-15. The soda pop and the coffee were poured on to the surface (as expected in a real accident) leaving a thick layer after drying. The water contact angle is zero as might be expected and the film is easily detected by ellipsometry and SPD. The lap shear strength is severely decreased and the percent interfacial failure severely increased as might be expected.

TABLE 2

Effect of Human Contamination on Bond Strength: Surface Properties, Contamination and Lap Shear Strength for PAA Al 7075-T6

Initial Preparation

Sample	Δ (deg)	ψ (deg)	SPD (volts)	θH_2O (deg)
1-6-6-78	155.0	37.0	0.21	6
2-6-6-78	158.2	35.0	0.22	7
3-6-6-78	155.6	34.2	0.20	5
4-6-6-78	167.0	37.2	0.22	6
5-6-6-78	159.6	36.8	0.20	8
6-6-6-78	167.0	35.8	0.17	4
7-7-6-78	168.0	36.7	0.14	6
8-7-6-78	166.4	35.8	0.15	8
9-7-6-78	154.2	36.7	0.15	8
10-7-6-78	159.4	37.2	0.17	8
11-7-6-78	170.0	37.7	0.20	7
12-7-6-78	169.8	36.6	0.19	4
Average	162±5	36.4±0.8	0.18±0.02	6±1

After Contamination

Contamination	Sample	Δ (deg)	ψ (deg)	Estimated Thickness Å	SPD (volts)	θH_2O (deg)	Lap Shear Strength (Ksi)	% Interfacial Failure
Control	1-6-6-78	155	37.0	0	0.21	6	5.00	15
Exhale Smoke	3-6-6-78	140	32.9	200	0.50	5	5.20	10
Cigarette Smoke	3-6-6-78	96	60.0	700	0.65	12	5.00	10
Fingerprint	6-6-6-78	134	37.8	300	0.41	20	5.00	15
Soda Pop (Coke)	5-6-6-78	159	24.9	Thick	0.76	0	3.40	70
Coffee	4-6-6-78	154	20.7	Thick	0.68	0	1.35	95

Table 3 gives results for a similar contamination experiment but for the durability wedge test. As for the lap shear specimens, all types of contamination were detected (i.e. parameters deviated significantly from control values). However, the contamination caused a significant degradation (increase in crack growth) and/or percent interfacial failure.

Table 4 gives results for controlled contamination by coughing on the wedge specimens. In the case of strong and extreme cough, mucous was sprayed on the specimen. This type of contamination is detected by ellipsometry and SPD, but not by water contact angle. The strong and extreme cough considerably degraded bond durability as noted by the increase in crack growth and percent interfacial failure.

Although soda pop is very unlikely to be a contaminant other than a direct spill, Table 5 gives results for varying thickness by diluting the coke in water. For film thickness between 0-700Å, the contamination is easily detected by ellipsometry and SPD, but not by water contact angle. For these thin films, the lap shear strength is only slightly decreased.

TABLE 3

Effect of Human Contamination on Durability:
Surface Properties, Contamination and Wedge Tests
for PAA Al 7075-T6

Initial Preparation

Sample	Δ (deg)	ψ (deg)	SPD (volts)	θH_2O (deg)
1-6-6-78	181.4	39.3	0.00	4
2-6-6-78	178.5	40.3	0.04	4
3-6-6-78	187.4	41.2	0.20	3
4-6-6-78	181.9	40.2	0.11	6
5-6-6-78	159.1	38.6	0.28	9
6-6-6-78	180.4	39.2	0.05	4
10-23-5-78	181.0	39.9	0.20	4
8-23-5-78	180.1	40.2	0.19	6
9-23-5-78	181.1	41.1	0.17	6
10-6-6-78	180.4	39.2	0.05	4
11-6-6-78	175.1	38.2	0.23	10
12-6-6-78	177.0	38.1	0.35	9

After Contamination

Contamination		Δ (deg)	ψ (deg)	Estimated Thickness Å	SPD (volts)	θH_2O (deg)	Crack Growth inches 1 hr	Crack Growth inches 24 hr	% Interfacial Failure
Control	10-6-6-78	180.4	39.2	0	0.05	4	0.06	0.50	5
Soda Pop	3-6-6-78	161.5	57.4	Thick	0.70	7	0.06	0.43	40*
Exhaled Smoke	5-6-6-78	161.6	35.8	0	0.18	15	0.03	0.69	50*
Coffee	2-6-6-78	260.1	59.0	Thick	0.72	5	0.31	0.75	30*
Finger print	6-6-6-78	80.6	37.6	1000	0.55	40	0.03	0.81	70
Cigarette Smoke	4-6-6-78	114.5	38.0	800	0.44	11	0.19	1.00	85*

* Interfacial failure at both interfaces although contamination was originally at only one interface.

TABLE 4
Effect of Extreme Cough (Spit) on Durability:
Surface Properties, Contamination and Wedge Test
for PAA Al 7075-T6

Initial Preparation

Sample	Δ (deg)	ψ (deg)	SPD (volts)	θH_2O (deg)
3-24-5-78	171.1	37.8	0.17	8
4-24-5-78	182.4	40.7	0.22	6
5-24-5-78	177.5	38.3	0.21	3
11-23-5-78	179.9	39.6	0.20	7
12-23-5-78	179.2	40.5	0.15	6
13-23-5-78	187.0	40.0	0.15	5

After Contamination

Contamination		Δ (deg)	ψ (deg)	Estimated Thickness Å	SPD (volts)	θH_2O (deg)	Crack Growth inches 1 hr	Crack Growth inches 24 hr	% Interfacial Failure
Control				0	0.20	6	0.06	0.50	5
Cough	5-24-5-78	126	33.3	600	0.36	0	0.03	0.50	10
Stronger Cough	4-24-5-78	149	31.1	4000	0.35	0	0.06	0.62	45
Extreme Cough	3-24-5-78	-	21.7	Thick	0.57	0	1.25	2.00	95

TABLE 5
Effect of Soda Pop (Coca Cola) Contamination:
Surface Properties, Contamination and Lap Shear Strength
for PAA Al 7075-T6

Initial Preparation

Sample	Δ (deg)	ψ (deg)	SPD (volts)	θH_2O (deg)
1-10-5-78	183.4	34.7	0.23	6
5-10-5-78	188.8	34.7	0.22	8
3-10-5-78	182.9	36.6	0.19	9
2-10-5-78	187.8	39.6	0.19	5
6-10-5-78	182.7	36.1	0.22	8
4-10-5-78	174.8	33.9	0.12	10
7-10-5-78	183.6	34.8	0.21	3
8-10-5-78	175.9	37.7	0.22	6
9-10-5-78	187.6	36.9	0.18	9
10-10-5-78	177.3	32.2	0.19	8
11-10-5-78	181.8	37.7	0.21	7
12-10-5-78	189.9	39.0	0.23	4

After Contamination

Contamination	Sample	Δ (deg)	ψ (deg)	Estimated Thickness Å	SPD (volts)	θH_2O (deg)	Lap Shear Strength (Ksi)
Control	1-20-5-78	183.4	34.7	0	0.23	6	5.43
Coke	5-10-5-78	102.1	30.5	100	0.36	0	5.25
Coke	3-10-5-78	135.8	32.2	235	0.36	0	5.40
Coke	2-10-5-78	108.8	39.9	400	0.51	0	---
Coke	6-10-5-78	92.2	41.0	455	0.29	0	5.25
Coke	4-10-5-78	43.3	41.0	700	0.58	0	4.96

2. Mechanical Damage

Table 6 gives surface properties before and after mechanical damage to the hydroxide film. Various levels of cotton glove smudge pressure, change Δ, SPD and θH_2O beyond the control values and cause only slight decrease in lap shear strength. This is in contrast to severe degradation in bond durability as measured by the wedge test. Although the ellipsometric values are interpreted as effective contamination thickness (0-65Å), they can also be interpreted as a change in optical properties of uncomtaminated hydroxide caused by increased density from crushing. Much larger thickness organic contamination has little, if any, effect on lap shear or wedge test results. Consequently, we are still inclined to attribute bond degradation to closing of the pores and fracture of the hydroxide by the cotton glove smudge.

3. Process Errors

A set of lap shear specimens were anodized for various lengths of time between 0 and 25 minutes to simulate a process error. The deviation of the ellipsometric parameters and contact angle from the control values (in Table 7) indicate easy detection of the process error for anodize times less than 20 minutes. Only the non-anodized sample deviates significantly in SPD values from the control. The control specimens (number 5), anodized 20 minutes, have normal cohesive failure and lap shear strength. Number 6 was contaminated during mapping, with resulting 4.0 Ksi bond strength. The other specimens have lower lap shear strength and higher interfacial failure.

Table 8 gives results for the simulation of another process error, viz. incorrect anodic voltage. The surface properties are reported as a function of voltage, 0, 2, 4, 6, 8, and 10 volts, and 20 minutes under the heading "Initial Preparation" in Table 8. The estimated hydroxide film thickness increases from about 300Å at 0 V to about 3400Å at 10 V. SPD at 0 V is 0.3 V and varies between about 0.1 and 0.25 for the other voltages. The water contact angle is about 130° for 0 V, but the surface is essentially wettable for 2-10 V. The lap shear strength is approximately independent of voltage, corresponding approximately to that for the control (5 Ksi) and failure is about 95% cohesive and 5% interfacial.

TABLE 6

Effect of Cotton Glove Smudge:
Surface Properties, Mechanical Damage and Lap Shear Strength
for PAA Al 7075-T6

Initial Preparation

Sample	Δ (deg)	ψ (deg)	SPD (volts)	θH_2O (deg)
1-3-5-79	184.5	39.3	0.08	4
2-3-5-78	183.1	39.7	0.17	5
3-3-5-78	182.2	39.9	0.07	9
4-3-5-78	183.6	40.0	0.08	9
5-3-5-78	184.3	40.9	0.08	5
6-3-5-78	185.8	39.8	0.08	8
7-4-5-78	180.3	41.5	0.22	4
8-4-5-78	183.7	40.9	0.27	5
9-4-5-78	180.3	41.7	0.22	8
10-4-5-78	182.3	38.4	0.22	8
11-4-5-78	185.6	42.1	0.21	5
12-4-5-78	181.8	38.2	0.22	8

After Mechanical Damage

Contamination	Sample	Δ (deg)	ψ (deg)	Estimated Thickness (Å)	SPD (volts)	θH_2O (deg)	Lap Shear Strength (Ksi)
Control	7-4-5-78	180.3	41.5	0	0.22	4	5.55
Cotton Glove	8-4-5-78	202.8		19	0.19	15	6.20
Cotton Glove	9-4-5-78	212.0		32	0.07	17	5.91
Cotton Glove	10-4-5-78	228.8		46	0.34	23	5.80
Cotton Glove	11-4-5-78	239.5		54	0.38	27	5.20
Cotton Glove	12-4-5-78	246.8		65	0.40	27	5.18

TABLE 7

Effect of Process Error (Anodize Time) on Bond Strength:
Surface Properties and Lap Shear Strength for
PAA Al 7075-T6

Initial Preparation

Sample	Δ (deg)	ψ (deg)	SPD (volts)	θH_2O (deg)
1-30-5-78	73.1	34.2	0.72	90
2-30-5-78	223.1	24.7	0.22	29
3-30-5-78	101.6	33.2	0.18	25
4-30-5-78	110.6	43.4	0.22	28
5-30-5-78	179.0	36.1	0.21	3
6-30-5-78	166.4	39.6	0.23	6
7-6-5-78	163.6	37.9	0.18	4
8-8-6-78	159.9	35.3	0.17	5
9-8-7-78	171.7	36.9	0.17	7
10-8-6-78	173.4	35.8	0.20	6
11-8-6-78	176.6	31.6	0.11	4
12-8-6-78	103.2	36.8	0.12	4

Lap Shear Results

	Anodize Time (min)	Estimated Hydroxide Thickness Å	Lap Shear Strength (Ksi)	% Interfacial Failure
1-30-5-78	0	100	3.40	60
2-30-5-78	5	2000	4.50	30
3-30-5-78	10	3000	4.10	20
4-30-5-78	15	3400	4.30	10
5-30-5-78	20	3500	4.80	10
6-30-5-78	25	3500	4.00*	10

* Contaminated during mapping.

TABLE 8

Effect of Process Error (Anodic Voltage) on Bond Strength:
Surface Properties and Lap Shear Strength for
PAA Al 7075-T6

Initial Preparation

Sample Voltage	Time (min)	Δ (deg)	ψ (deg)	SPD (volts)	θH_2O (deg)
0	20	80	33.8	0.30	138
2	20	86	37.6	0.09	5
4	20	128	49.2	0.17	8
6	20	186	44.5	0.14	6
8	20	181	40.0	0.12	4
10	20	168	37.5	0.25	3
1-6-7-78		158	37.4	0.22	3
2-6-7-78		164	35.2	0.21	4
3-6-7-78		165	31.0	0.23	6
4-6-7-78		164	38.1	0.21	5
5-6-7-78		165	36.9	0.24	4
6-6-7-78		152	34.0	0.27	3

Lap Shear Results

Anodic Voltage	Estimated Hydroxide Thickness (Å)	Lap Shear Strength (Ksi)	% Interfacial Failure
0	300	5.00	10
2	800	4.40	5
2	800	5.25	5
2	800	4.40	5
4	1400	4.95	5
4	1400	4.90	5
4	1400	4.77	5
6	2400	4.75	5
6	2400	4.95	5
6	2400	5.10	5
8	2900	4.90	5
8	2900	4.60	5
8	2900	4.30	5
10	3400	4.90	5

It was a surprise that exposure to phosphoric acid for 20 minutes without anodizing yielded the same lap shear strength as anodized samples. To check this, a set of nine samples were exposed to the phosphoric acid anodize bath for 20 minutes, then bonded to standard PAA samples and tested. Table 9 reveals the average lap shear strengsh (5.0±0.1 Ksi) is even higher than the average (4.8±0.2 Ksi) for the anodized samples. One sample was degreased, but not exposed to acid or anodized. The results in Table 9 indicate the expected lower lap shear strength (2.5 Ksi) and increased interfacial failure (~40%). A set of five wedge test specimens were exposed to the phosphoric acid bath for 20 minutes without anodizing. Table 9 reveals that although lap shear strength is equivalent to anodized samples, the endurance in humid atmosphere is very poor. PAA crack growth is normally about 0.2"/24 hrs with about 10% interfacial failure, without anodizing the crack growth averaged 2.2"/24 hrs.

The effect of anodic voltage on the wedge test is given in Table 10. Six samples were given the standard PAA treatment and yielded normal surface properties (Initial Preparation, Table 10). Six more samples were anodized at 0, 2, 4, 6, 8 and 10 volts. The wedge test results in Table 10 reveal that for potentials greater than 4 volts, the crack growth drops to a constant value of about 0.2"/24 hrs and the interfacial failure drops to 10-15%. Below 4 volts (<1000Å), the treatment fails the durability test.

TABLE 9

Lap Shear and Wedge Endurance Tests for Al 7075-T6 After Degreasing and Exposure to Phosphoric Acid for 20 min (No Anodic Voltage)

Time in H_3PO_4 (min)	Lap Shear Strength (Ksi)	% Inter-Facial Failure	Wedge Test inches 1 hr	Wedge Test inches 24 hr
20	5.10	5	1.1	3.5
20	5.15	4	1.0	2.2
20	4.85	9	0.7	2.2
20	5.10	5	0.7	2.0
20	5.00	6	0.3	1.0
20	4.70	10		
0	2.55	40		

TABLE 10

Effect of Anodic Voltage on Surface Properties and Wedge Endurance Test for PAA Al 7075-T6

Initial Preparation

Sample	Anodic Volts	Δ (deg)	ψ (deg)	SPD (volts)	θH_2O (deg)
1	10	169	35.9	0.19	4
2	10	164	34.7	0.20	0
3	10	162	36.1	0.21	7
4	10	164	36.4	0.18	3
5	10	171	39.9	0.17	5
6	10	168	34.6	0.19	6
7	0	94	36.9	0.32	100
8	2	96	37.1	0.3	33
9	4	91	42.9	0.38	3
10	6	167	47.9	0.21	6
11	8	177	45.1	0.18	4
12	10	186	39.7	0.16	4

Wedge Test Results

		Estimated Hydroxide Thickness (Å)	Crack Growth Inches		% Interfacial Failure
			1 hr	24 hrs	
7-1	0	100	1.5	1.50	100
8-2	2	600	1.0	1.00	100
9-3	4	1000	0.8	0.25	15
10-4	6	1600	0.5	0.20	15
11-5	8	3000	0.5	0.25	13
12-6	10	3200	0.2	0.20	10

4. Smog Simulation

Three constituents of smog (stearic acid, hexadecylamine and erucic acid) were dissolved in pentane and sprayed near PAA samples to simulate smog aerosol. The samples were then bonded and tested to correlate smog constituent thickness with lap shear bond strength and wedge crack extensions. Table 11 gives the surface properties for samples prepared for contamination with stearic acid. Note that in this case, the ellipsometric measurements were performed at 60^{o} angle of incidence for comparison with the automated ellipsometer. The SPD and water contact angles are slightly high, 0.3 vs the usual 0.2 volts, and 10^{o} vs the usual 7^{o}, respectively.

The contamination was put on extremely thick for some of these samples, as it had been observed that thin films had little effect on bond strength or durability. Table 11 reveals that, although the surface properties are dramatically affected (easily detected), the lap shear strength averages 5.0 Ksi.

Table 12 gives wedge test results for stearic acid contaminated samples. Stearic acid films ~1300Å have a large effect on the water contact angle, but little effect on crack extension. However, there is a notable increase in percent interfacial failure for the heavier contamination. This indicates that the contamination does affect bond durability, but the wedge test is not of sufficient severity to reveal it by crack extension.

To determine how tolerant the H_3PO_4 anodize surface treatment is to stearic acid contamination, lap shear bond tests were conducted on Al 7075-T6 with very thick (up to 70,000Å) films. Seven lap shear test specimens were prepared. Contamination was deposited by an aerosol spray technique. Films of different thicknesses were achieved by varying mixture ratios of stearic acid saturated pentane and MEK. Although the resulting films were not perfectly uniform in thickness, the calculated (by weight difference) thickness should give a reasonable average value.

The seven contaminated specimens were mated to clean specimens using FM-73 as the adhesive. The samples, including a control, were then cured in the usual manner. After curing, it was noted that the stearic acid films were depleted in the region just next to the lap joint (see Fig. 8). The area

TABLE 11

Effect of Smog Constituent (Stearic Acid): Surface Properties and Lap Shear Strength for PAA Al 7075-T6

Initial Preparation

Sample	Angle of Incidence 60 Δ (deg)	ψ (deg)	SPD (volts)	θH_2O (deg)
1	155	41.5	0.27	10
2	154	41.0	0.27	13
3	155	40.6	0.21	9
4	153	40.6	0.25	6
5	154	40.6	0.25	9
6	155	40.2	0.24	6
7	163	41.2	0.33	10
8	161	40.8	0.33	14
9	162	40.8	0.35	9
10	162	41.0	0.36	8
11	159	40.5	0.20	12
12	160	40.7	0.26	7

After Contamination

	Δ	ψ	Estimated Contamination Thickness (Å)	SPD	θH_2O (deg)	Lap Shear Strength (Ksi)
6	155	40.2	0	0.24	6	5.44
12	149	40.9	80	0.76	21	4.84
11	144	42.2	100	0.72	67	4.54
10	117	50.2	1000	0.66	80	4.74
9	196	62.0	2000	0.59	90	4.84
5	161	47.2	3000	0.57	120	5.34

TABLE 12
The Effect of Stearic Acid Contamination on Surface Properties and Wedge Tests

Sample	Ellipsometry λ=6328Å, AI=70 Δ (deg)	ψ (deg)	Estimated Stearic Acid Thickness (Å)	Water Contact Angle (deg)	Wedge Test Extension (in/hr)	(in/24hr)	Est % Interfacial Failure
Avg. 12 samples before contamination	175.0	43.4	0	7			
After Contamination							
2-7-1	161.6	45.3	0	20	0.12	0.20	1
2.7-10	164.8	33.7	175	115	0.04	0.20	10
2-7-12	194.4	41.0	150	119	0.12	0.16	5
2-7-8	188.6	38.3	1300	124	0.12	0.20	30
2-7-6	113.2	29.2	1300	157	0.12	0.22	60
2-7-3	196.4	38.4	1250	161	0.16	0.24	5

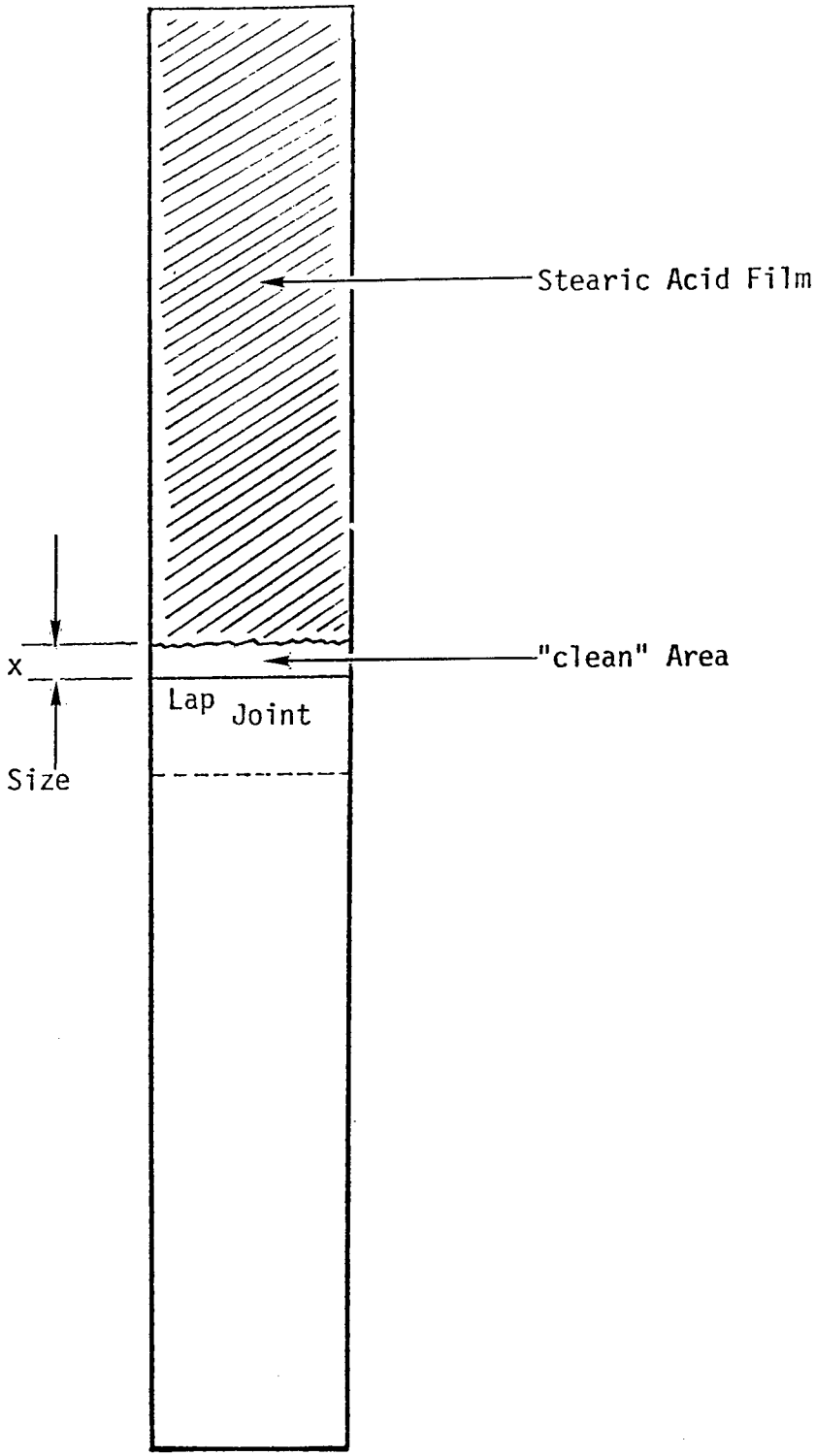

Fig. 8 Diagram of depleted contamination after curing.

almost looked clean, but some interference colors could be seen indicating a thin film. It was possible to measure this area on sample #3 using a manual ellipsometer. Delta and psi were 107^{o} and 39.2^{o}, respectively, indicating a film thickness of about 700Å. The size of this depleted area is tabulated in Table 13 for the various samples, and a rough correlation between the thickness of the stearic acid film and the size of the area seems to be indicated. This result suggests that the FM-73 is absorbing some of the stearic acid. To investigate this hypotheses, the following experiment was carried out. Three samples were prepared. Number 1 was a 3"x3" Al foil with a thick layer of sprayed stearic acid. Number 2 was a 3"x3" Al foil with a 2½"x2½" piece of FM-73 adhesive. Number 3 was a duplicate of number 2 with a thick layer of stearic acid sprayed on the FM-73. The samples were weighed at various stages of preparation. All three samples were then placed in an oven for the standard curing cycle for FM-73. The samples were weighed again after cooling, then cleaned in pentane and weighed a final time. The results are tabulated in Table 14.

Sample 1 lost approximately 11 mg in the cure cycle, indicating that the stearic acid evaporated at temperature. Cleaning in pentane dissolved the remaining stearic acid and the sample returned to the starting weight.

Sample 2 lost approximately 11 mg in the cure cycle, indicating a loss of some components of FM-73. Cleaning in pentane did not appreciably change the weight.

Sample 3 only lost about 2 mg. Cleaning in pentane did not appreciably change the weight, indicating that no stearic acid was on the surface. This result seems to confirm the hypothesis that the FM-73 is absorbing the stearic acid. Assuming that Sample 3 should lose the same proportional amount of FM-73 as Sample 2, then the ending weight (ignoring possible loss of stearic acid) would be 1.06736 gm. The actual end weight indicates that 0.01294 gm of the available stearic acid was absorbed by the FM-73 adhesive, allowing approximately 1 mg of stearic acid to evaporate.

These results are consistent with Table 13, the FM-73 is absorbing stearic acid from regions x adjacent to the adhesive.

Table 15 summarizes the characterization of the specimens and the resulting lap shear bond strengths. Bond strength is not degraded and there is no appreciable interfacial failure in any of the samples.

TABLE 13

Distance x vs Contamination Thickness

Sample No.	Film Thickness (Å)	x (cm)
1	0	control
3	4100	0.38
7	6100	0.23
8	7700	0.20
6	17000	0.10
5	26300	0.08
4	69900	0.10

TABLE 14
Experiment to see if FM-73 Absorbs Stearic Acid

Stage	Weight (gms)	Weight Change (gms)	Weight (gms)	Weight Change (gms)	Weight (gms)	Weight Change (gms)
1 - Clean Al	0.26191		0.26194		0.26350	
2 - Al + Stearic Acid	0.27635	0.01444				
3 - Al + FM-73			0.85303	0.59109	1.06815	0.80465
4 - Al + FM-73 + Stearic Acid					1.08210	0.1395
5 - After FM-73 Cure Cycle	0.26575	-0.01060	0.84220	-0.01083	1.08030	-0.00180
6 - After Cleaning in Pentane	0.26190	-0.00385	0.84225	0.0005	1.08024	-0.0006

TABLE 15

Effect of Controlled Contamination of H_3PO_4
Anodized Al 7075-T6 with Stearic Acid

Sample	Weight Change (gm)	Calc. Thickness (Å)	θH_2O (deg)	Lap Shear Bond Strength (Ksi)	Est. % Adhesive Failure
Control	-	-	8	5.70	0
1	.00041	1670	102	5.60	0
3	.00101	4116	114	6.10	0
4	.01717	69900	115	5.60	0
5	.00643	26300	100	5.70	0
6	.00422	17300	102	2.64	0
7	.00151	6100	107	5.54	0
8	.00190	7700	105	5.50	0

Table 16 gives the effect of another smog constituent (hexadecylamine) on the lap shear strength. Thick films dramatically affect $\theta H_2 0$, but have little effect on the lap shear strengths (average 5.4 Ksi), and cause essentially zero interfacial failure.

Table 18 gives results for tests to check for absorption of hexadecylamine in FM-73 adhesive. Three aluminum foil samples (3"x3") were prepared, #1 with a thick layer of contaminant, but no adhesive, #2 with adhesive, but no contaminant, and #3 with both. The samples were put through the same cure cycle and weighed at the appropriate times. The last steps, hexane cleaning, is to remove any contaminant that has not been absorbed by the adhesive. #1 lost the 15 mg of contaminant during the cure cycle, returning to its original weight, indicating that the hexadecylamine exaporates at or below 240°F. #2 lost 2.5 mg during the cure cycle and gained about 1 mg when cleaned in hexane. #3 lost 4.5 mg during the cure cycle and gained about 2 mg when cleaned in hexane. These results indicate that about 8 mg of hexadecylamine was absorbed by the FM-73.

Table 19 reveals that another smog constituent (erucic acid) behaves as the other constituents, a large effect on $\theta H_2 0$, but no effect on lap shear strength or interfacial failure.

5. Factory Contaminants

Table 20 gives results for contaminants with machine lubricating oil. For films 100Å and much thicker, no effect is observed on the lap shear strength or interfacial failure, although the water contact angle increases. Table 21 also indicates no effect on crack growth in the wedge test, although the thicker films cause $\theta H_2 0$ to increase to 100°.

Table 22 reveals that the machine oil is absorbed strongly by the adhesive. The effect of another factory contaminant (silicone or vacuum grease) is given in Table 23. In this case, relatively thin films dramatically degrade the lap shear strength and increase the interfacial failure. Table 24 reveals that silicone grease is not absorbed by the adhesive.

TABLE 16

Effect of Smog constituent (Hexadecylamine): Surface Properties and Lap Shear Strength for PAA Al 7075-T6

Initial Preparation

Sample	Δ (deg)	ψ (deg)	θH_2O (deg)
5	185	42.4	3
13	183	40.0	2
14	180	37.4	7
15	178	39.3	7
17	186	41.9	5
18	185	41.4	10

After Contamination

	Δ	ψ	Estimated Thickness (Å)	θH_2O	Lap Shear Strength (Ksi)	% Interfacial Failure
13	183	40.0	0	2	5.80	0
14	115	35.2	650	128	4.76	1
5	106	40.8	800	118	5.78	2
17	95	41.5	900	113	5.00	0
15	194	13.9	Large	74	6.15	0
18	130	30.7	Large	135	4.79	1

TABLE 17

Effect of Smog Constituent (Hexadecylamine) and Durability:
Surface Properties, Contamination and Wedge Tests
for PAA Al 7075-T6

Initial Preparation

Sample	Δ (deg)	ψ (deg)	SPD (volts)	θH_2O (deg)
13-5-3-78	176	36.1	0.26	5
16-5-3-78	174	38.0	0.1	4
9-5-3-78	175	40.1	0.15	5
17-5-3-78	172	36.2	0.19	4
15-5-3-78	174	36.9	0.26	9
14-5-3-78	176	37.5	0.24	7
12-5-3-78	169	36.0	0.23	7
8-5-3-78	169	36.1	0.22	6
9-5-3-78	169	35.7	0.22	3
10-5-3-78	151	35.6	0.21	5
11-5-3-78	163	36.0	0.23	7
12-5-3-78	171	38.3	0.23	8

After Contamination

	Δ	ψ	Estimated Thickness (Å)	SPD	θH_2O	Wedge Test Crack Growth Inches 1 hr	24 hrs
13	176	36.1	0	0.26	5	0.04	0.27
16	326	66.0	Thick	0.93	--	0.04	0.27
9	82	45.9	Thick	0.92	122	0.03	0.16
17	94	42.6	Thick	0.87	68	0.05	0.20
15	310	47.4	Thick	0.92	130	0.18	0.23
14	47	70.1	Thick	0.93	85	0.05	0.23

TABLE 18

Experiment to see if FM-73 Absorbs 1-Hexadecylamine

Stage	Sample #1		Sample #2		Sample ##	
	Weight (gms)	Weight Change (gms)	Weight (gms)	Weight Change (gms)	Weight (gms)	Weight Change (gms)
1 - Clean Al	0.26343		0.25956		0.25895	
2 - Al + Hexadecylamine	0.27842	0.01499				
3 - Al + FM-73			0.85854	0.59898	0.82542	0.56647
4 - Al + FM-73 + Hexadecylamine					0.83545	0.01003
5 - After FM-73 Cure Cycle	0.26343	-0.01499	0.85601	-0.00253	0.83096	-0.00449
6 - After Cleaning in Hexane	0.26343	0	0.85600	0.00009	0.83331	0.00235

All weights are average of at least 3 measurements

TABLE 19

Effect of Smog Constituent (Erucic Acid):
Surface Properties and Lap Shear Strength
for PAA Al 7075-T6

Initial Preparation

Sample	Δ (deg)	SPD (volts)	θH_2O (deg)
1	163.7	0.17	2
2	165.8	0.22	2
3	161.9	0.15	2
4	162.1	---	2
5	153.1	0.19	2
6	165.7	---	2
7	164.6	0.20	2
8	164.9	---	2
9	162.8	0.18	2
10	163.0	---	2
11	162.3	0.18	2
12	161.9	---	2

After Contamination

	Δ	Estimated Thickness (Å)	SPD	θH_2O	Lap Shear Strength (Ksi)	% Interfacial Failure
1	163.7	0	0.17	2	5.5	5
11	163.2	0	0.22	35	5.5	5
5	162.3	5	0.43	42	5.9	5
7	152.6	82	0.49	62	5.6	5
3	152.3	83	0.43	90	5.9	5
9	156.2	68	0.40	92	5.7	5

TABLE 20

Effect of Oil Contamination:
Surface Properties, Contamination and Lap Shear Strength for
PAA Al 7075-T6

Initial Preparation

Sample	Δ (deg)	ψ (deg)	θH_2O (deg)
1	184	43.0	8
2	171	38.8	6
3	172	37.9	15
4	178	39.3	13
5	172	38.1	15
6			14

After Contamination

	Δ	ψ	Estimated Thickness (Å)	θH_2O	Lap Shear Strength (Ksi)	% Interfacial Failure
6	-	--	0	14	5.73	0
2	153	37.3	150	9	6.01	0
4	153	36.8	150	18	5.80	0
3	125	38.7	430	29	5.63	0
5	96	46.5	1000	54	5.50	0
1	0	80.8	Thick	21	5.64	0

TABLE 21

Effect of Factory Contaminant (Oil) on Durability: Surface Properties, Contamination and Wedge Tests for PAA Al 7075-T6

Initial Preparation

Sample	Δ (deg)	ψ (deg)	θH_2O (deg)
1	175	36.9	5
2	167	36.2	6
3	169	35.7	3
4	172	37.7	9
5	164	33.2	7
6	169	36.9	4

After Contamination

	Δ (deg)	ψ (deg)	Estimated Contamin. Thickness (Å)	θH_2O (deg)	Crack Growth Inches 1 hr	Crack Growth Inches 24 hrs	% Interfacial Failure
1	173	36.9		5	0.12	0.24	20
5	124	36.4	500	33	0.08	0.24	1
2	270	41.0	3400	101	0.08	0.20	0
3	30	11.1	Thick	82	0.12	0.25	1
4	121	81.6	Thick	90	0.00	0.18	1
6	260	71.2	Thick	75	0.10	0.24	5

TABLE 22

Experiment to see if FM-73 Absorbs Industrial Oil

Stage	Sample #1		Sample #2		Sample #3	
	Weight (gms)	Weight Change (gms)	Weight (gms)	Weight Change (gms)	Weight (gms)	Weight Change (gms)
1 - Clean Al	0.24769		0.24775		0.24870	
2 - Al + Oil	0.40586	0.15817				
3 - Al + FM-73			0877803	0.63005	0.83824	0.58954
4 - Al + FM-73 + Oil					0.95195	0.11371
5 - After FM-73 Cure Cycle	0.40586	--	0.87702	-0.00078	0.95090	-0.00105
6 - After Cleaning in Acetone	0.24861	-0.15725	0.87702	--	0.85330	-0.0976

All weights are average of at least 3 measurements

TABLE 23

Effect of Factory Contaminant Silicone Grease:
Surface Properties, Contamination of Lap Shear Strength for
PAA Al 7075-T6

Initial Preparation

Sample	Δ (deg)	ψ (deg)	θH_2O (deg)
1	179	39.3	9
2	171	37.9	14
3	174	38.4	9
4	181	40.0	13
5	182	44.0	10
6	---	-----	--

After Contamination

			Estimated Thickness (Å)	θH_2O	Lap Shear Strength (Ksi)	% Inter-facial Failure
6	---	-----	0	--	5.5	5
1	163	35.6	130	43	5.3	5
2	142	38.7	270	66	5.7	20
3	118	46.4	500	74	4.9	40
4	94	50.7	1100	89	3.2	90
5	73	62.5	Large	105	2.6	95

TABLE 24

Experiment to see if FM-73 Absorbs Silicone Grease

Stage	Sample #1		Sample #2		Sample #3	
	Weight (gms)	Weight Change (gms)	Weight (gms)	Weight Change (gms)	Weight (gms)	Weight Change (gms)
1 - Clean Al	0.26156		0.26566		0.26746	
2 - Al + Silicone	0.30242	0.04086				
3 - Al + FM-73			1.03636	0.77070	1.03852	0.77106
4 - Al + FM-73 + Silicone					1.19630	0.15778
5 - After FM-73 Cure Cycle	0.30242	0	1.03274	-0.00362	1.19245	-0.00395
6 - After Cleaning in MEK	0.26165	-0.04077	1.06385	0.06023	1.09645	-0.09600

All weights are average of at least 3 measurements

In view of the compatibility of the PAA surface with organic contamination, a more severe durability test was investigated. To provide a more severe durability test, hexadecylamine contaminated specimens (see Table 25) were bonded and placed in boiling tap water. Although little effect was noted in 1 hr, after 24 hrs, the cracks had grown 1.6 inches and failure was 100% interfacial. The interfacial failure occurred on the control PAA specimen as well as on the contaminated specimen and the adhesive was strongly attacked. Although all specimens were degraded by boiling water, the heavily contaminated samples increased the crack extension on both sides of the adhesive, to about 2"/24 hrs.

B. Comparison of PAA with FPL Etch

It is of interest to compare the lap shear test for PAA treatment with that for the standard FPL etch treatment. Therefore, samples that had been given the FPL etch were contaminated with stearic acid, machine oil, silicone grease and with the cotton glove smudge. Table 26 shows results for stearic acid contamination on FPL etched samples. A small stearic acid film thickness (30Å or about 1 monolayer) increases $\theta H_2 0$ to 90^o and decreases the lap shear strength to 4.4 ksi. This is about a 600 psi decrease from the normal 5.0 Ksi control value. The low value of 4.64 Ksi for the control sample (#6) in Table 26 is attributed to the high initial contact sample of 20^o. For an unknown reason, all of the initial samples were slightly contaminated for this test. An increase of stearic acid contamination from 30 to 500Å decreases the lap shear strength by about 1.5 Ksi and increases interfacial failure to about 20%.

Table 28 gives the results for silicone grease contamination on FPL etched aluminum. Relatively small amounts (35-200Å) of silicone grease drastically increases the water contact angle and decreases the lap shear strength causing almost 100% interfacial failure. The same average thickness on PAA samples actually increased the lap shear strength, but larger amounts strongly decrease it.

TABLE 25

Effect of Smog Constituent (Hexedecylamine) on Durability: Surface Properties, Contamination and Wedge Tests in Boiling Water for PAA Al 7075-T6

Initial Preparation

Sample	Δ (deg)	ψ (deg)	SPD (volts)	θH_2O (deg)
1-25-5-78	184.1	40.7	0.18	9
2-25-5-78	184.0	40.8	0.21	7
3-25-5-78	188.7	40.6	0.22	6
4-25-5-78	184.7	40.4	0.27	4
5-25-5-78	183.7	41.1	0.20	2
6-25-5-78	169.5	39.8	0.10	6
7-25-5-78	175.6	38.5	0.18	3
8-25-5-78	180.2	38.6	0.21	5
9-25-5-78	179.1	40.2	0.19	4
10-25-5-78	181.4	38.9	0.20	4
11-25-5-78	179.5	39.1	0.20	3
12-25-5-78	175.1	37.8	0.21	6

After Contamination

Contamination		Δ (deg)	ψ (deg)	Estimated Thickness (Å)	SPD (volts)	θH_2O (deg)	Crack Growth Inches 1hr	Crack Growth Inches 24hr
Control	1-25-5-78	184.1	40.7	0	0.18	9	0.05	1.62
Hexadecyl amine	2-25-5-78	175.8	37.2	87	0.77	115	0.00	1.62
Hexadecyl-amine	3-25-5-78	153.2	34.7	355	0.84	132	0.06	1.56
Hexadecyl-amine	4-25-5-78	137.0	35.9	477	0.90	136	0.06	1.69
Hexadecyl-amine	5-25-5-78	127.6	36.2	561	0.90	183	0.09	1.87
Hexadecyl-amine	6-25-5-78	95.6	39.7	739	0.85	129	0.12	2.06

TABLE 26

Effect of Stearic Acid Contamination: Surface Properties Contamination and Lap Shear Strength for FPL Etched Al 7075-T6

Initial Preparation

Sample		Δ (deg)	SPD	θH_2O (deg)
1	99	38.0	0.60	17
2	100	38.2	0.80	29
3	99	38.3	0.58	18
4	100	37.9	1.30	17
5	102	37.7	1.80	19
6	100	38.0	1.90	20

After Contamination

	Δ	ψ	Estimated Thickness (Å)	SPD	θH_2O	Lap Shear Strength (Ksi)	% Interfacial Failure
6	100	38.0	0	1.90	20	4.64	0
2	96	40.0	30	0.27	90	4.40	2
3	87	43.5	200	0.13	114	3.90	10
1	82	44.6	280	0.07	104	3.79	2
4	87	47.1	500	0.17	118	3.35	30
5	85	47.1	500	0.16	117	3.53	20

TABLE 27

Effect of Oil Contamination: Surface Properties, Contamination and Lap Shear Strength for FPL Etched Al 7075-T6

Initial Preparation

Sample	Δ (deg)	ψ (deg)	θH_2O (deg)
1	87.1	35.6	3
2	90.2	36.8	2
3	89.1	35.6	4
4	86.7	37.3	3
5	88.0	35.2	5
6	85.4	35.4	2
7	86.0	36.5	3
8	90.0	35.5	4
9	96.0	36.5	2
10	92.0	35.4	3
11	95.0	36.2	5
12	90.0	35.9	3

After Contamination

		Δ	ψ	Estimated Thickness (Å)	θH_2O	Lap Shear Strength (Ksi)	% Interfacial Failure
4	Control	86.7	37.3	0	3	5.00	0
1		83.2	36.9	20	20	4.85	0
3		78.7	35.4	50	32	4.60	0
2		17.0	53.5	350	59	4.45	20
5		7.6	19.2	400	63	4.05	25
6		82.7	36.8	Thick	20	3.75	30

TABLE 28

Effect of Silicone Grease Contamination: Surface Properties Contamination and Lap Shear Strength for FPL Etched Al 7075-T6

Initial Preparation

Sample	Δ (deg)	ψ (deg)	θH_2O (deg)
1-15-6-78	91.3	37.0	4
2-15-6-78	89.2	36.1	3
3-15-6-78	84.0	34.7	3
4-15-6-78	83.4	35.6	2
5-15-6-78	92.2	36.2	5
6-15-6-78	87.5	34.9	2
7-15-6-78	89.0	36.3	2
8-15-6-78	87.7	36.5	4
9-15-6-78	89.0	36.3	2
10-15-6-78	93.6	35.3	7
11-15-6-78	90.3	35.1	4
12-15-6-78	85.6	36.2	3

After Contamination

	Δ	ψ	Estimated Thickness (Å)	θH_2O	Lap Shear Strength (Ksi)	% Interfacial Failure
1-15-67-78	91.3	37.0	0	4	5.10	0
2-15-6-78	82.5	37.2	35	109	1.75	90
3-15-6-78	75.3	37.7	45	96	0.90	100
4-15-6-78	63.0	47.1	100	100	0.60	98
5-15-6-78	51.7	44.3	200	141	---	100
6-15-6-78	80.7	38.2	35	92	1.3	99

TABLE 29

Effect of Cotton Glove Smudge: Surface Properties, Mechanical Damage and Lap Shear Strength for FPL Etched Al 7075-T6

Initial Preparation

Sample	Δ (deg)	ψ (deg)	θH_2O (deg)
1-14-6-78	90.1	34.1	2
2-14-6-78	91.3	36.1	2
3-14-6-78	93.1	33.6	5
4-14-6-78	92.2	32.9	4
5-14-6-78	89.1	35.5	3
6-14-6-78	94.1	35.1	5
7-14-6-78	90.0	34.9	2
8-14-6-78	92.4	35.5	5
9-14-6-78	90.1	36.1	2
10-14-6-78	88.7	35.8	2
11-14-6-78	88.4	34.7	3
12-14-6-78	91.1	34.9	4

After Contamination

	Δ	ψ	Estimated Thickness (Å)	θH_2O	Lap Shear Strength (Ksi)	% Interfacial Failure
1	90.1	34.1	0	2	5.00	5
2	81.7	36.8	50	25	4.60	25
3	81.1	31.5	60	39	4.70	40
4	74.4	32.1	110	41	5.00	10
5	70.1	31.9	95	42	4.70	25
6	91.3	31.8	15	32	4.45	15

C. Relation Between Computer Maps and Bond Quality

Al 7075-T6 panels were cut for lap shear and wedge test specimens and anodized. These samples were then contaminated to varying levels and placed side by side on the computerized mapping table and mapped by the "OFF NULL" technique. The contaminanted samples were then bonded to uncontaminated samples and tested as lap shear, or wedge test joints. The lap shear strengths and wedge crack extensions were then correlated.

1. Lap Shear Mapping

Figure 9 shows lap shear couples after the lap shear test and aligned with the map. The 1.5 cm wide mapped strip corresponds to the adjacent lap shear region but prior to bonding. The mating surface has been placed on top for reference. Figure 10 shows the same map and the corresponding lap shear data from Table 6. Figures 11 through 14 show similar maps for panels that were contaminated with stearic acid, hexadecylamine, oil, and silicone grease. Note that Fig. 11 is for an FPL etched surface and the rest for PAA surfaces. The table that corresponds to each map is indicated at the end of the figure title.

2. Wedge Test Mapping

Figure 15 is a map of specimens prepared for wedge tests, then damaged to varying degrees by the cotton glove smudge technique. In this case, serious damage to the joint durability is indicated. The data corresponding to Fig. 15 is given in Table 30.

There is a good correlation between the dot map and crack growth (Fig. 15). To quantify the relationship between bond degradation (crack growth) and photometric reflected light intensity, data from Table 30 are plotted in Fig. 16. An excellent relation exists between intensity and bond degradation as a function of map position. The relationship is further evidenced as % interfacial failure and intensity as a function of map position in Fig. 17. Finally, there is a direct correlation between crack growth and reflected light intensity in Fig. 18.

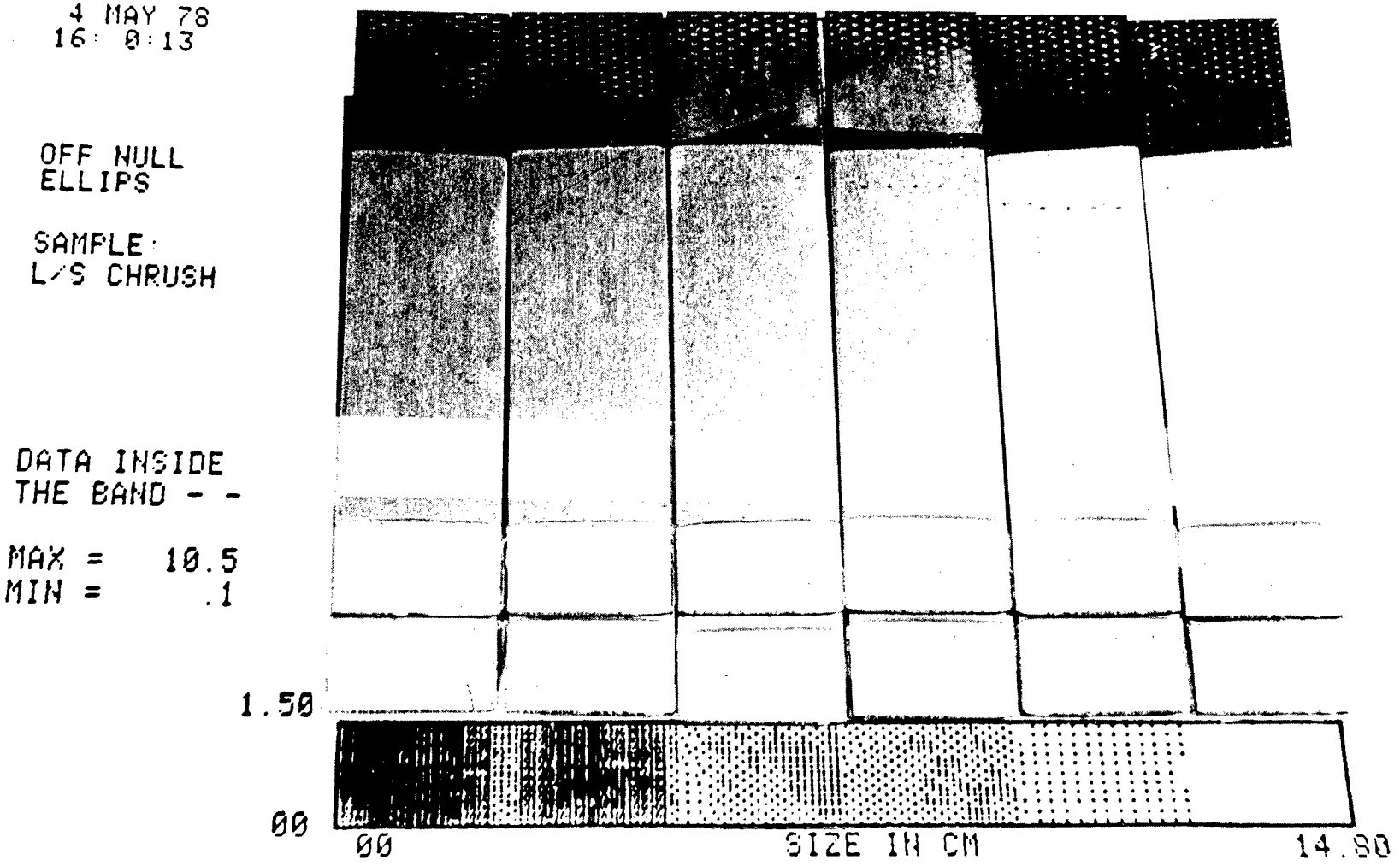

Fig. 9 Computer map of contamination on the lower half inch of lap shear specimens.

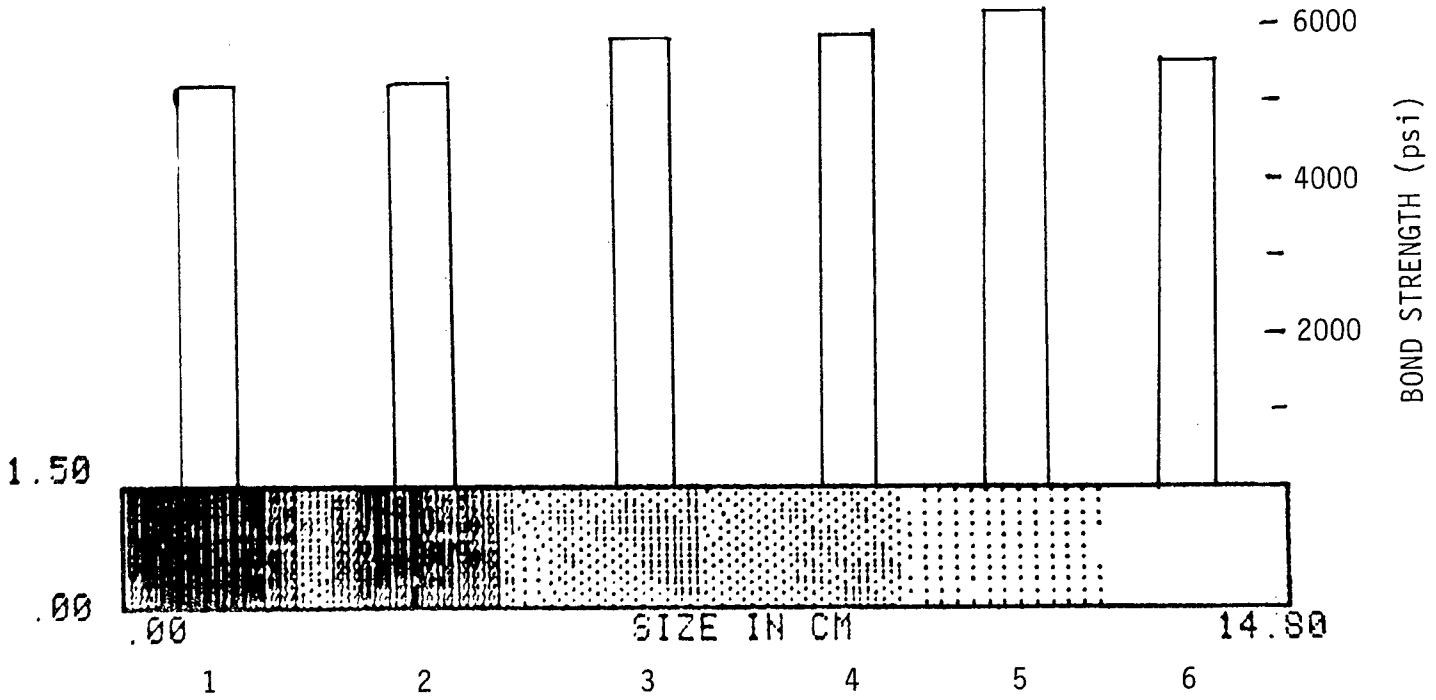

Fig. 10 Computer contamination plot for cotton glove smudge on PAA Al 7075-T6. Bars indicate relative lap shear strength.

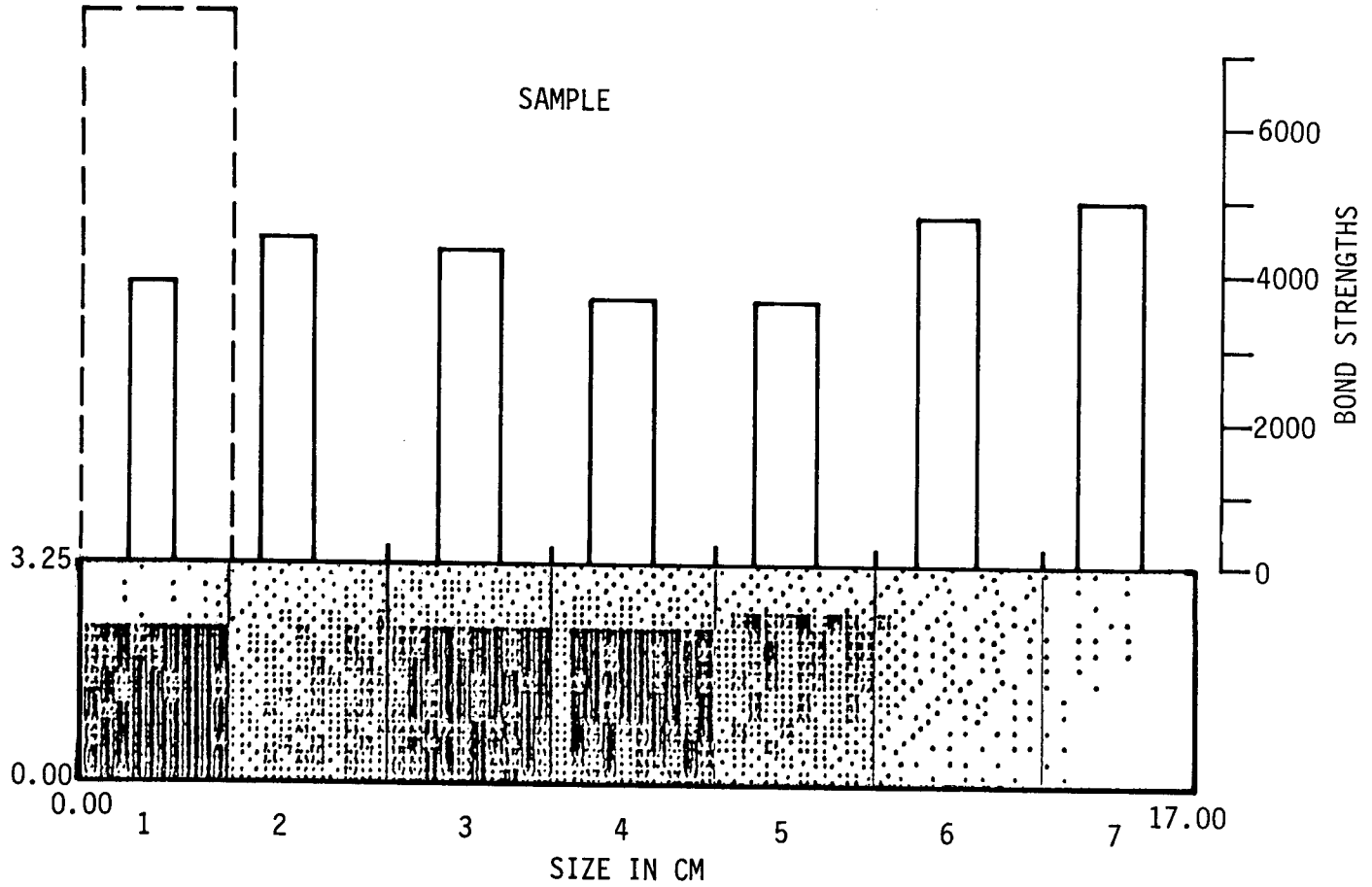

Fig. 11 Computer contamination plot for stearic acid on FPL etched Al 7075-T6. Bars indicate relative lap shear bond strengths. (Table 26)

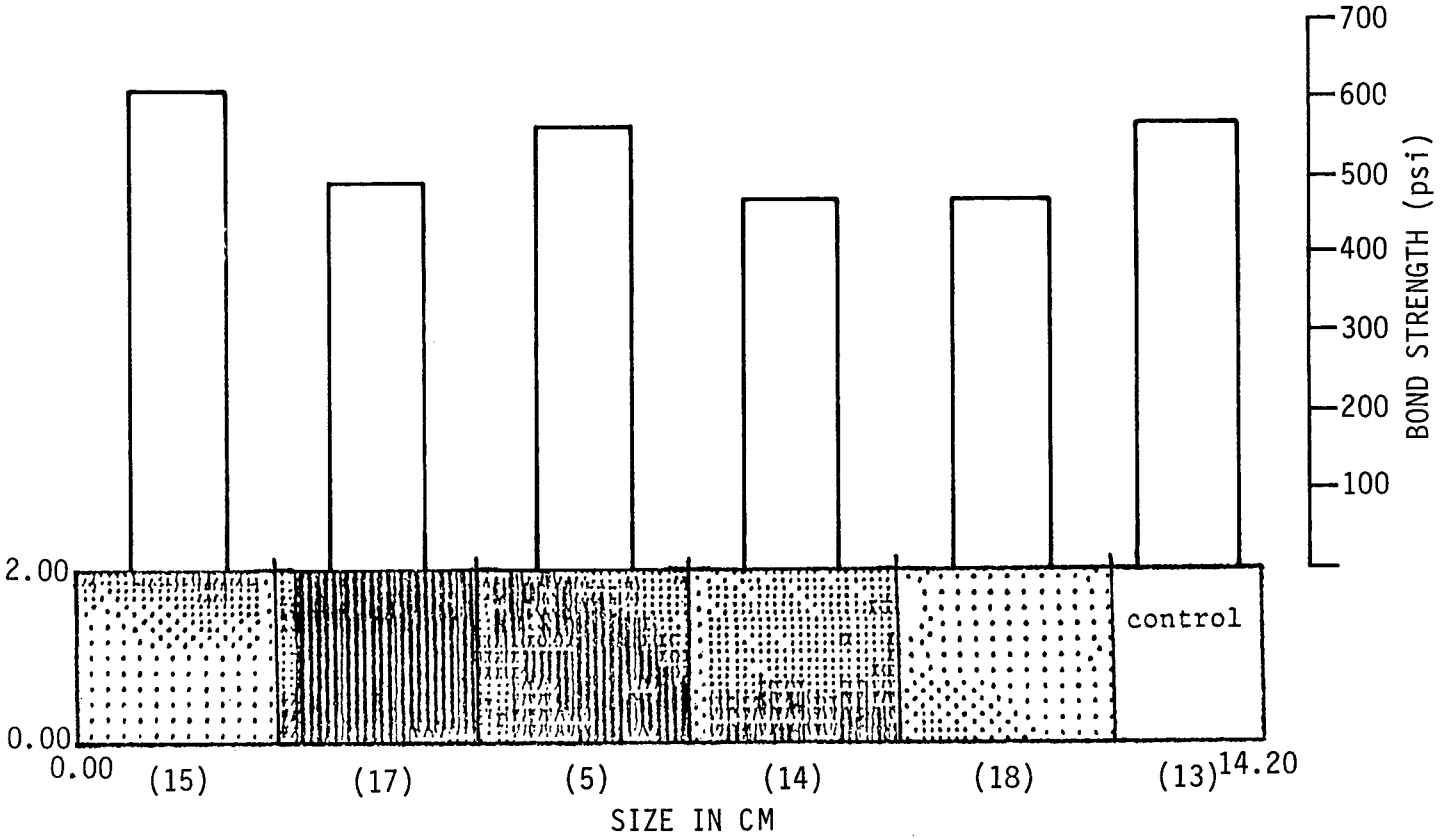

Fig. 12 Ellipsometric intensity map for hexadecylamine on phosphoric acid anodized Al 7075-T6. Bars indicate relative lap shear bond strengths. (Table 16)

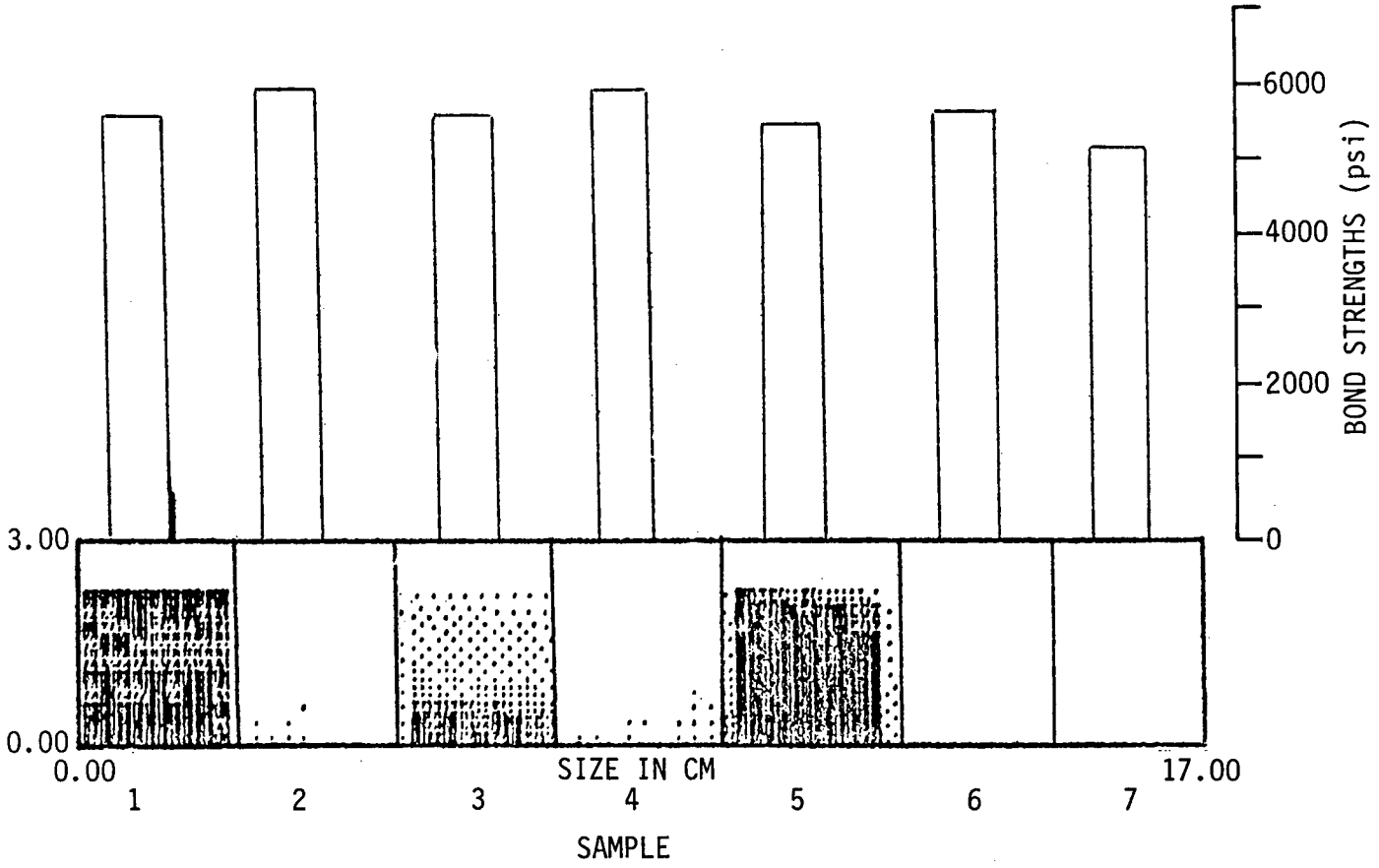

Fig. 13 Computer contamination plot for lub oil on anodic Al 7075-T6. Bars indicate relative lap shear strengths. (Table 20)

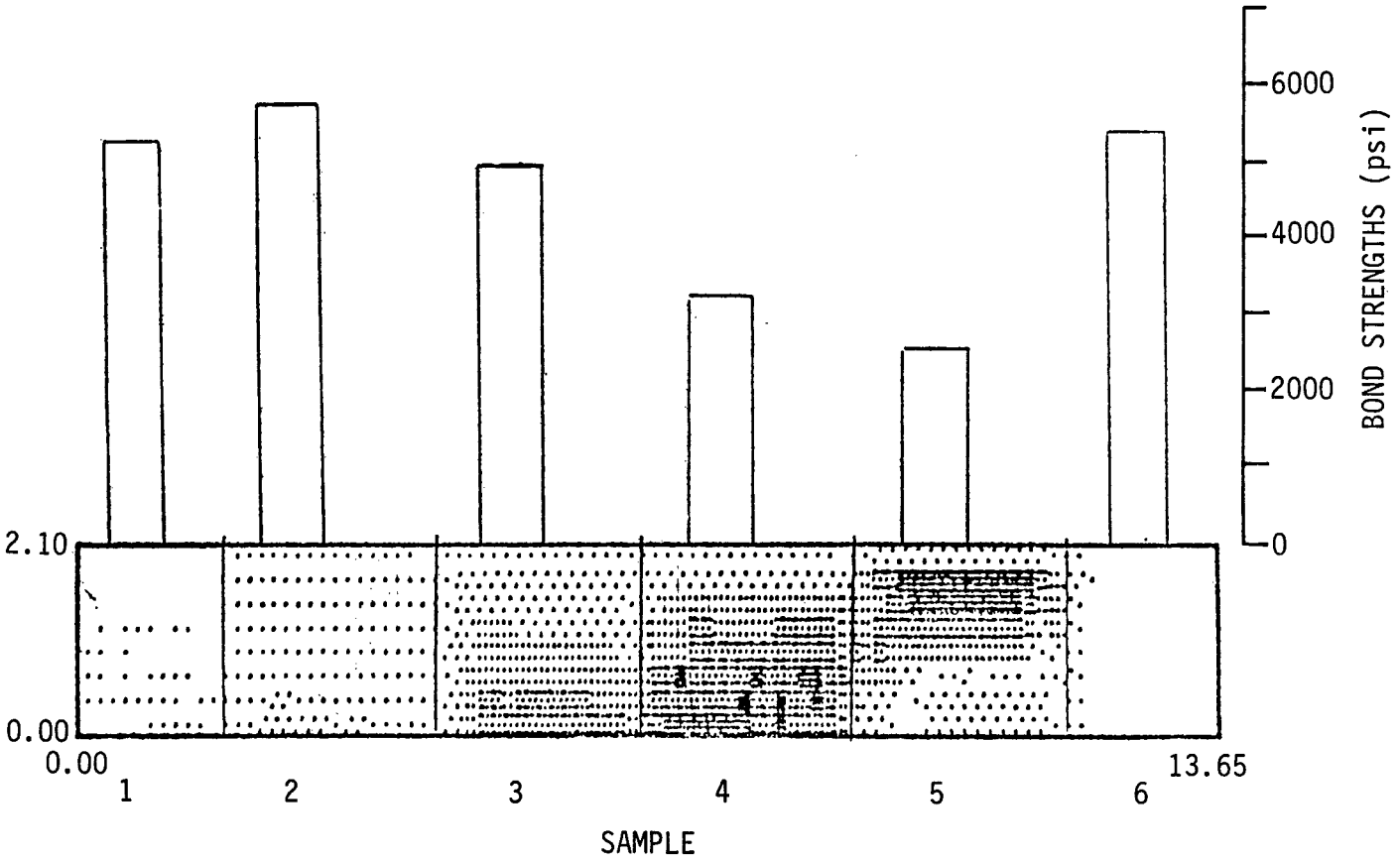

Fig. 14 Computer contamination plot for silicone grease on phosphoric acid anodized Al 7075-T6. Bars indicate relative lap shear bond strengths. (Table 23)

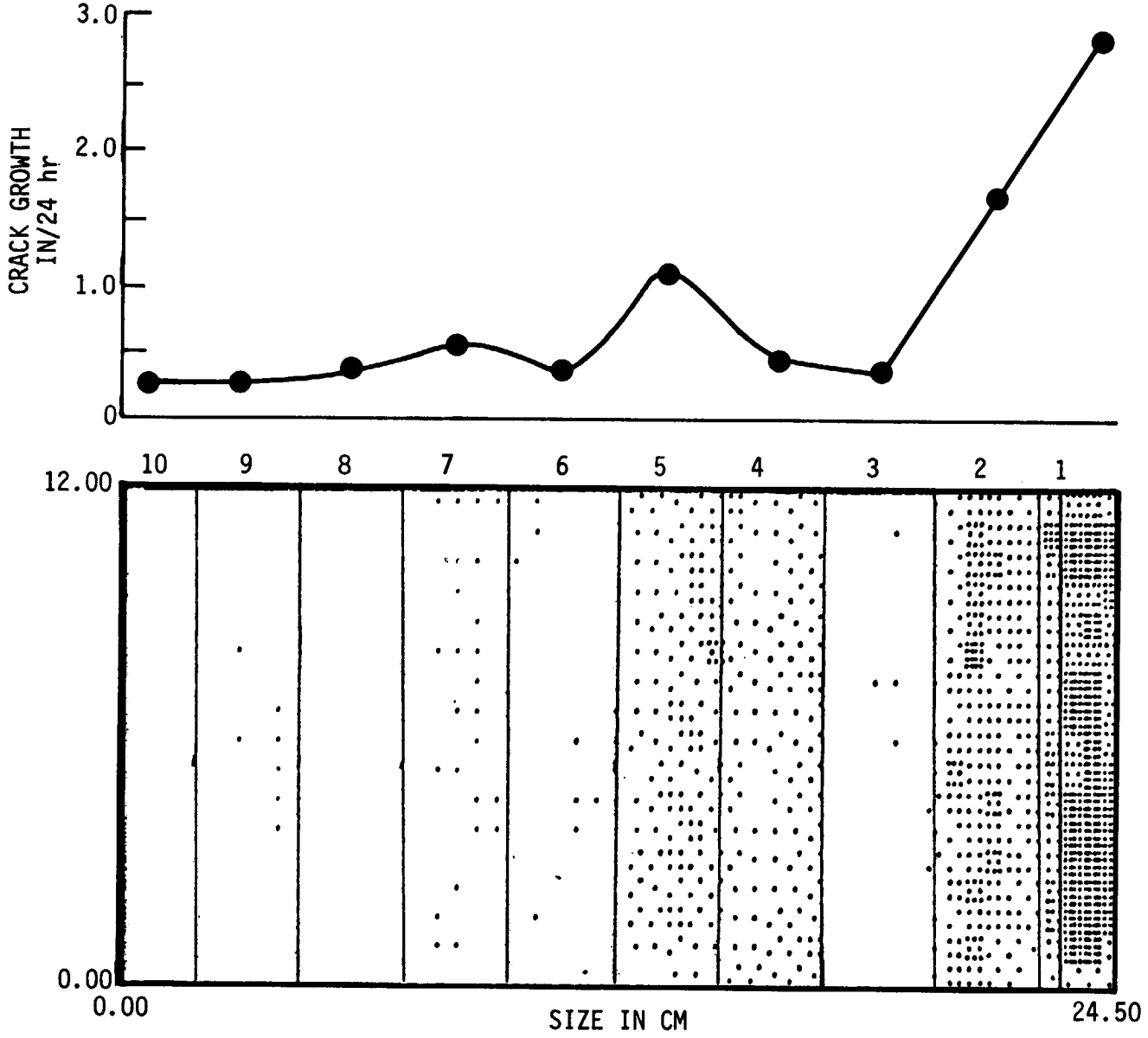

Fig. 15 Ellipsometric intensity map for cotton glove damaged Al 7075-T6 (phosphoric acid anodized).

TABLE 30

Average Ellipsometric Light Intensity vs Crack Growth and % Interfacial Failure for Cotton Glove Damaged Al 7075-T6 (Phosphoric Acid Anodized)

Sample	Crack Growth (in/1hr)	Crack Growth (in/24hr)	% Interfacial Failure	I
1	2.23	2.90	100	4.48
2	0.85	1.70	100	3.56
3	0.06	0.35	90	2.26
4	0.07	0.42	60	3.44
5	0.07	1.11	100	3.49
6	0.08	0.35	50	2.24
7	0.10	0.56	95	2.68
8	0.08	0.42	95	1.98
9	0.06	0.34	50	2.22
10	0.07	0.36	25	1.60
11(Control)	0.07	0.35	0	--
12(Control)	0.07	0.35	0	--

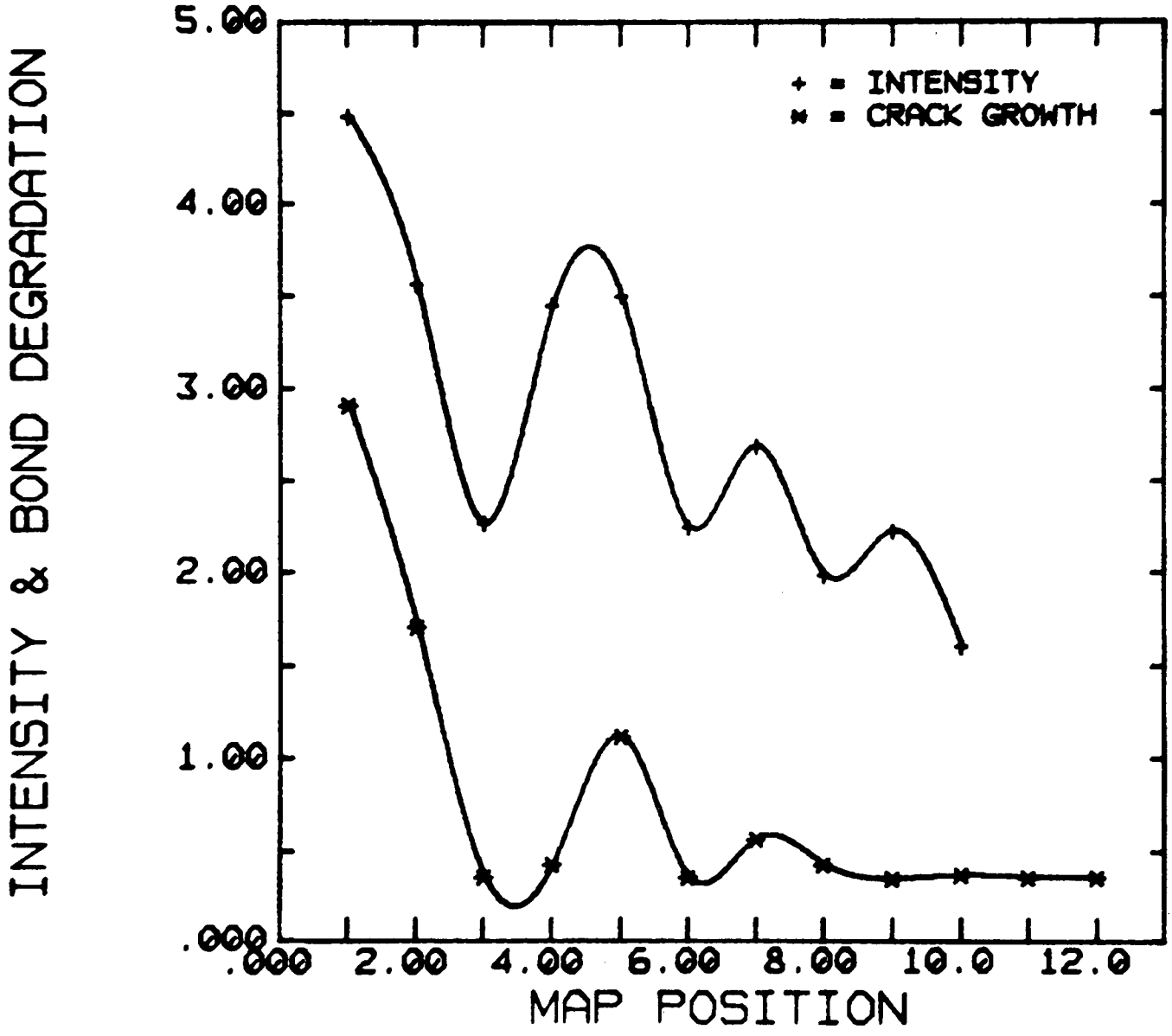

Fig. 16 Correlation between ellipsometric and failure maps.

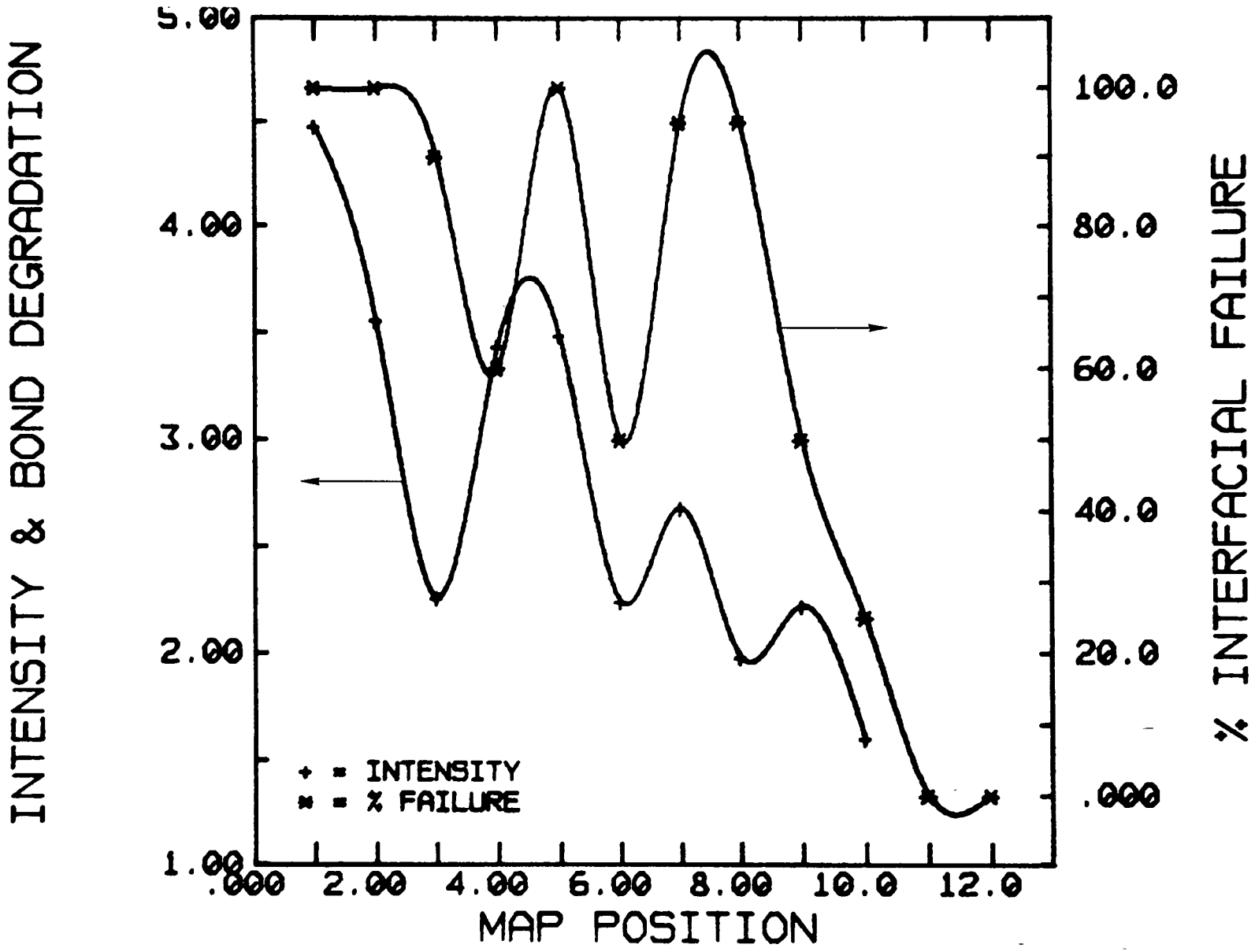

Fig. 17 Correlation between ellipsometric and failure maps.

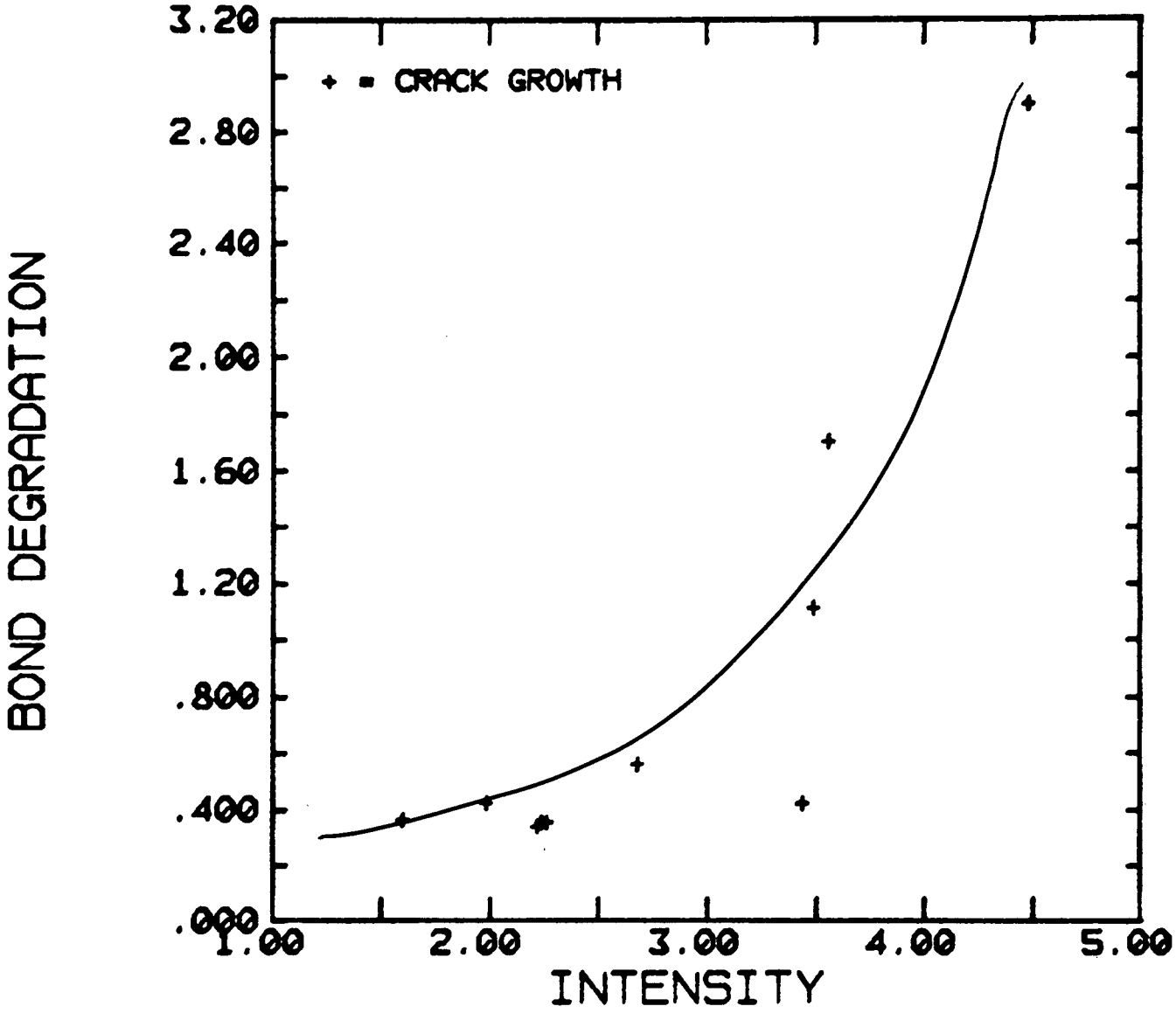

Fig. 18 Correlation between ellipsometric and failure maps.

Figure 19 is a map of wedge test samples that were anodized at various potentials to simulate a possible process error. There is a serious degradation in bond durability below 4 volts (<1000Å) and this is very distinctly revealed by the computer map. Figure 20 is a similar map for oil contamination. As observed for lap shear tests, oil is easily mapped, but has little effect on bond durability.

Production Panels

One square foot production panels were anodized at McDonnel Douglas. These panels were contaminated to varying levels along a 1 inch strip across the center of the panel and mapped. Table 31 gives results of this test. The table gives the type of contamination, the level L (Low), M (medium), H (high), VH (very high), the corresponding map figure number, the average water contact angle θH_2O, the lap shear strength and the percent interfacial failure. The corresponding maps and relative bond strength bar graphs are presented in Figs. 21 to 28.

As for the Science Center panels, the maps reveal contamination below the level that significantly affects the bond tests.

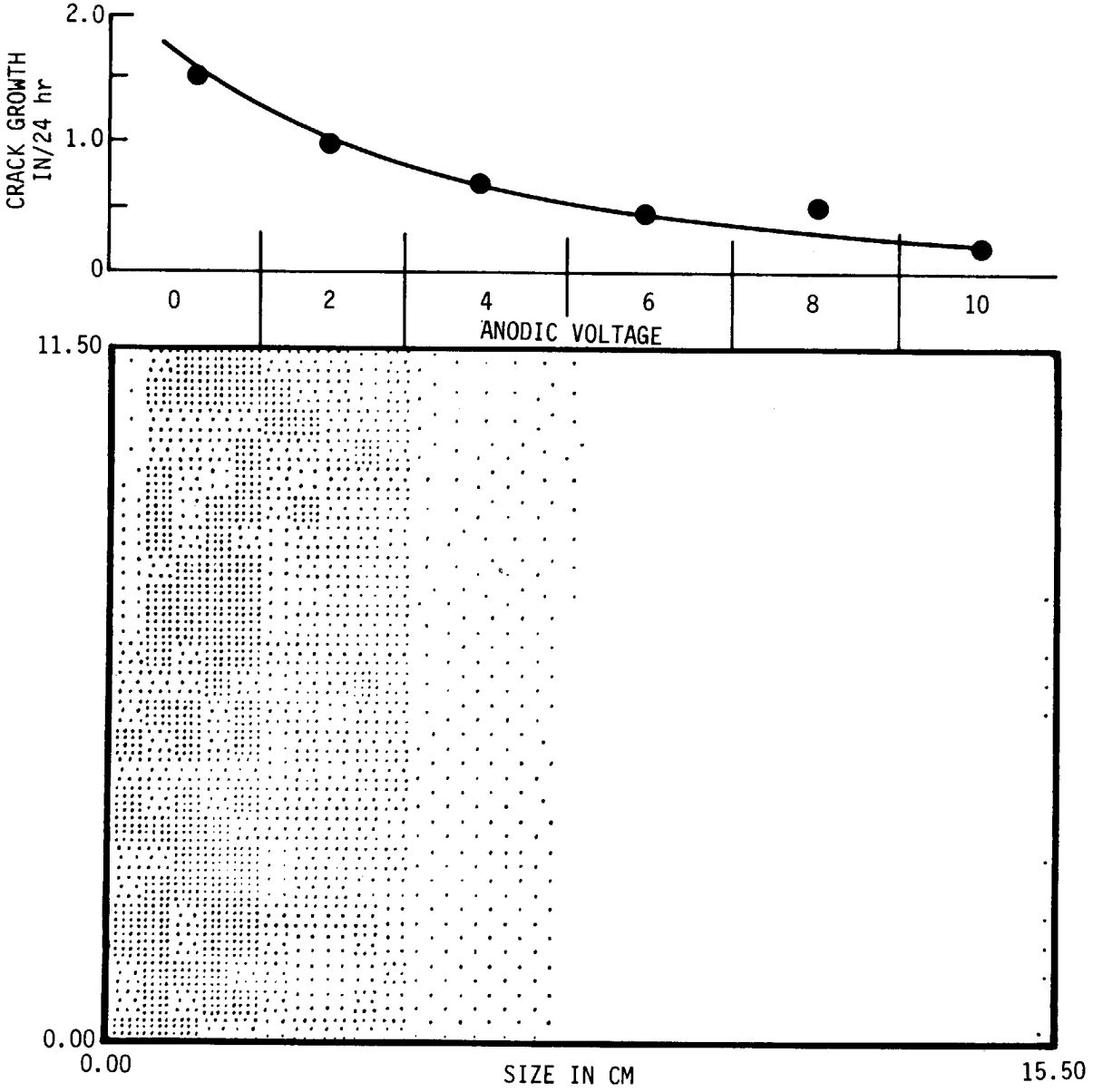

Fig. 19 Computer map for wedge specimens anodized at various voltages and corresponding crack extension curve from Table 10.

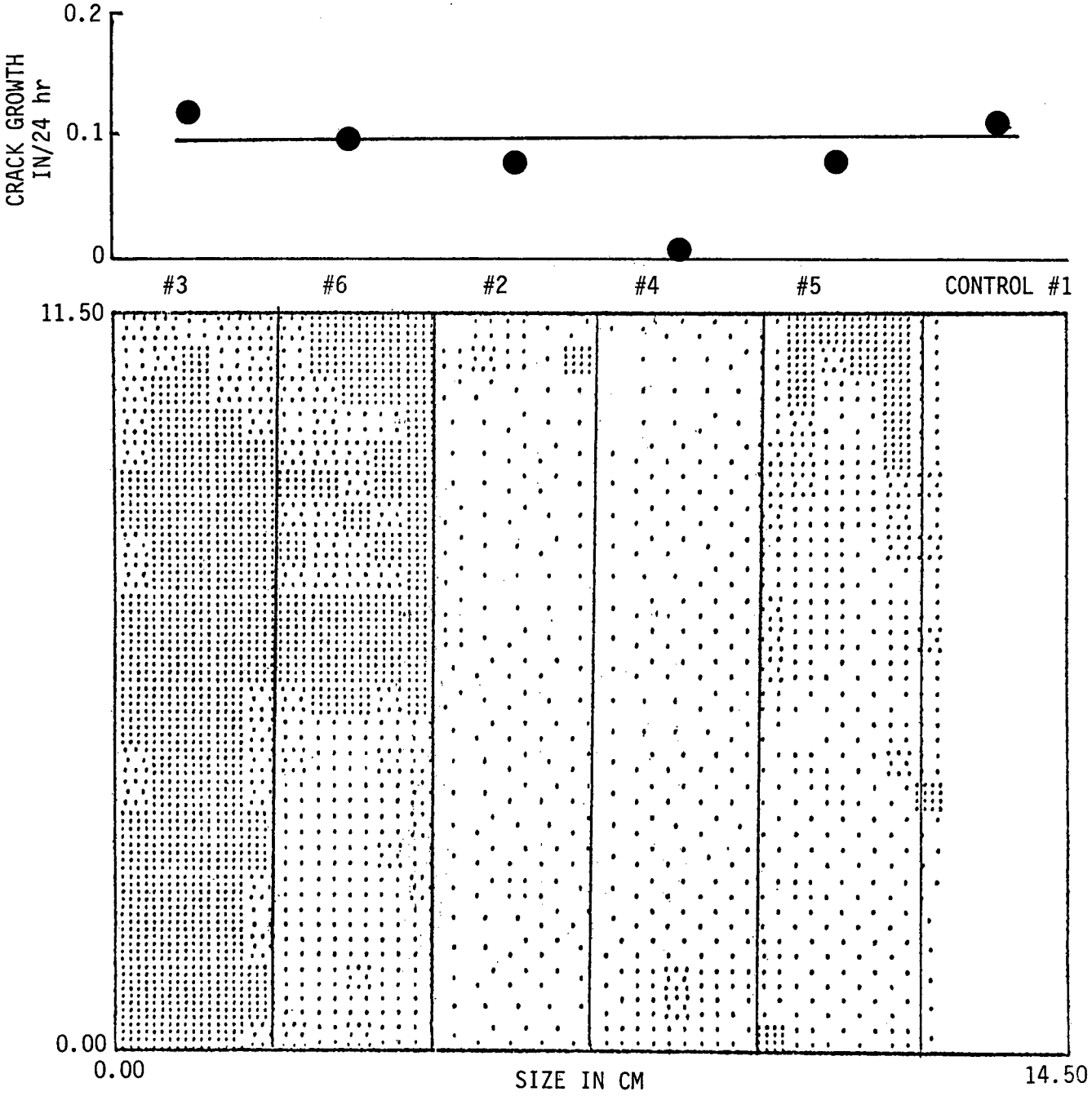

Fig. 20 Computer map of oil contaminated PAA wedge specimens and corresponding crack extension curve from Table 21.

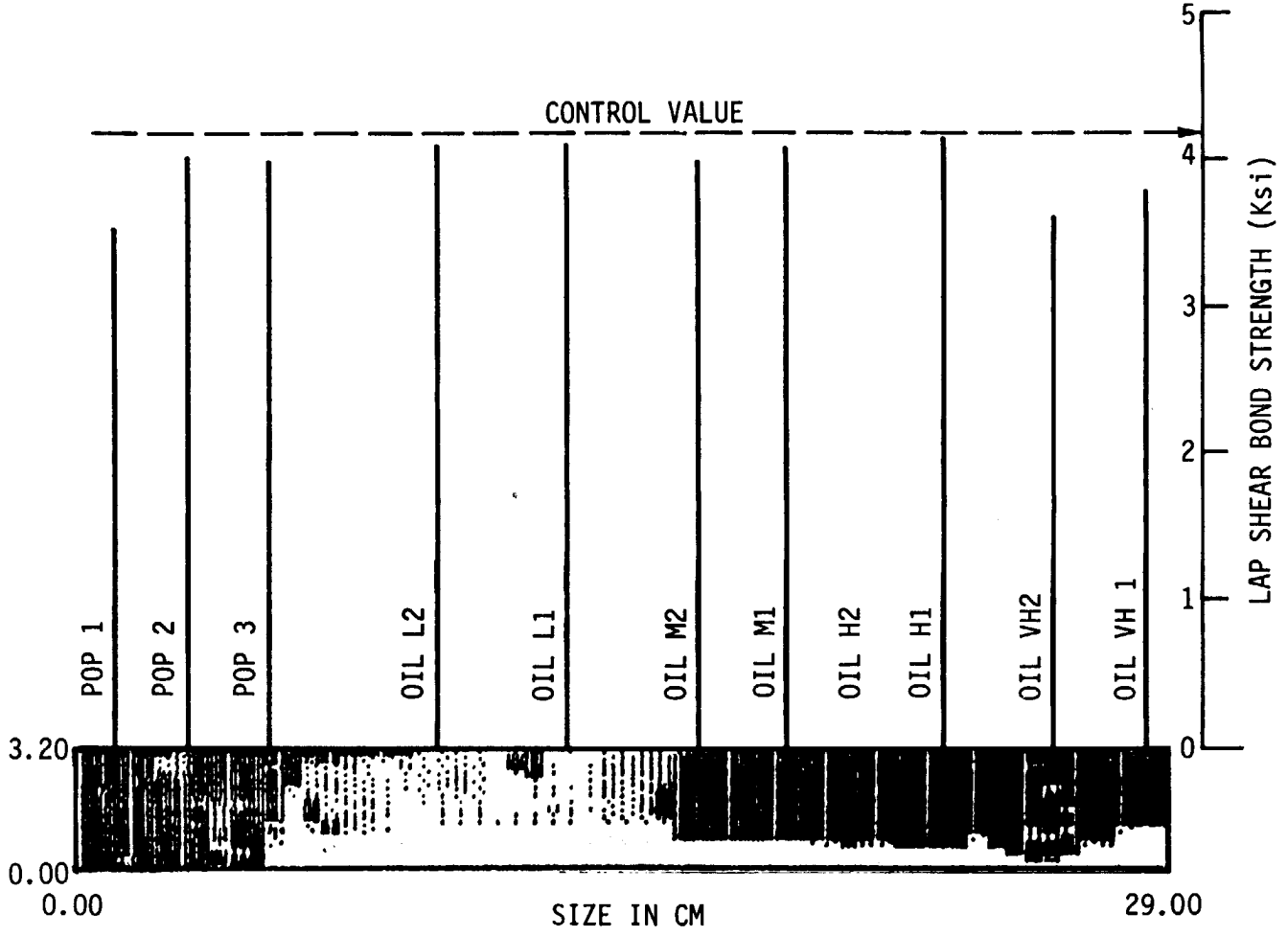

Fig. 21 Computer map of oil and soda pop (Coca Cola) contamination on PAA Al 7075-T6 production panel from McDonnel-Douglas.

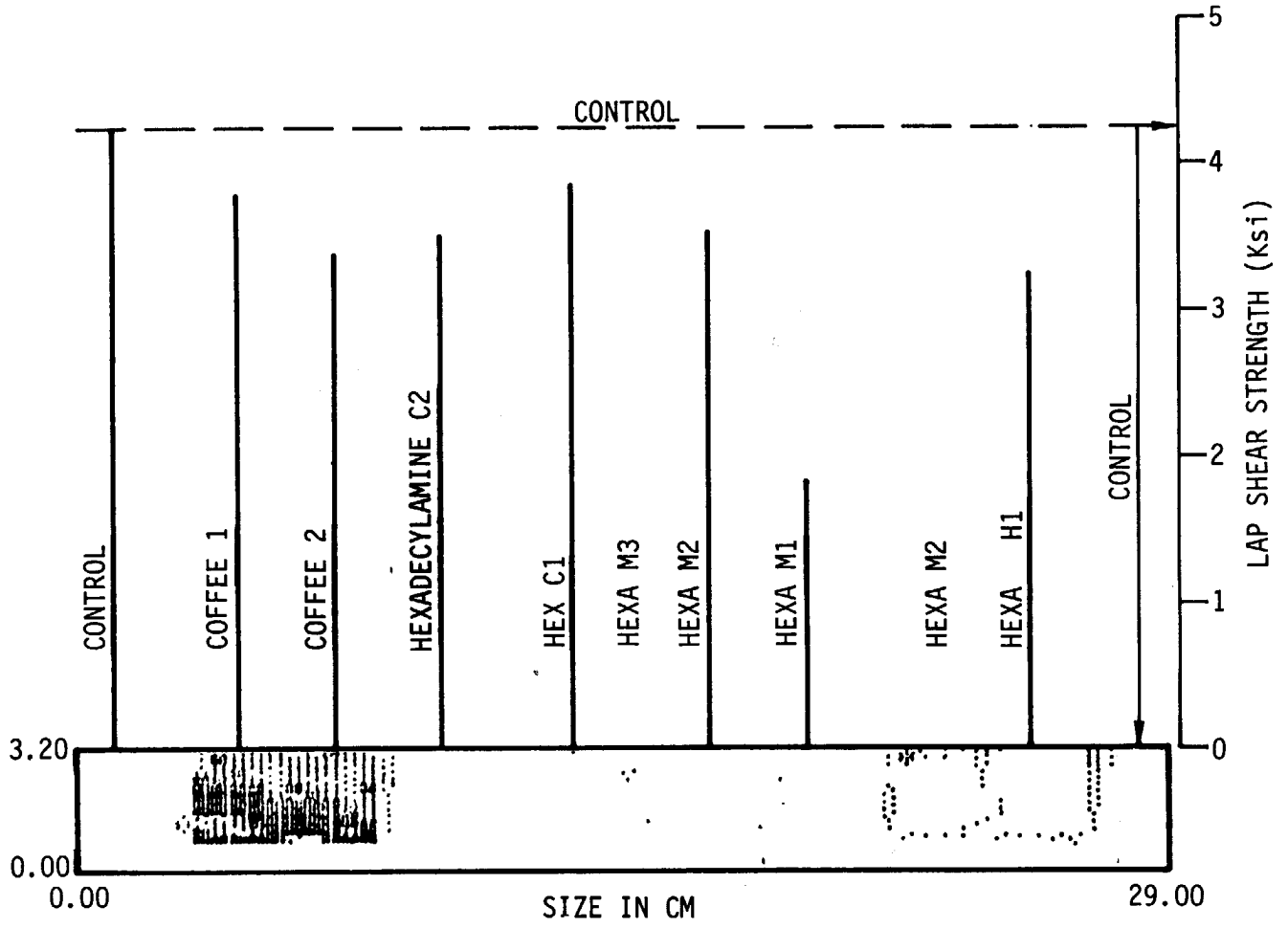

Fig. 22 Computer map of coffee and hexadecylamine contamination PAA McDonnel-Douglas production panel.

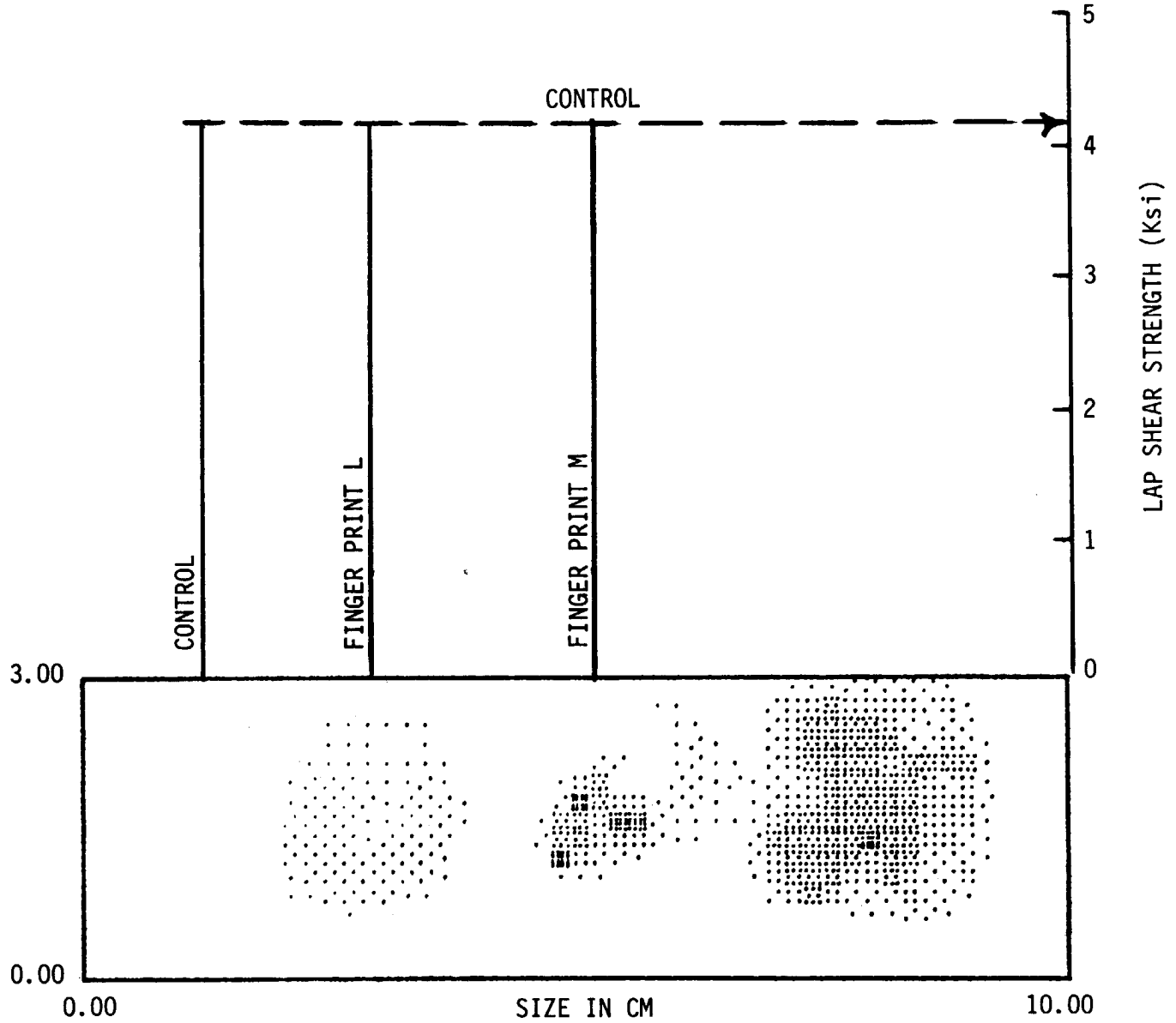

Fig. 23 Computer map of finger print contamination. PAA McDonnel-Douglas production panel.

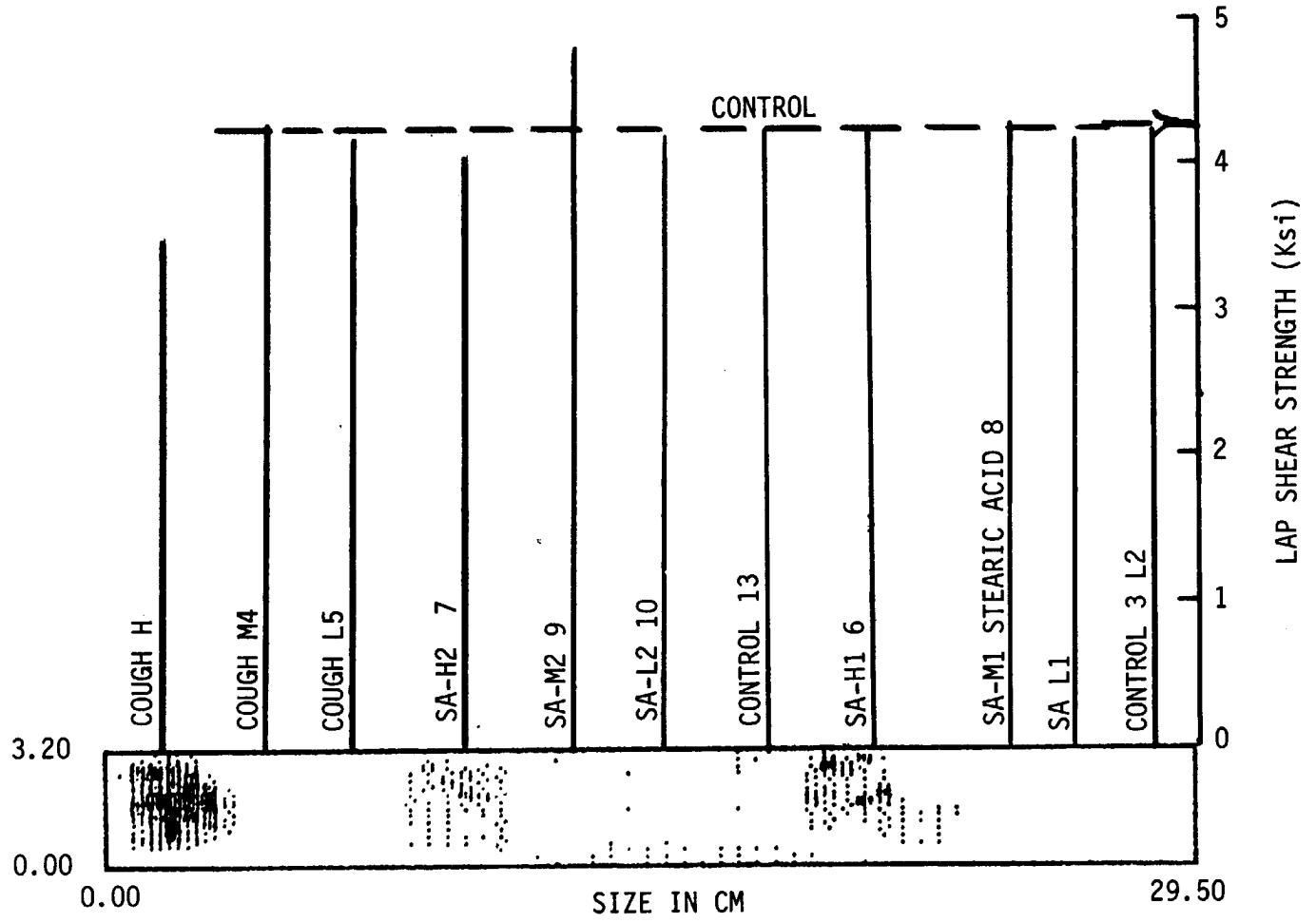

Fig. 24 Computer map of smog constituent (stearic acid (SA)) and cough. PAA McDonnel-Douglas production panel

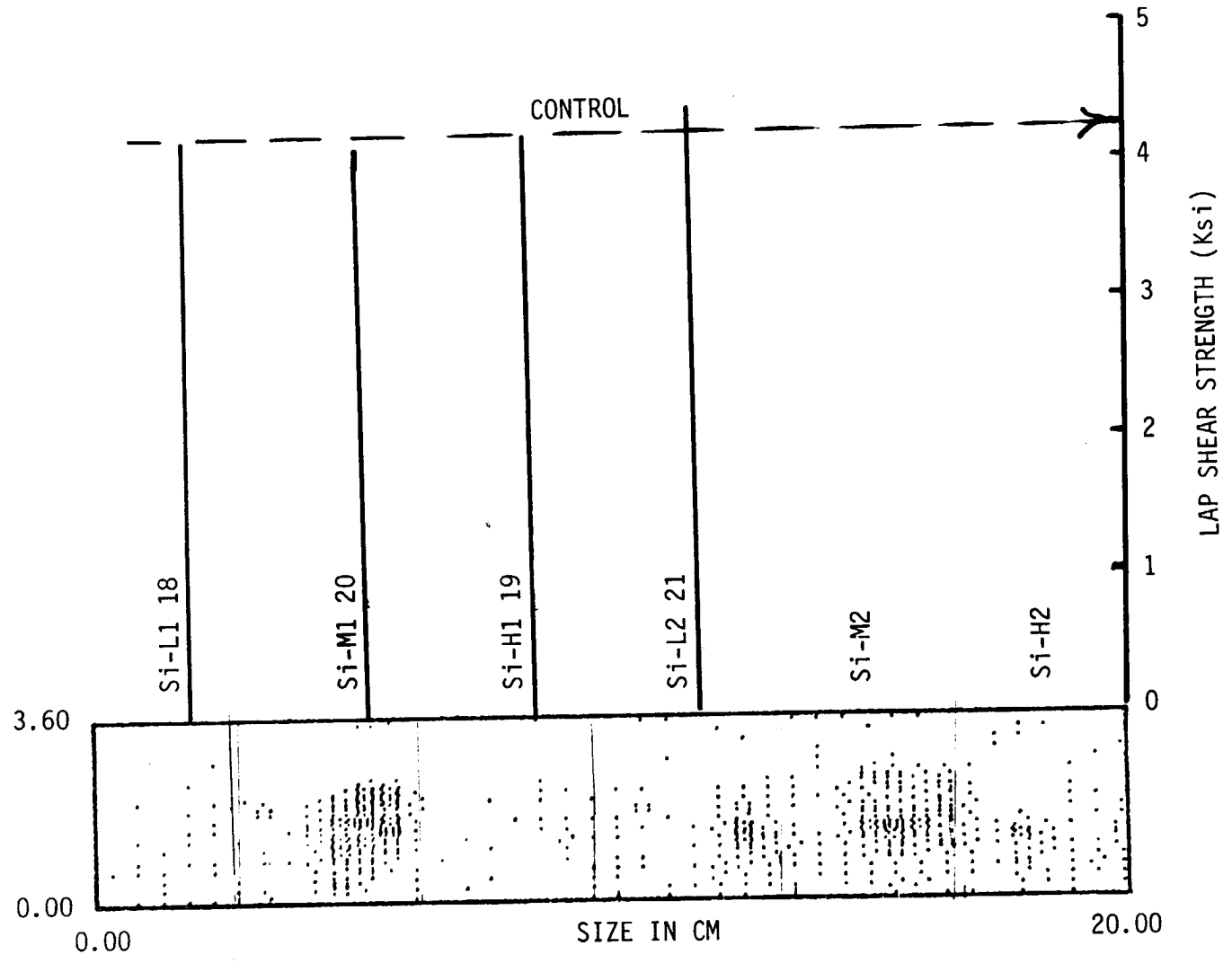

Fig. 25 Computer map of silicone grease contamination. PAA McDonnel-Douglas production panel.

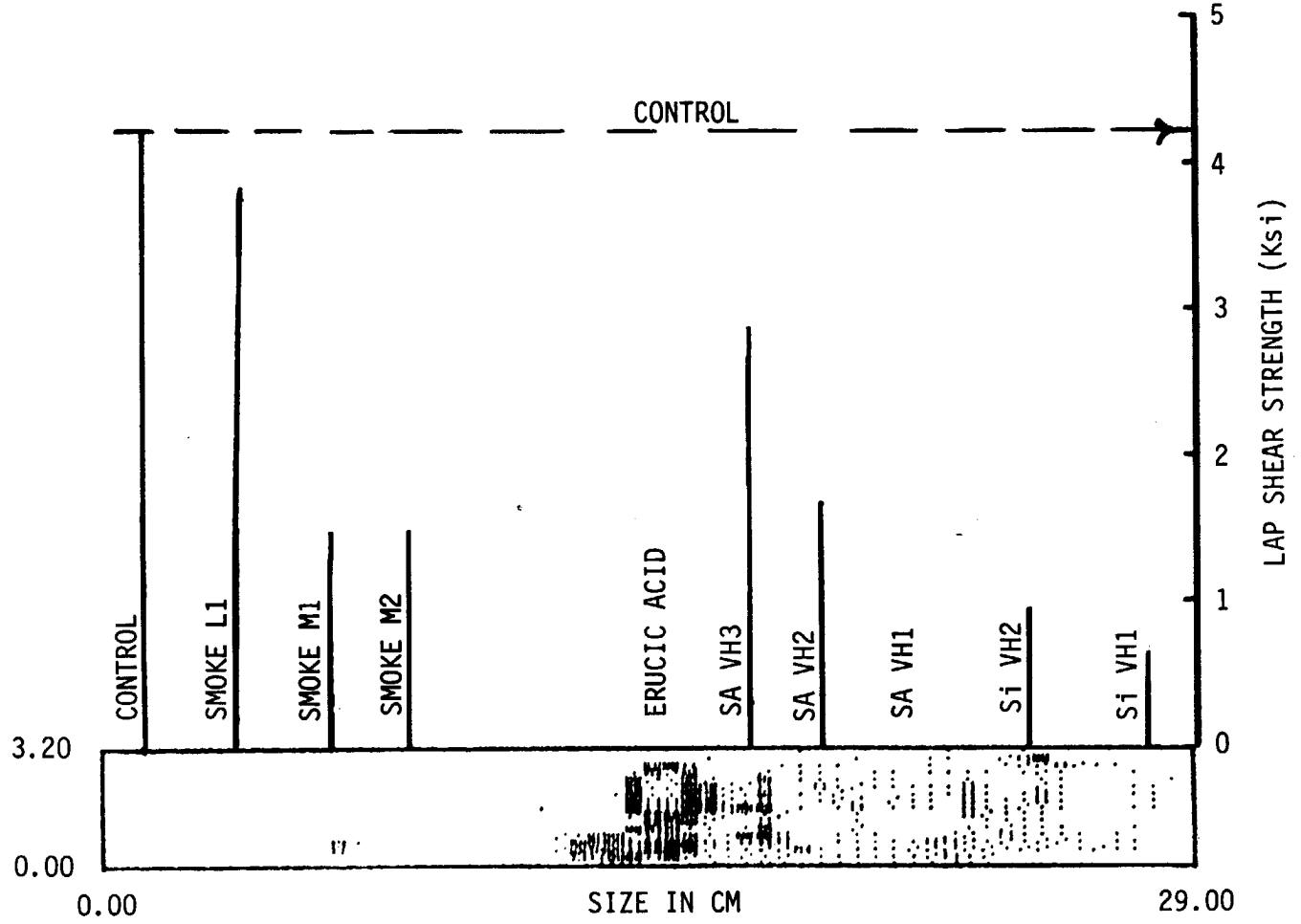

Fig. 26 Computer map of silicone grease, stearic acid, erucic acid, and cigarette smoke. PAA McDonnel-Douglas production panel.

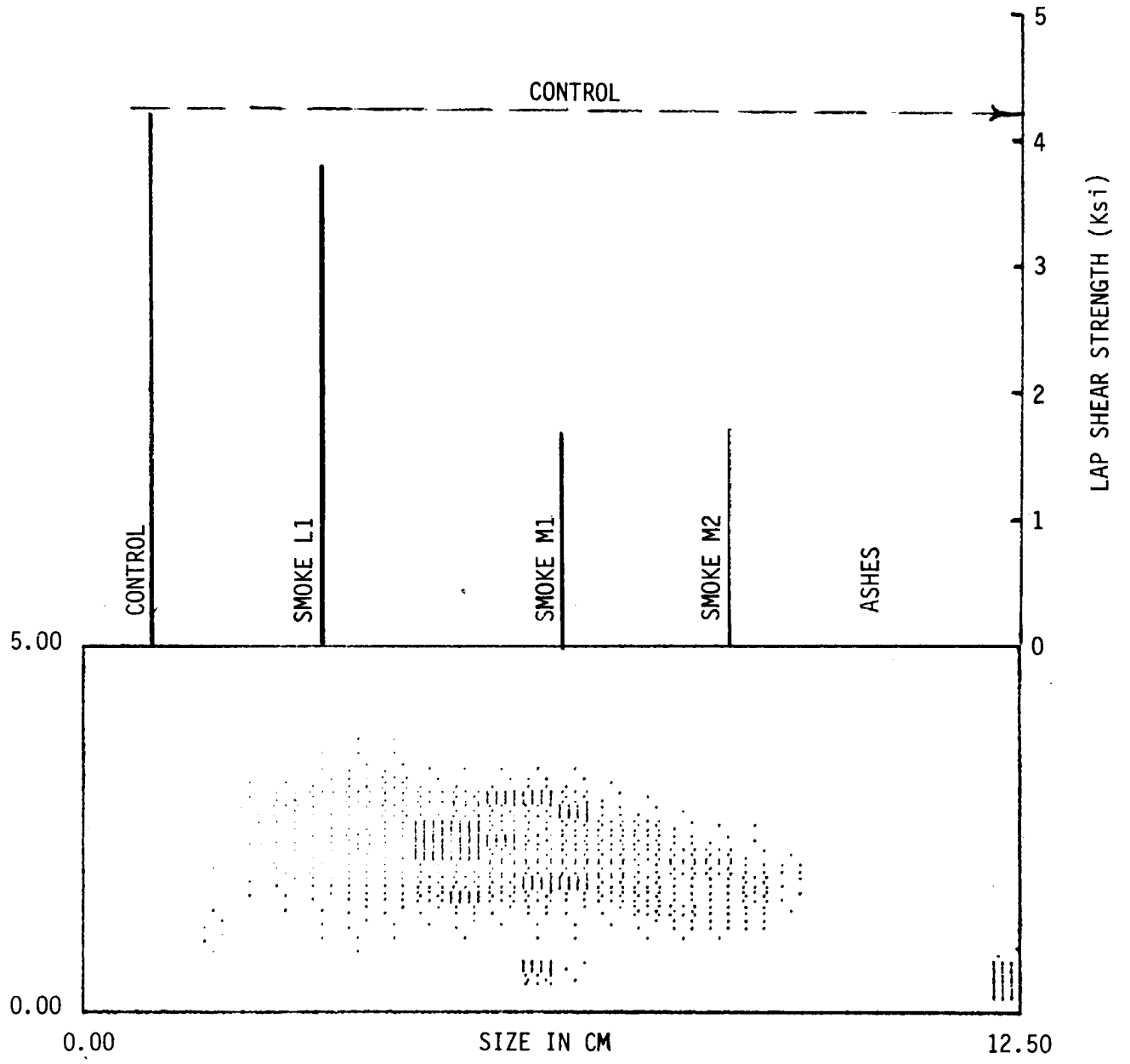

Fig. 27 Expanded computer map of cigarette smoke contamination area. PAA Mc-Donnel-Douglas production panel.

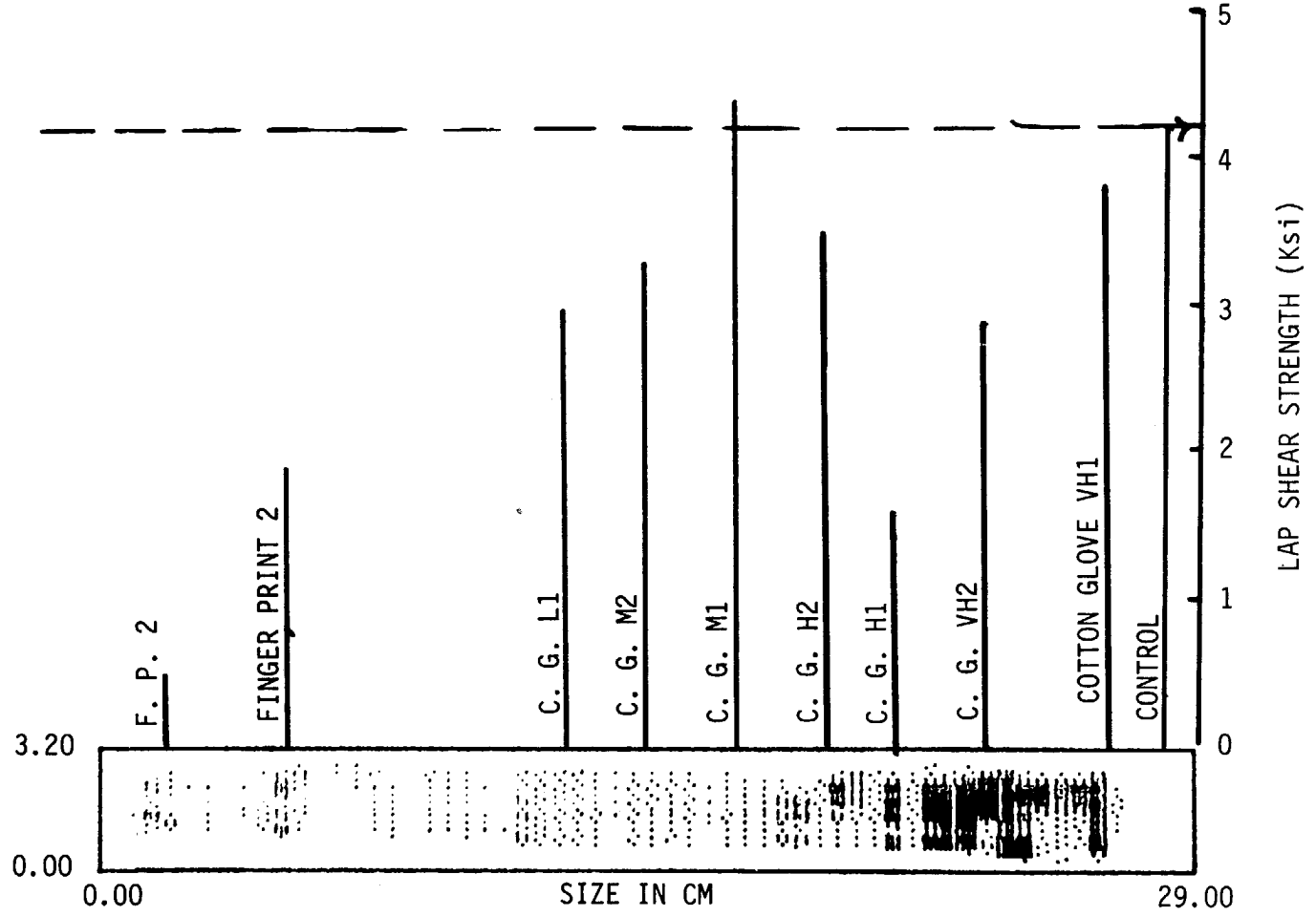

Fig. 28 Computer map of cotton glove smudge and finger prints. PAA McDonnel-Douglas production panel.

TABLE 31
Effect of Contamination on Production Panels for
McDonnel Douglas

Panel 1

Contaminant	Level	Map Figure	θH_2O	Lap Shear Strength (Ksi)	% Inter-facial Failure
Control	0	18	-	4.25	1
Control	0	18	6	4.10	10
Control	0	19	8	4.10	10
Control	0	20	7	4.25	10
Machine Oil	L1	17		4.10	1
Machine Oil	L2	17		4.10	2
Machine oil	M1	17		4.10	10
Machine Oil	M2	17		4.07	5
Machine Oil	H1	17		4.20	6
Machine Oil	VH1	17		3.82	20
Machine Oil	VH2	17		3.65	20
Soda Pop & Oil	1	17		3.50	6
Soda Pop & Oil	2	17		4.05	9
Soda Pop & Oil	3	17		3.97	10
Coffee	1	18		3.80	4
Coffee	2	18		3.42	10
Fingerprints	L	19	30	4.20	5
Fingerprints	M	19	90	4.30	5
Cough (Spit)	L	20	5	4.20	5
Cough (Spit)	M	19	90	4.30	5
Silicone Grease	L1	21	30	4.40	25
Silicone Grease	L2	21	20	4.00	5
Silicone Grease	M1	21	30	4.10	20
Silicone Grease	H1	21	40	4.20	25
Smog Constituents Stearic Acid	L1	20	15	4.20	6
Smog Constituents Stearic Acid	L2	20	50	4.20	10
Smog Constituents Stearic Acid	M1	20	30	4.30	5
Smog Constituents Stearic Acid	H1	20	120	4.25	10
Smog Constituents Stearic Acid	H2	20	110	4.05	12
Hexacecylamine	L1	18		3.85	10
Hexacecylamine	L2	18		3.50	10
Hexacecylamine	L3	18		3.45	10
Hexacecylamine	M1	18		1.80	30
Hexacecylamine	M2	18		3.55	15
Hexacecylamine	H1	18		3.20	40
Hexacecylamine	H2	18		---	--

TABLE 2 (Cont'd)

Panel 2

Contaminant	Level	Map Figure	Lap Shear Strength (Ksi)	% Inter-facial Failure
Control		22	4.25	0
Control		24	4.20	0
Silicone Grease	VH1	22	0.65	95
Silicone Grease	VH2	22	0.95	50
Fingerprints	1		0.50	90
Fingerprints	2		1.95	80
Cigarette Smoke	L1	22,23	3.80	5
Cigarette Smoke	M2	22,23	1.52	90
Cigarette Smoke	M3	22,23	1.50	90
Stearic Acid	VH1	22	1.71	40
Stearic Acid	VH2	22	2.90	15
Cotton Glove & Si	L1	24	3.00	20
Cotton Glove	M1	24	4.45	3
Cotton Glove	M2	24	3.30	20
Cotton Glove	H1	24	1.60	80
Cotton Glove	H2	24	3.50	20
Cotton Glove	VH1	24	3.90	5
Cotton Glove	VH2	24	2.90	15

D. Effect of Panel Curvature on Mapping

1. "OFF NULL" Technique

Figure 29 is a computer map of a contaminated Al 7075-T6 PAA curved panel by the "OFF NULL" technique. The radius of curvature of this panel is 7 cm. It is considered that if the mapping techniques are as sensitive on this sharp curvature, they would be equally as sensitive on panels of larger curvature. Figure 29 reveals that, with a given sensitivity setting, all three levels of cotton glove smudge and stearic acid contamination can be detected. The highest level of silicone grease is detected. Also, the pencil grid lines are detected. Level 1 is a control area that was not contaminated and should be blank as observed.

Figure 29 emphasizes a property of the present mapping technique. The photometer signal values in the -2.5 to +10.5 range are divided into levels. All data above the top level is compressed into that level, resulting in saturation of dots in levels 2, 3 and 4 for the cotton glove smudge. A lower sensitivity removes this saturation effect in Fig. 30, but leaves the silicone grease undetected. In the field, it may be necessary to map at various sensitivity levels if different types of contamination are expected. Details of the computer mapping logic are given in Ref. 2. There may be better ways to program for mapping which have not been tried as yet.

2. Automated Scanning Ellipsometer Technique

Figure 31 is a Δ map using the automated scanning ellipsometer, rather than the "OFF NULL" technique. The automatic scanning ellipsometer is not quite as sensitive as the "OFF NULL" technique and monitors a larger area, but reveals contamination very well. The silicone grease, not detected in Fig. 31, is revealed at higher sensitivity in Fig. 32. A map similar to Fig. 31 is obtained in Fig. 33 for the concave side of the panel.

It is of interest to note, that the ψ maps (Fig. 34 and 35) for the concave and convex side reveal the silicon grease, but not the stearic acid. Both Δ and ψ maps reveal cotton glove smudge very well.

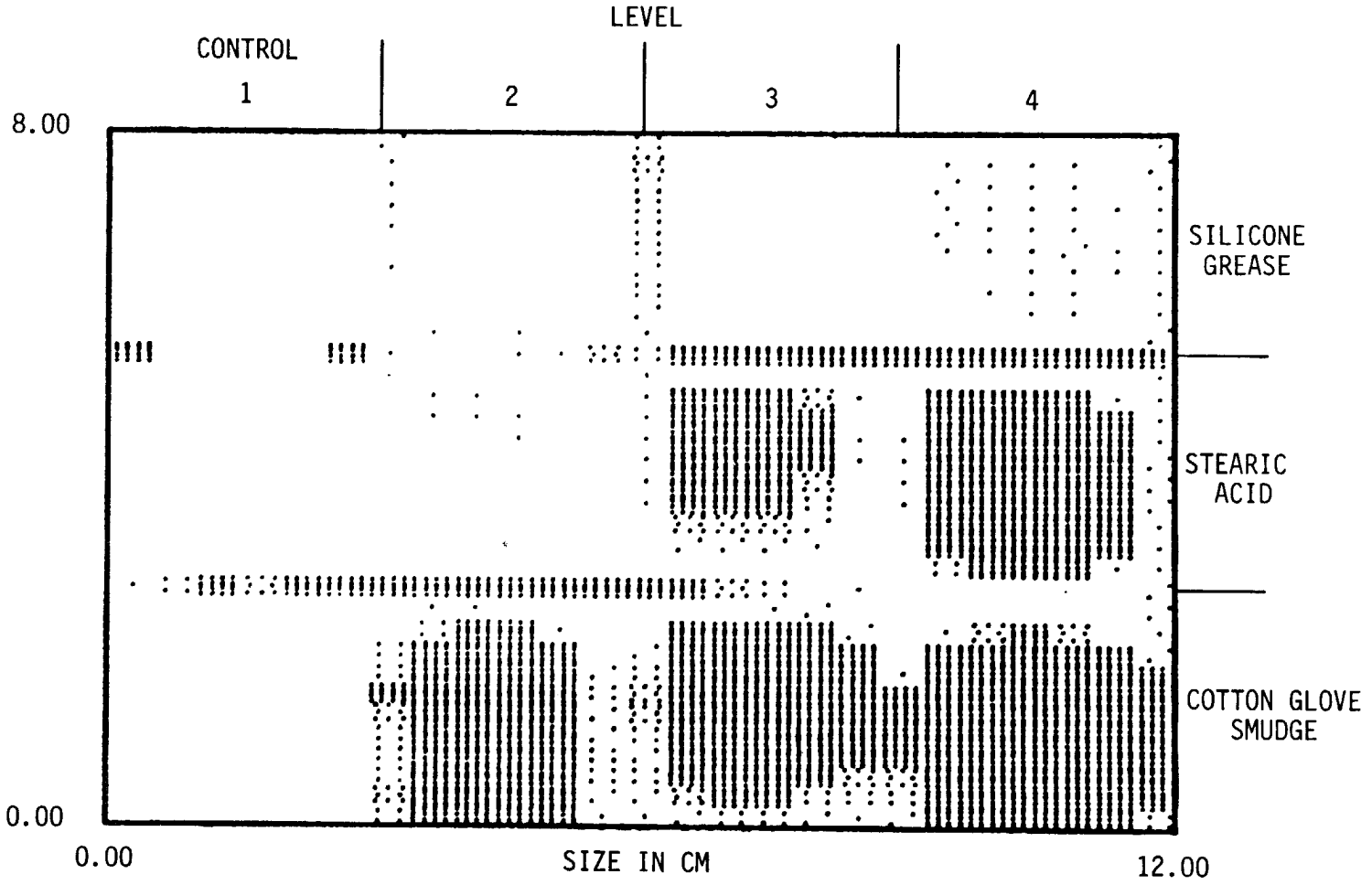

Fig. 29 Computer map of control (clean) and three levels of silicone grease, stearic acid and cotton glove smudge on a PAA AL 7075-T6 curved panel. Convex side by the Off Null technique.

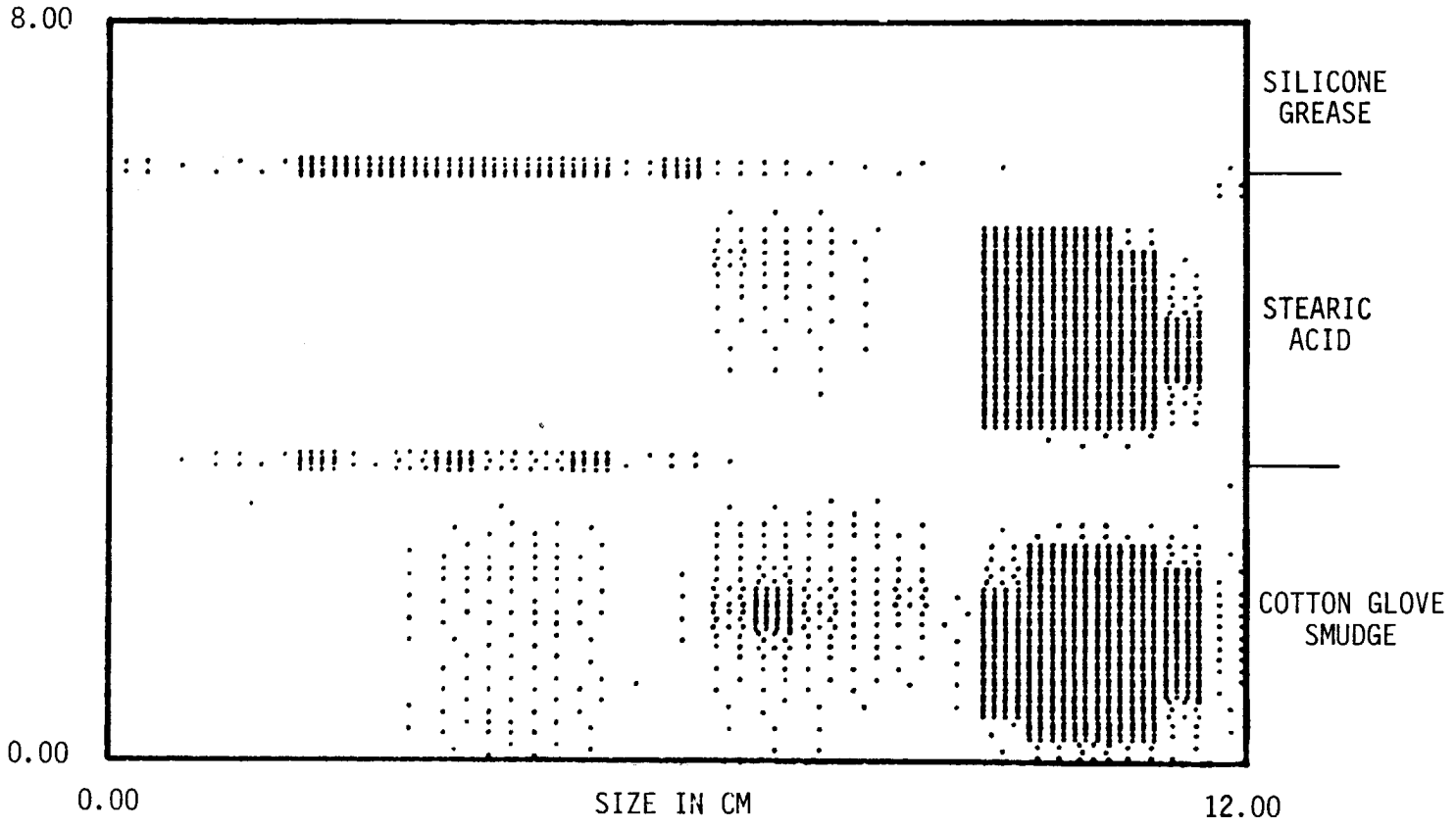

Fig. 30 Computer map at lower sensitivity than Fig. 29.

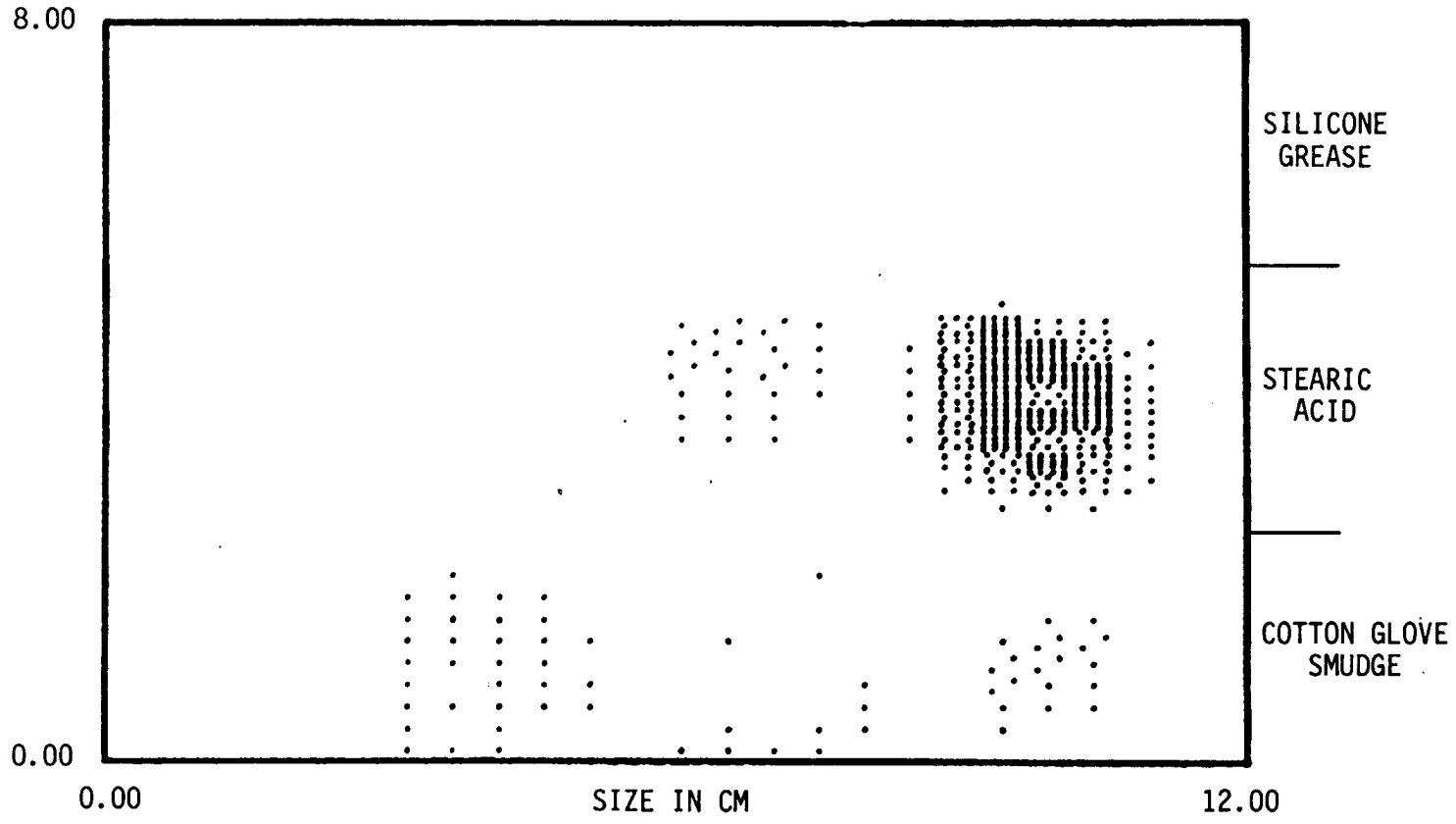

Fig. 31 Computer map using the automated ellipsometer. Δ map on the convex side.

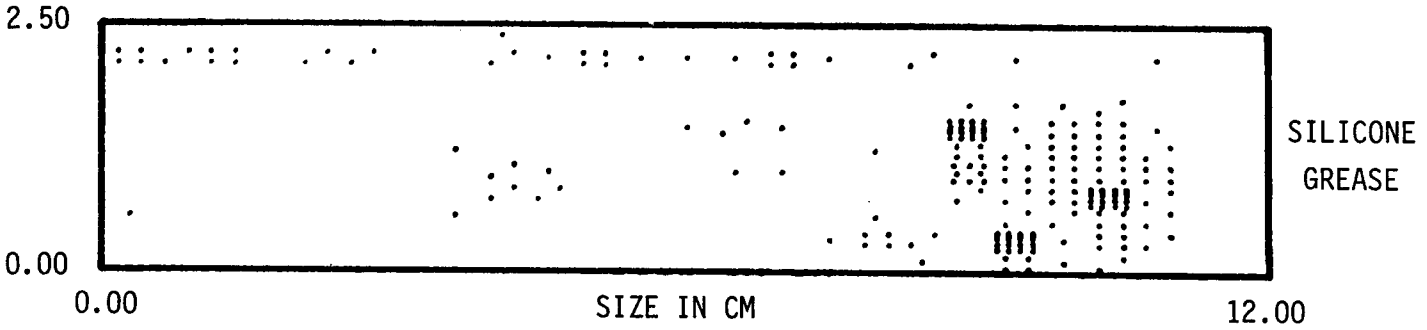

Fig. 32 Computer map using the automated ellipsometer in the silicone grease region. Δ plot of convex side with higher sensitivity.

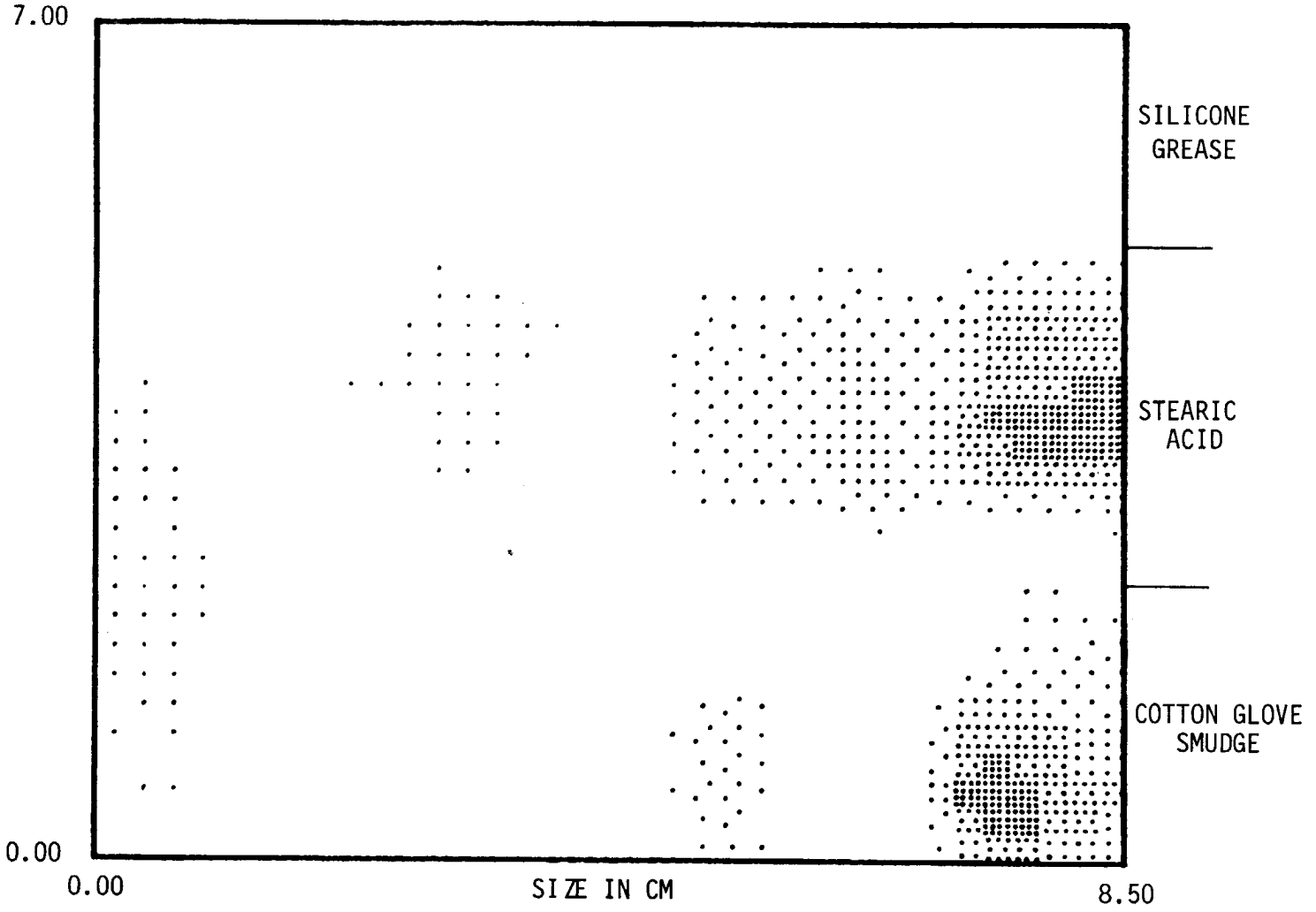

Fig. 33 Computer map using the automated ellipsometer rather than the Off Null technique. Δ plot on concave side.

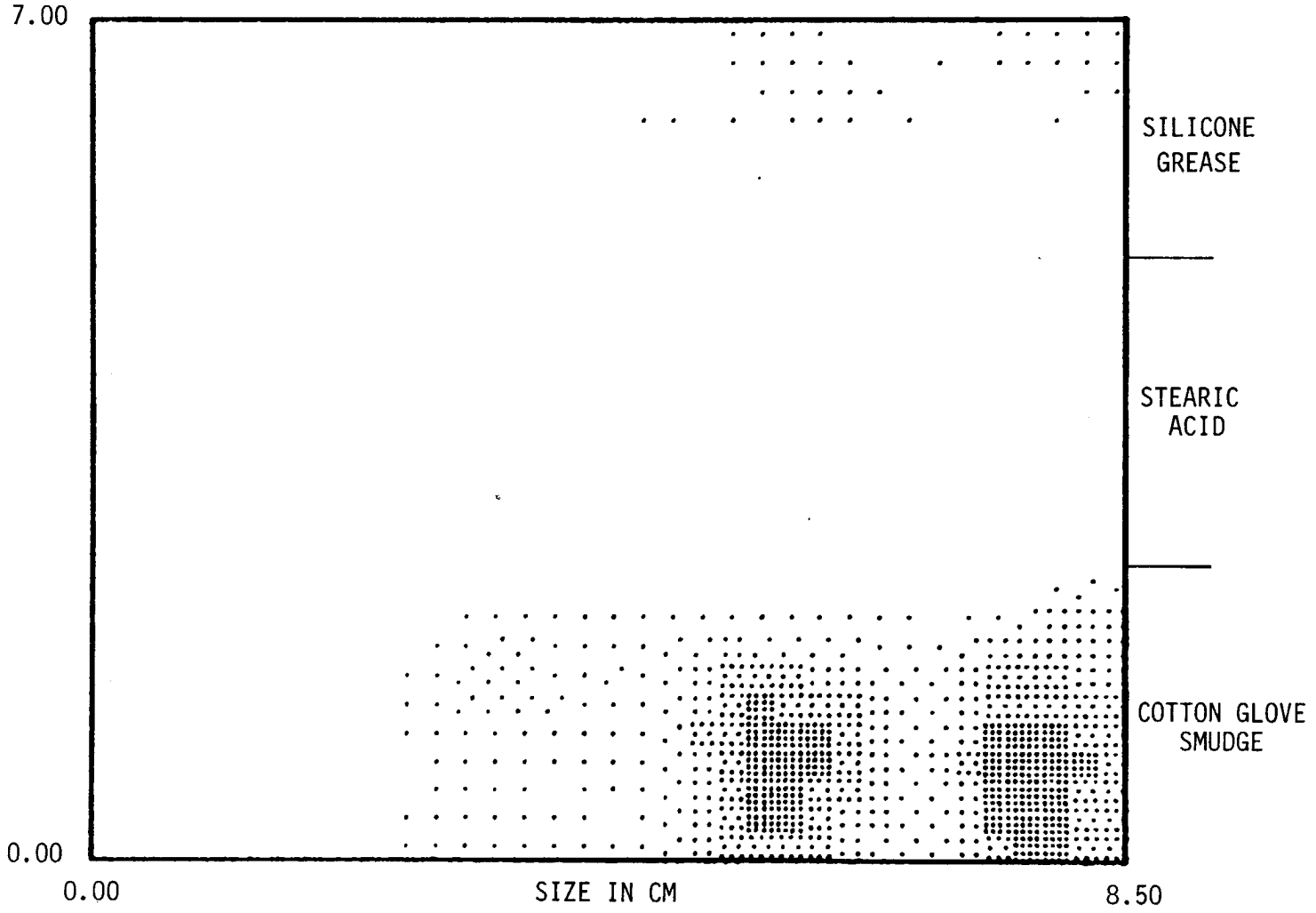

Fig. 34 Computer map using the automated ellipsometric ψ plot on concave side.

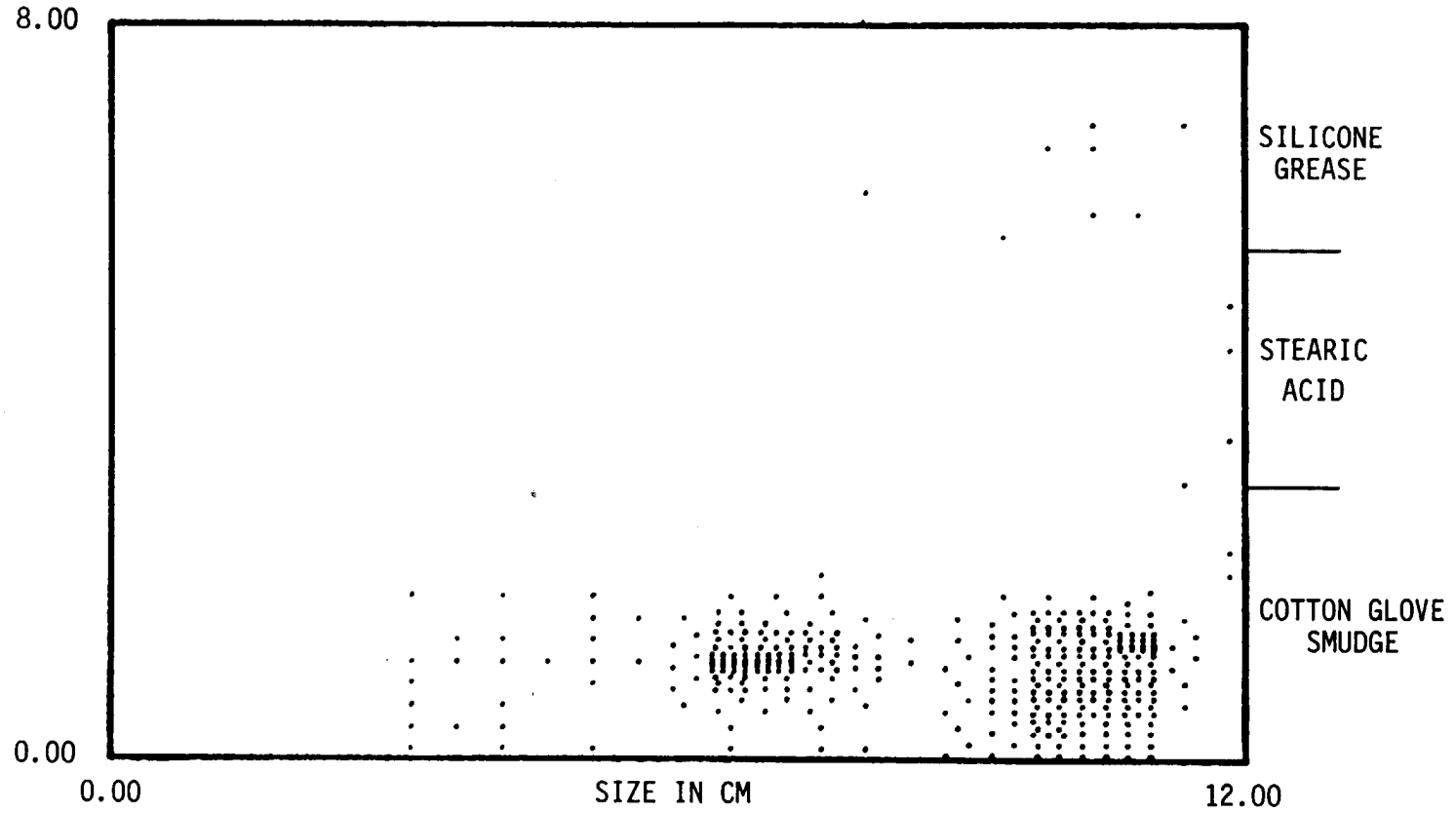

Fig. 35 Computer map using the automated ellipsometric ψ map of the convex side.

SECTION IV

DISCUSSION OF RESULTS

The contamination results of PAA and FPL etched Al 7075-T6 with various contaminants are summarized in Tables 32 and 33, respectively. Figure 36 is a plot of lap shear bond strength vs contamination thickness for oil, silicone grease, stearic acid, hexadecylamine and Coca Cola. Figure 36 and the results presented in the text indicate that very thick layers of organic contamination (to 60,000Å) have only small effect on lap shear strength. This is attributed to two phenomena.

1) Organic contamination is absorbed by the FM-73 adhesive
2) Organic contamination not absorbed by the adhesive, is absorbed within the porous structure of the anodic hydroxide layer.

In spite of the contamination absorption by the adhesive, FPL etched aluminum cannot accommodate that which is left. This is evidenced by Fig. 37, where bond strength degradation occurs for small contamination thickness in the case of FPL etch.

Silicone grease degrades lap shear strength for PAA surfaces, but much more strongly for FPL etched surfaces. The reason for the above behavior can be inferred from Figs. 38 and 39.

The FPL etched surface has been shown[2], to be very pitted, but the pits are shallow and not porous as for the PAA anodic hydroxide. The oxide thickness on FPL etched aluminum is only 100-200Å as compared to 3000 to 5000Å for PAA aluminum.

Thus as schematically represented in Fig. 38 and 39, contamination (as low as a monolayer) forms a continuous weak boundary layer on an FPL etched surface, but not on the PAA surface. Because silicone grease is not absorbed by the adhesive and perhaps because the molecules are larger, silicone grease can be accomodated by neither system.

TABLE 32

Summary of Contamination Results for PAA Al 7075-T6

Cont. Thickness (Å)	θH_2O (deg)	Bond Strength (Ksi)	% Interfacial Failure
Oil/PAA Al 7075-T6			
0	14	5.73	0
150	9	6.01	0
180	18	5.98	1
430	29	5.53	0
1000	54	5.53	0
Silicon Grease/PAA Al 7075-T6			
0	9	5.47	0
130	43	5.29	5
270	66	5.71	20
500	74	4.93	40
1100	89	3.21	90
Large	105	2.58	95
Stearic Acid (SA)/PAA Al 7075-T6			
0	6	5.44	--
80	21	4.84	--
100	67	4.54	--
1000	80	4.74	--
2000	90	4.84	--
3000	120	5.34	--
Hexadecylamine/PAA Al 7075-T6			
0	2	5.8	0
650	128	4.76	1
800	118	5.78	2
900	113	5.00	0
Large	74	6.15	0
Large	135	4.79	1
Soda Pop/PAA Al 7075-T6			
0	--	5.43	--
200	--	5.25	--
470	--	5.40	--
800	--	----	--
900	--	5.25	--
1400	--	4.96	--

TABLE 33

Summary of Contamination Results for FPL Etched Al 7075-T6

Cont. Thickness (Å)	θH_2O (deg)	Bond Strength (Ksi)	% Interfacial Failure
Oil/FPL Etched Al 7075-T6			
0	3	5.00	0
20	20	4.85	0
50	32	4.60	0
350	59	4.45	20
400	63	4.05	25
Silicon Grease/FPL Etched Al 7075-T6			
0	4	5.10	0
35	109	1.75	90
35	92	1.30	99
45	96	0.90	100
100	100	0.60	98
200	141	---	100
Stearic Acid (SA)/FPL Etched Al 7075-T6			
0	20	4.87	0
30	90	4.40	2
200	114	3.90	10
280	104	3.79	2
500	118	3.35	30
500	117	3.53	20

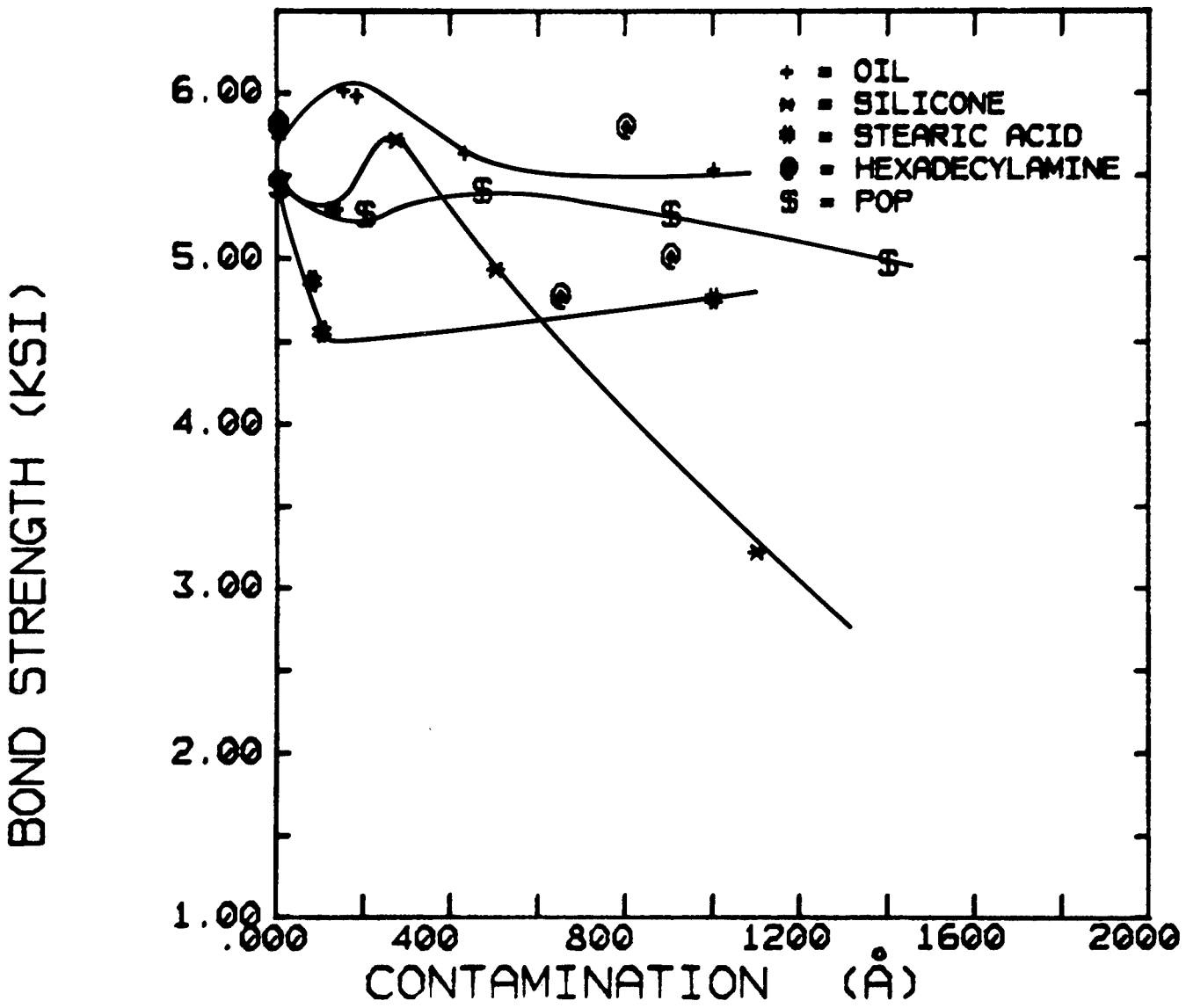

Fig. 36 Bond strength vs contamination for PAA AL 7075-T6.

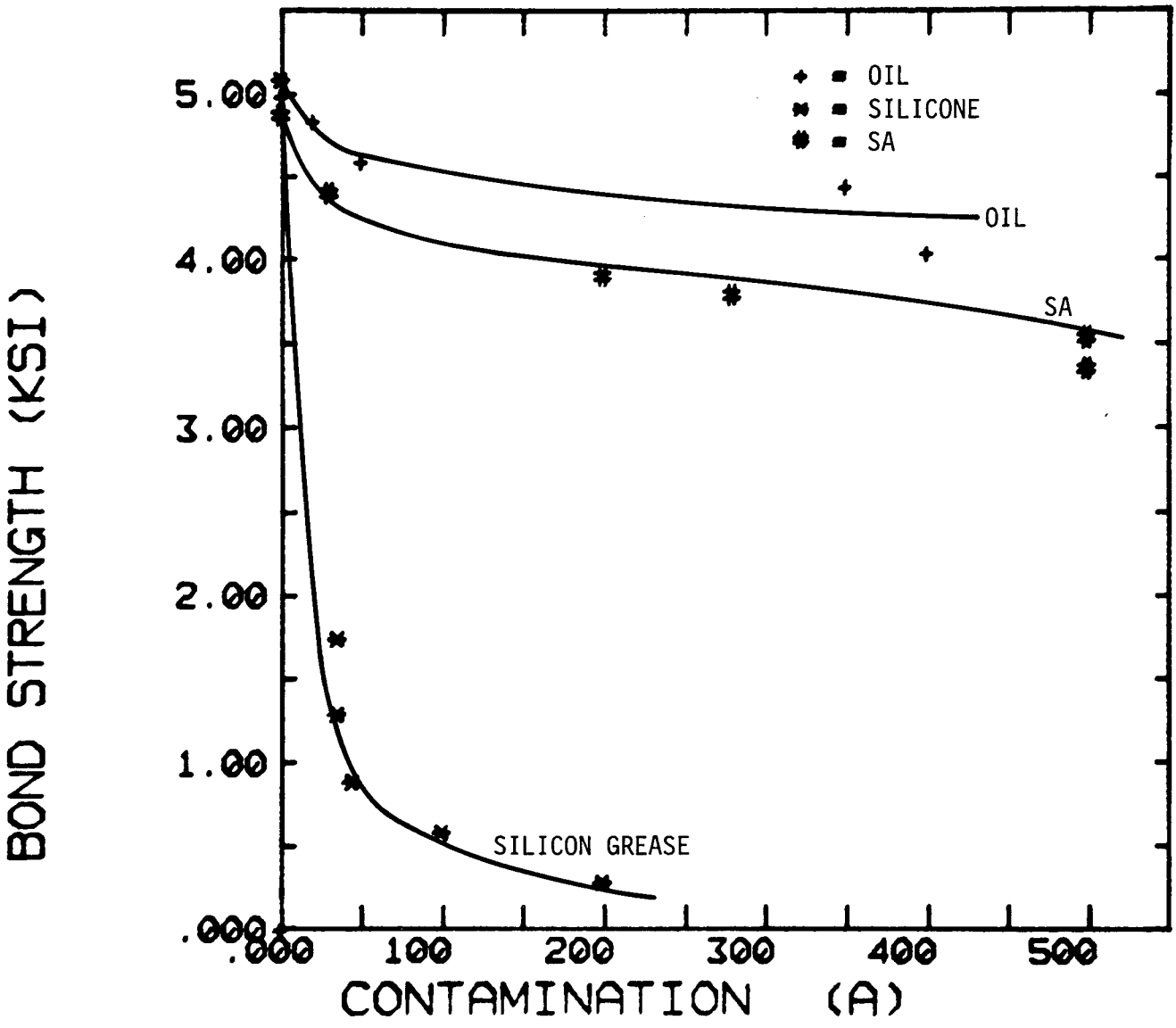

Fig. 37 Bond strength vs contamination for FPL etched AL 7075-T6.

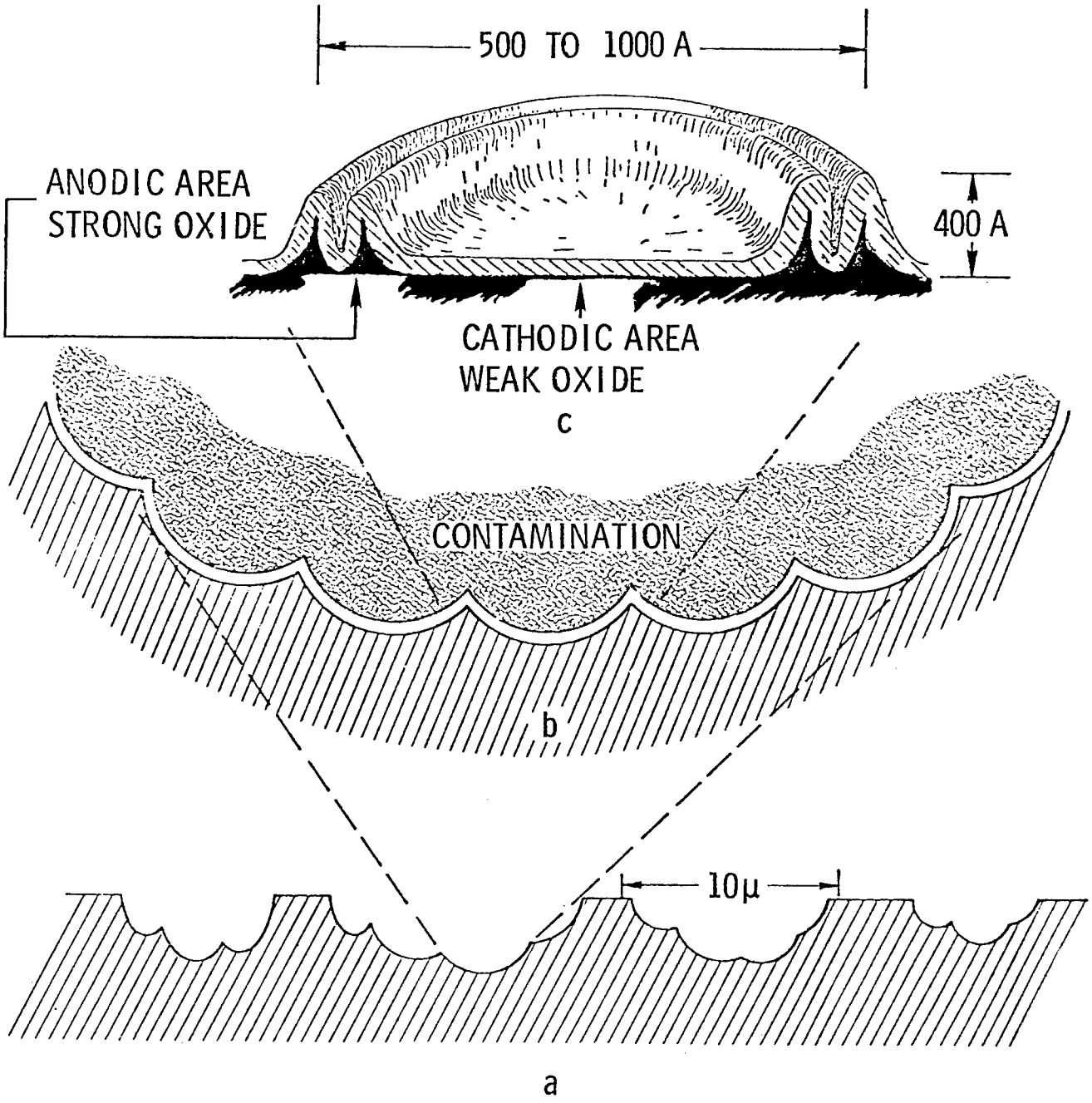

Fig. 38 Schematic representation of FPL etched aluminum with contamination, three magnifications.

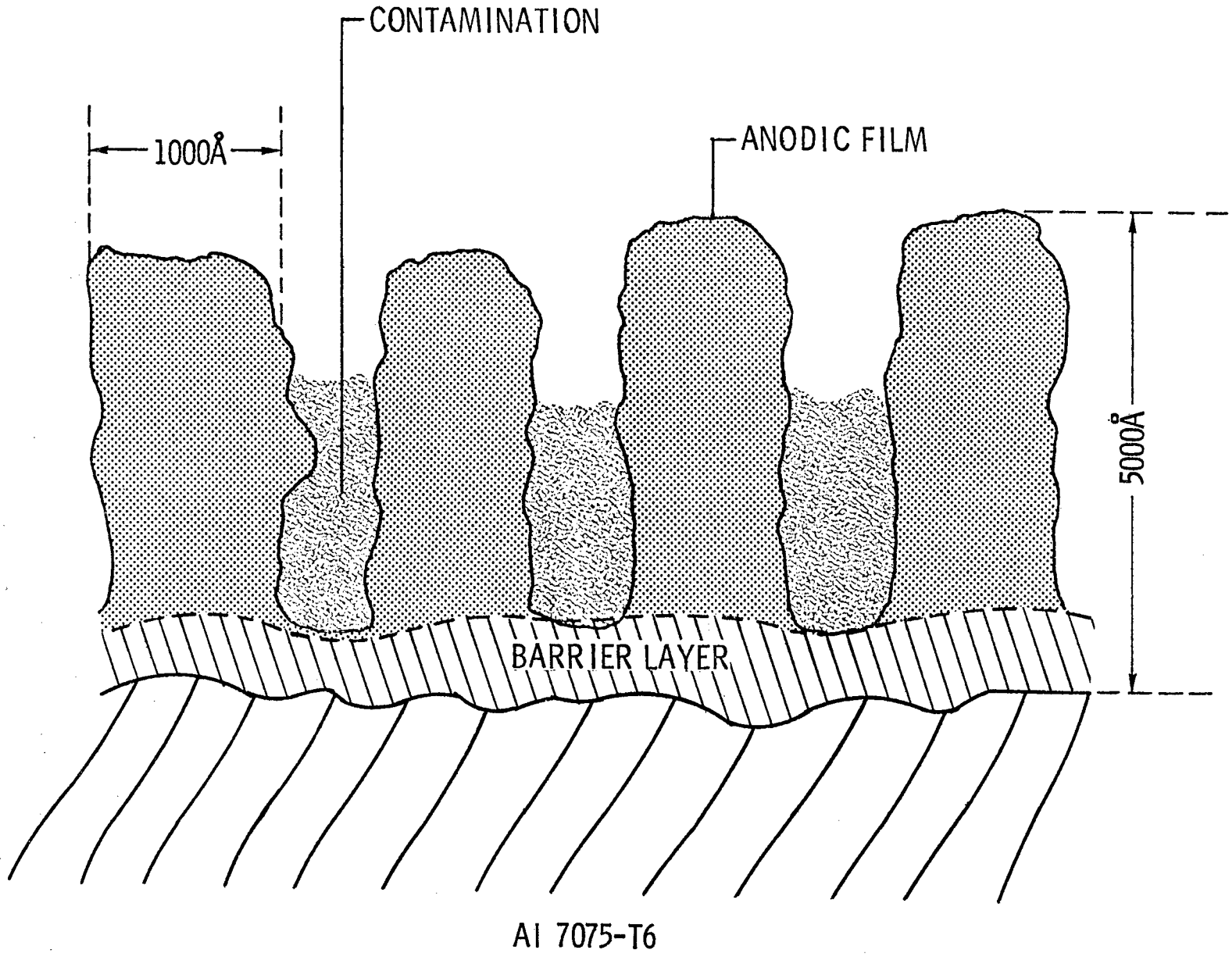

Fig. 39 Schematic representation of phosphoric anodized Al 7075-T6.

Figure 40 is a plot of water contact angle vs contamination thickness on PAA aluminum. The low molecular weight oil has considerably less effect on θH_2O than the same average thickness of the other contaminants. The same is noted in Fig. 41 for contamination on the FPL etched surface. However, the water contact angle is increased to a much greater value at small contamination levels. The relationship between bond strength and water contact angle is plotted in Fig. 42 for PAA and Fig. 43 for FPL etched surfaces. The lap shear bond strength decreases approximately linearly with θH_2O for all the contaminants except silicone grease. The rate of decrease is greater for the FPL etch than the PAA. The bond strength drops off sharply above $\theta H_2O \sim 60^o$ for both surfaces.

As might be expected, there is a general decrease in bond strength with increase in the percent interfacial failure, as noted in Fig. 44.

C. Hand Held Contamination Detector

There are two main reasons for the development of a miniaturized hand held contamination tester.

1. Most of the adhesive bonding in the aerospace industry is for small batches of varying shapes and size panels rather than large numbers of a particular panel. There is therefore a need for a small hand held (about the size of a flashlight) instrument for spot checking.
2. The instrument developed in this study (see Fig. 3, AFML-TR-77-42) is not conducive to mapping large curved parts. It would be much better to move the detection head over the panel, than the panel under a fixed head. In order to facilitate motion of the head and decrease the radius of curvature that can be inspected, a miniaturized head is needed. Such a hand held contamination tester has been designed, but needs to be developed and tested.

A schematic representation of the instrument is given in Fig. 45. A small cylindrical container holds a battery pack A or can have an extension cord to standard electrical outlets. The power source is connected to a lamp

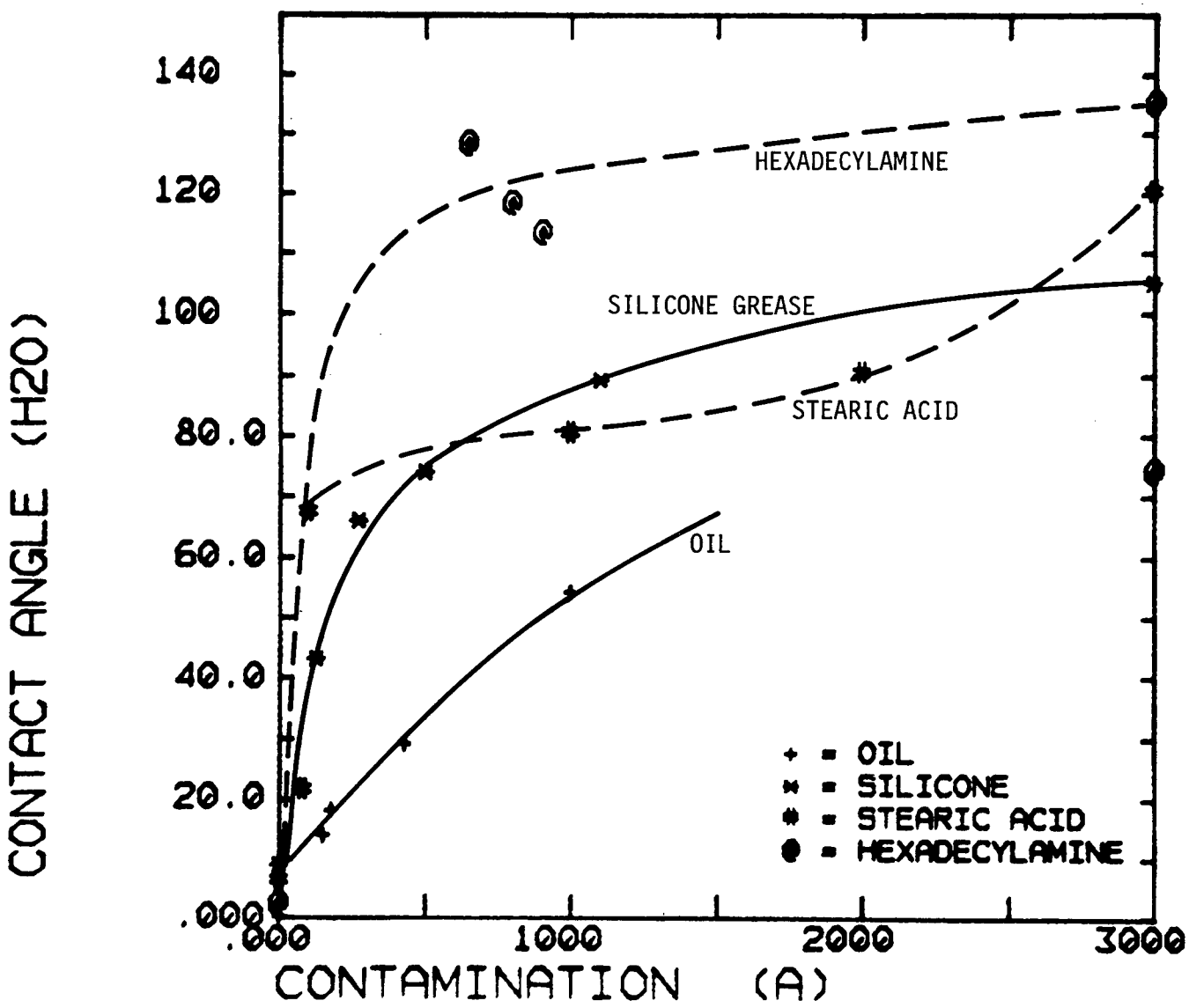

Fig. 40 Contact angle vs. contamination for PAA AL 7075-T6.

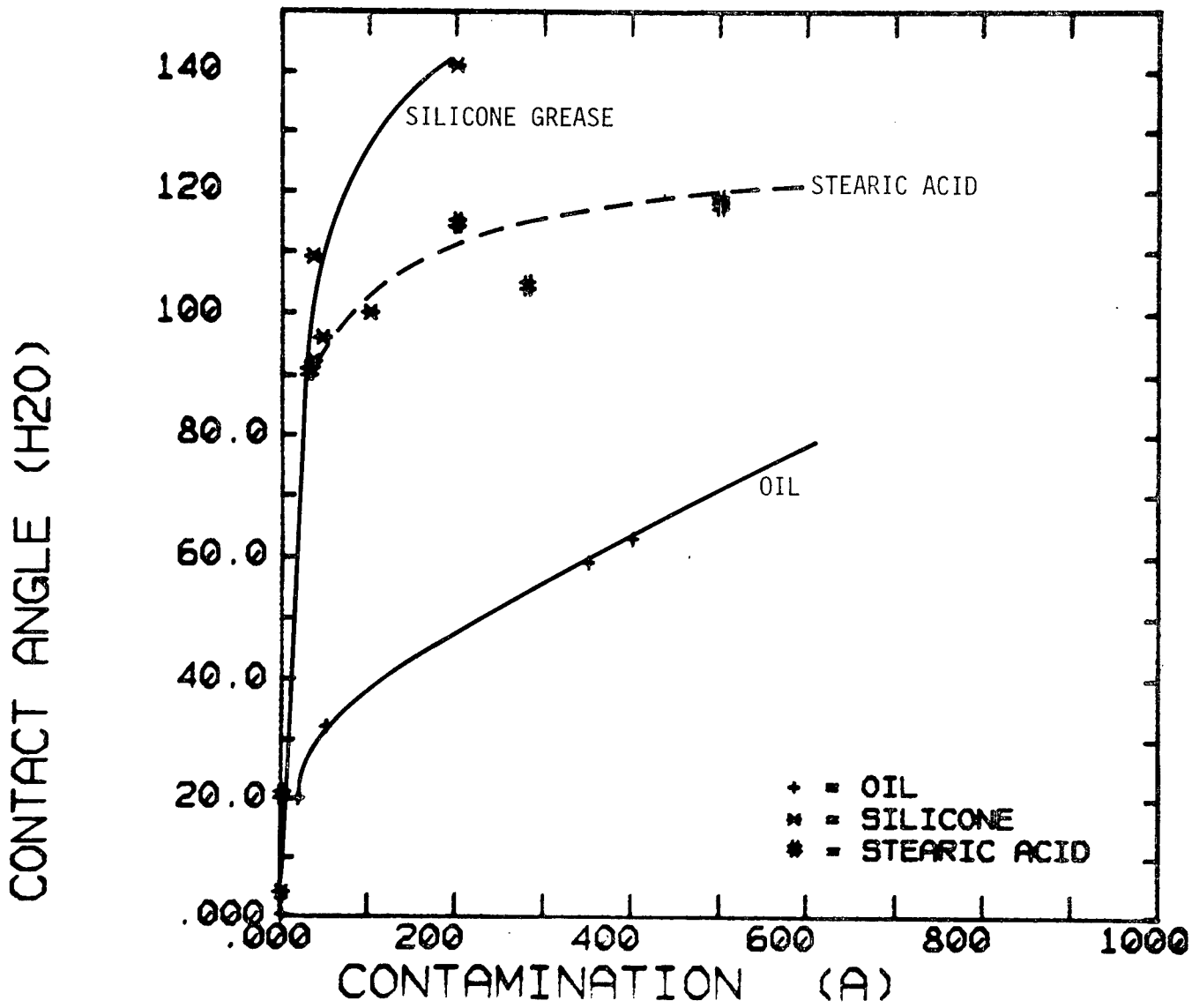

Fig. 41 Contact angle vs contamination for FPL etch AL 7075-T6.

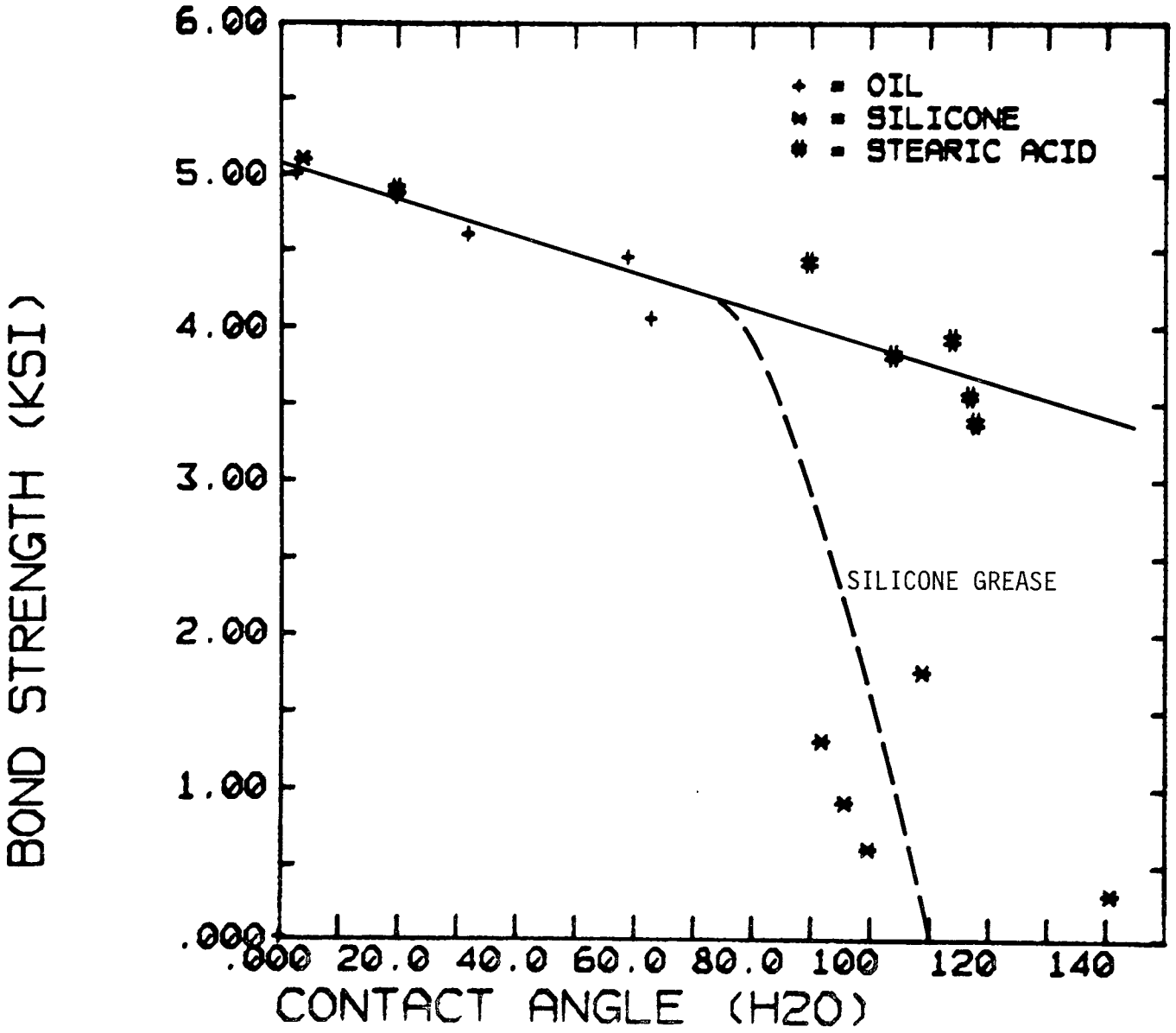

Fig. 42 Bond strength vs. contact angle for FPL etch AL 7075-T6.

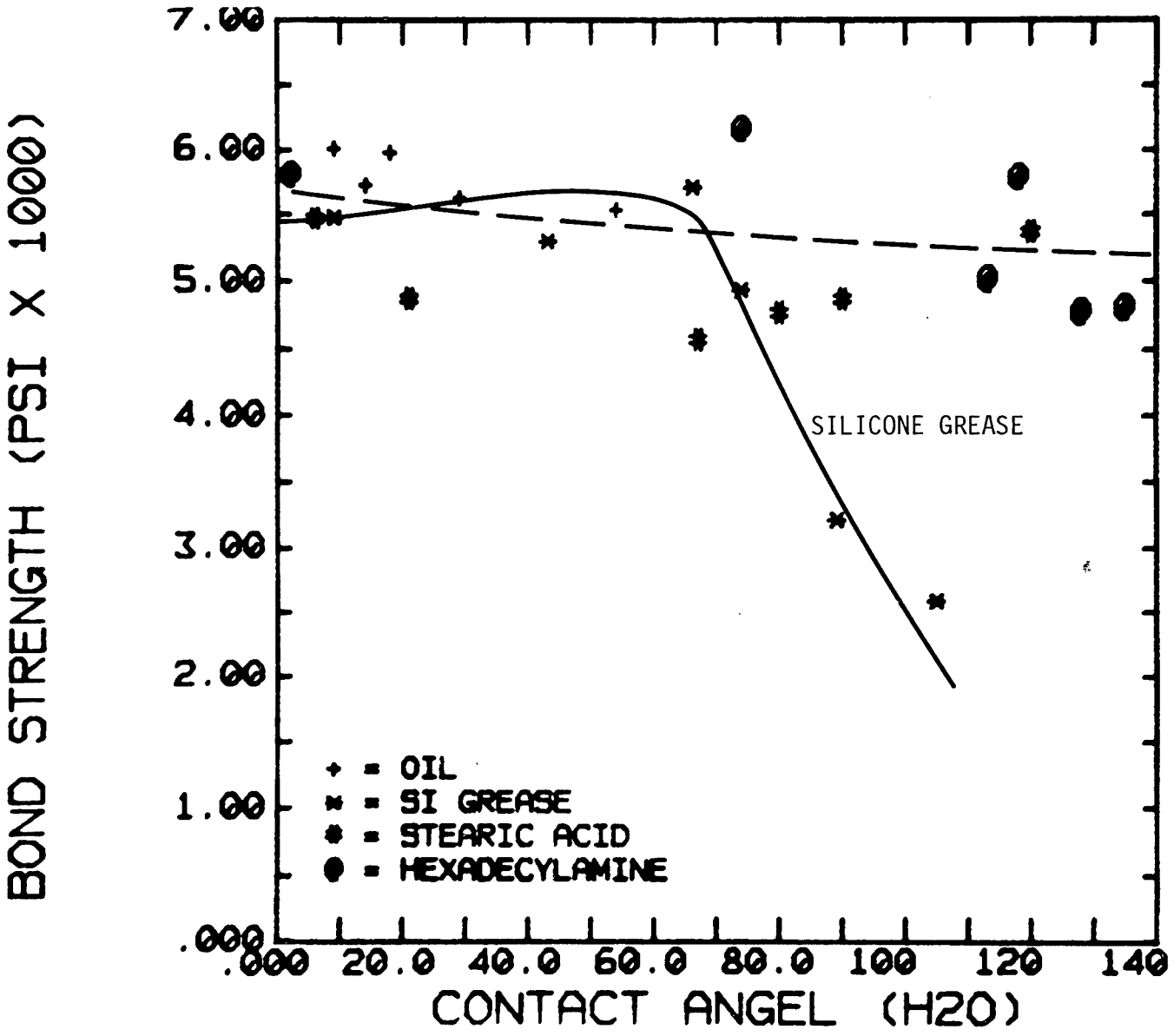

Fig. 43 Bond strength vs contact angle for PAA AL 7075-T6.

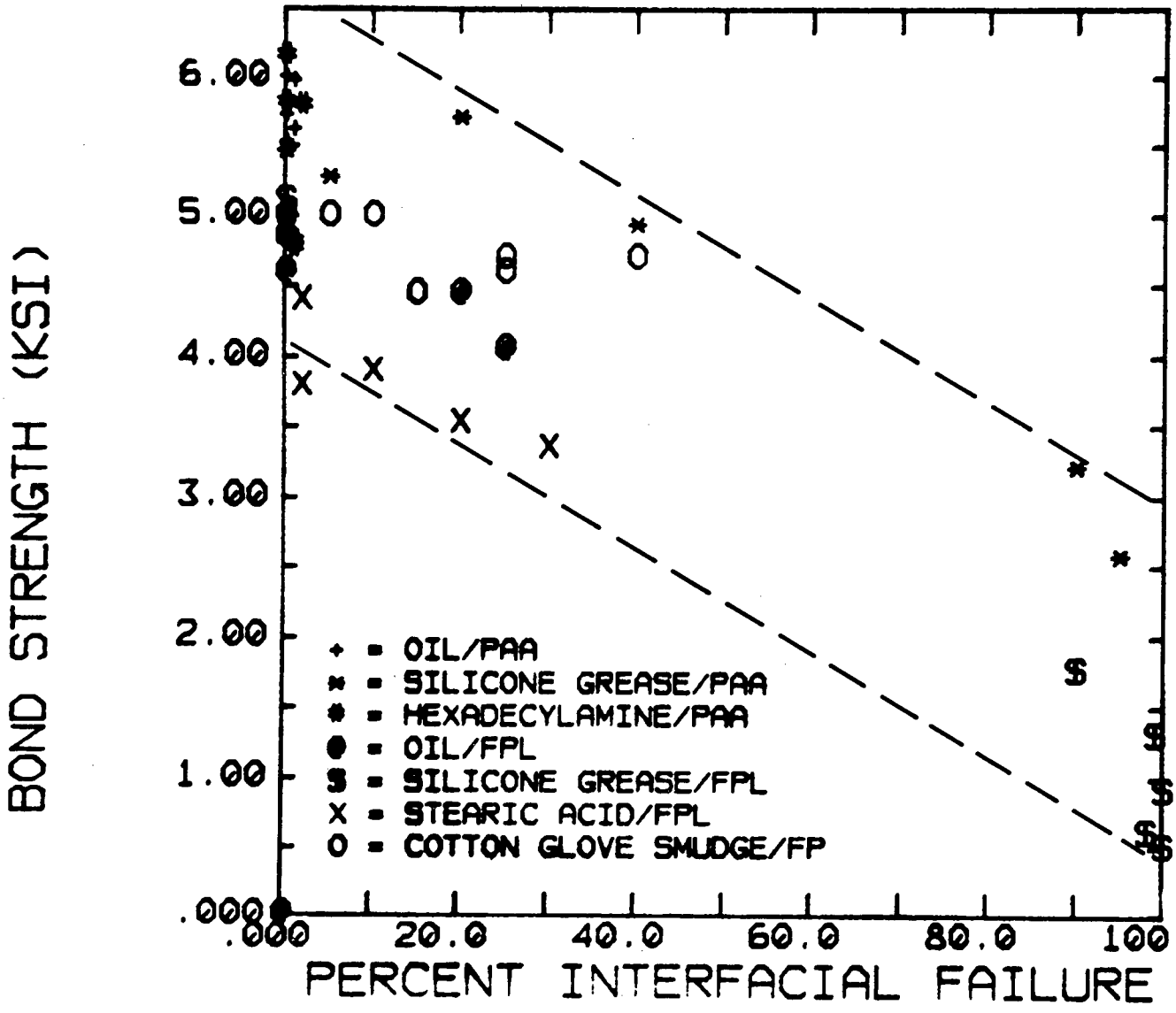

Fig. 44 Bond strength vs % interfacial failure.

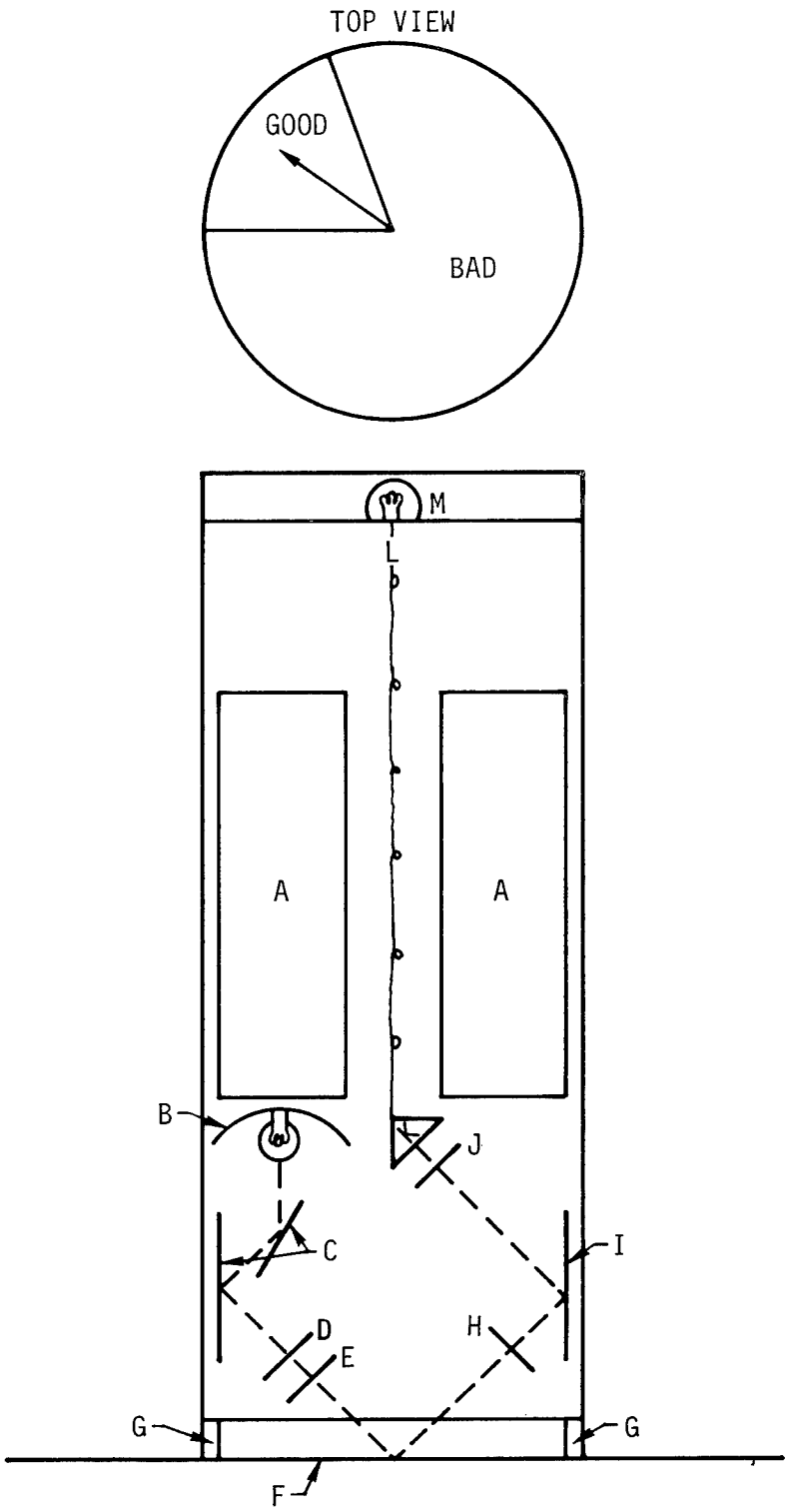

Fig. 45 A schematic presentation of the Off Null ellipsometric contamination tester.

and reflector B that reflects light off mirrors C and through a polarizer D and compensator E. The light passes through a window in the bottom of the instrument and reflects from the surface F, to be tested. The feet G are placed against the surface to provide a precise angle of incidence for the beam. If the surface cannot be touched, it will be necessary to provide mechanical arm and holder that position the tester in the correct orientation with respect to the surface. The alignment technique is described below.

The light beam reflects from the surface, passes through the analyzer H, reflects from the mirror I, passes through monochromator filter J, and is detected by photodetector K. The electronic control for K is held in the container at L and the lamp M lights up in direct proportion to the light striking detector K. The photodetector amplifier is adjusted such that the warning lamp M does not light up for any position on the acceptable control sample. The tester is then ready to test surfaces that have been prepared for painting, adhesive bonding, etc. The tester is placed with feet against the surface to be contamination tested. If the lamp M lights up, or an indicator needle moves out of the good region, the surface falls outside the acceptance band of the control sample.

It is concluded that the "OFF NULL" technique will provide an excellent means for a portable hand held contamination tester. The advantage is that no computer is needed and high sensitivity is possible. The increased sensitivity makes this technique promising for our computer operated mapping facility as well.

SECTION V
CONCLUSIONS

The solution to the problem posed in the introduction has been fully demonstrated. The ellipsometric technique can detect contamination below and over the range that significantly degrades the bond strength and durability of Al 7075-T6 - FM-73 joints as measured by the lap shear and wedge tests.

It was gratifying to discover the great insensitivity of PAA surfaces to organic contamination. It appears that contamination such as oils, fingerprints, smog, etc. have minimal effect on joint integrity. However, handling damage, processing errors and certain other types of contamination can cause serious degradation.

It is concluded that the mapping facility developed in this study can be used to detect all types of contamination and damage and is particularly suited to assembly line NDI of large numbers of flat parts.

For spot checking smaller batches of varying shaped parts, a hand held contamination tester should be developed. This instrument has been designed upon the same principle used for our mapping facility, but miniaturized. Miniaturization may introduce problems concerning sensitivity due to low intensity light source. This may be overcome by using a high intensity laser, as at present, with flexible line light pipes to place the light where needed.

REFERENCES

1. T.P. Remmel, "Characterization of Surfaces Prior to Adhesive Bonding," AFML Tech. Rep. NOR-75-145, October 1975.

2. T. Smith, "Nondestructive Inspection of Phosphoric Acid Anodized Aluminum Panels for Contamination," AFML-TR-77-42, April 1977.

3. T. Smith, "An Automated Scanning Elliipsometer," Surf. Sci. 56, 212 (1976).

☆U.S.Government Printing Office: 1979 — 657-002/644